University of Alberta

Zic transcription factors regulate retinoic acid metabolism during zebrafish neural development.

by

Danna Lynne Drummond

A thesis submitted to the Faculty of Graduate Studies and Research
in partial fulfillment of the requirements for the degree of

Master of Science
in
Molecular Biology and Genetics

Department of Biological Sciences

Spring 2012
Edmonton, Alberta

Abstract

Retinoic acid (RA) has a crucial role in embryonic nervous system development - controlling anterior-posterior patterning, neural differentiation, and cell proliferation. During zebrafish embryogenesis, levels of RA are tightly regulated by the combinatorial action of synthesis and degradation enzymes, such as *aldh1a2* and *cyp26a1*. We have identified a novel regulatory interaction between Zinc finger of the cerebellum 2a/2b, Zic2a2b, transcription factors and RA metabolism genes. Using morpholino-mediated knockdown in conjunction with exogenous alterations to RA levels, we found that Zic2a2b regulates both *cyp26a1* and *aldh1a2* gene expression. Phenotypes resulting from Zic2a2b-depletion are reminiscent of reduced embryonic RA levels – reduction in size of posterior rhombomeres and the spinal cord. Additionally, defects in the posterior-most class of branchiomotor neurons, the vagal neurons, are visible - a defect that is completely rescued with exogenous RA supplementation. We suggest a model whereby Zic2a2b acts upstream of *aldh1a2* in modulating RA levels during embryogenesis.

Acknowledgements

I would like to extend my sincere thanks to the following people:

To Andrew Waskiewicz for your inspiration, understanding, and scientific conversations.

To those within the department, Dr. David Pilgrim and Dr. Martin Srayko, and my committee members, Dr. Ted Allison and Dr. Roseline Godbout, for help and advice throughout the years. To James MacLagan, Dawn MacRitchie, and Mark Wolansky for making TAing fun and a great learning experience. To Aleah McCorry for taking care of fish.

To Dr. Joshua Waxman for graciously supplying Tg(12XRARE-*ef1a:gfp*)sk71 transgenic zebrafish line.

To previous and current Waskiewicz lab members (in alphabetical order):
Tim Erickson and Curtis French - for patiently answering the obtuse and redundant questions of a first year graduate student, you guys are the best.

To Caroline Cheng, Jakub Famulski, Jen Hocking, Vanessa Holly, Lindsey March, Laura Pillay, Lyndsay Selland, and Tara Stach – for scientific and personal help and support, for making everyday different and interesting, and for shamelessly promoting coffee-addiction.

To Caroline and Vin – special thanks for keeping me laughing, being my shoulders to cry and complain to, and for just plain being awesome.

To my parents, grandparents, and family for their unending love and support through this process. And Craig - words do not seem to do justice, but thank you for making me smile, for your understanding, your unwavering support, and for watching Harry Potter more times than any human alive. I love you.

Table of Contents

List of Tables

List of Figures

Figure 4.5 Zics can modulate each other's transcription.

Abbreviations

A-P	Anterior-posterior
Aldh	Aldehyde dehydrogenase
Bcox	beta-carotene 15,15'-monooxygenase 1
BMP	Bone morphogenetic protein
Cyp	Cytochrome p450 oxidase
D-V	Dorsal-ventral
DEAB	Diethylaminobenzaldehyde
FGF	Fibroblast growth factor
Gli	Human glioma
HB	Hindbrain
Her	Hairy-enhancer of split-related
Hox	Homeobox transcription factor
HPE	Holoprosencephaly
MHB	Midbrain-hindbrain boundary
r	Rhombomere
RA	Retinoic acid
RAR	Retinoic acid receptor
RARE	Retinoic acid response element
RXR	Retinoid-X receptor
S	Somite
SC	Spinal Cord
Shh	Sonic Hedgehog
VAD	Vitamin-A deficient
Zic	Zinc finger of the cerebellum
ZOC	Zic-Opa conserved domain

Chapter 1. Introduction

1.1 Vertebrate neural development

The vertebrate nervous system is responsible for all motor function and movement, autonomic activity such as coordination of breath and heart rate, and cognitive thought. Development of the nervous system is a complex and highly regulated process that has been the focus of study for a century. In the simplest terms, neurobiologists have been seeking to understand how specific cell types develop at the right time and place.

This process begins in the earliest stages of embryonic development, such that the overall architecture of the nervous system is already established by late -gastrulation (Appel, 2000; Keller, 1991; Keller, 1975, 1976). In addition to morphological movements, presumptive neural cells acquire regional identity based on a complex set of intracellular signaling mechanisms and extracellular signals. This ultimately gives rise to the neural tube – consisting of the forebrain, midbrain, hindbrain, and spinal cord (Figure 1.1 A) (Blader and Strahle, 2000). As development continues, these broad regions become further subdivided; for example, the forebrain includes the telencephalon, diencephalon, prethalamus, and hypothalamus, while the hindbrain is comprised of seven or eight lineage-restricted rhombomere segments. Neuronal identity and cell behaviors are completely dependent on the precise specification of regional identity. Therefore, within each segment or region there is a distinct array of transcription factors and markers expressed that determine the identity of cells within the segment – properties including cell morphology, axon trajectories, and neurotransmitters (Appel, 2000).

1.1.1 Early steps of neural development

The major subdivisions of the nervous system are established early, as fate mapping and explant studies show prospective forebrain and midbrain are specified at the beginning of gastrulation while the hindbrain is specified

slightly later (Appel, 2000; Grinblat et al., 1998; Woo and Fraser, 1998). By late gastrulation, presumptive anterior neural tissue (to become the forebrain and midbrain) is located dorsally at the animal pole while posterior tissue (to become the hindbrain and spinal cord) is adjacent, located closer to the embryonic margin (Figure 1.1 B) (Kimmel et al., 1990; Trevarrow et al., 1990).

Strict regional and temporal signals originating from embryonic signaling centers regulate neural development and specification. The embryonic organizer (the zebrafish shield) is a region of BMP-antagonism that specifies dorsal and neural tissue by blocking non-neural, ventralizing BMPs (Moens and Prince, 2002; Wilson et al., 1997). Interestingly, this step of neural induction has little effect on the hindbrain, as the hindbrain still forms and undergoes patterning with ablation of the embryonic shield (Fekany et al., 1999; Saude et al., 2000; Shih and Fraser, 1996). This suggests that there is a separate inductive event in formation of posterior neural tissue.

1.1.2 Posterior neural induction

The existence of separate signals coordinating A-P neural development was hypothesized decades ago; i.e. anterior neural induction is followed by a graded transforming signal that promotes posterior neural fates (Nieukoop, 1952; Toivonen and Saxen, 1968). These posteriorizing signals have been identified as Fibroblast Growth Factor (FGF), Wnts, and Retinoic Acid (RA) – originating from the lateral and ventral embryonic margin (Koshida et al., 1998). Xenopus and zebrafish studies have demonstrated the importance of FGF signaling; for example morpholino-mediated knockdown of zebrafish Fgf24 and Fgf8 prevents posterior neural development and causes loss of trunk mesodermal tissue (Draper et al., 2003). Loss of FGF signaling with dominant negative FGF receptors or pharmacological FGF inhibition (SU5402) prevents tail, trunk mesoderm, and spinal cord formation (Griffin and Kimelman, 2003; Kudoh et al., 2002;

Londin et al., 2005). Additionally, zebrafish Fgf8 and Fgf3 are required for posterior neural development as treatment with a pan-FGF-antagonist causes loss of trunk and tail tissue (Amaya et al., 1991; Griffin et al., 1995).

Disruption of zebrafish Wnt8 using a deletion mutant causes severe neural defects with a complete loss of ventral and posterior fates and concurrent expansion of dorsal fate (Lekven et al., 2001). Conversely, the *headless* mutant, which lacks activity of the Wnt repressor Tcf3, develops with expanded posterior neural tissue at the expense of eyes, forebrain and midbrain – demonstrating the additional requirement for Wnt signaling (Kim et al., 2000). Finally, RA is a critical factor in posterior neural development – whereby RA reduction or exogenous treatment causes severe posterior or anterior truncations, respectively (Glover et al., 2006). It is the combinatorial action of these signaling pathways that mediates precise induction of posterior neural tissue during early development.

1.1.3 Hindbrain patterning and *hox* genes

Following induction of posterior neural tissue, the hindbrain passes through a transient segmental organization of seven or eight rhombomeres. This reiterative organization of rhombomeres is regulated by one family of homeobox transcription factors (Hox) and is intimately linked to neural fates that arise within each region. *Hox* genes were first discovered as regulators of the Drosophila body plan (Lewis, 1978). In this experiment, mutation of one Drosophila *Hox* gene, *Ultrabithorax*, resulted in regional duplication causing an additional set of wings to develop. Since this discovery, *Hox* genes have become known as highly conserved master regulators of anterior-posterior identity – whereby the complement of *Hox* genes within each hindbrain segment determines the morphology and fate of cells within that segment (Moens and Selleri, 2006).

Hox paralogs are organized in discrete gene cluster arrays. Mouse and humans have four *Hox* clusters (*HoxA/B/C/D*) each located on a different chromosome (totaling 39 genes), while zebrafish, as a result of an additional

whole genome duplication, has 7 *hox* gene clusters (totaling 48 genes). Interestingly, following the genome duplication, zebrafish have lost almost an entire *hoxD* paralog cluster. As a result, many Hox family members have lost their hindbrain-specific functions (Moens and Prince, 2002).

Overlapping expression domains, partial redundancy, and regulatory relationships between *hox* genes have made study of individual *hox* genes difficult. However, in murine *Hoxb1* mutants, rhombomere 4 is partially converted to rhombomere 2 identity (Studer et al., 1996). *Hoxa1* mutant mice have lost rhombomere 5 such that rhombomere 4 and rhombomere 6 are directly adjacent to each other (Mark et al., 1993). Further, a regulatory relationship has been identified whereby Hoxa1 initiates *Hoxb1* transcription within rhombomere 4 (Gavalas et al., 1998; Studer et al., 1998). Ectopic over-expression of *Hoxa1* causes *Hoxb1* over-expression and conversion of rhombomere 2 to rhombomere 4 identity (Zhang et al., 1994). Factors directly upstream of *hox* are also crucially important – Valentino is one example of a transcription factor required for specification of r5 and r6. Zebrafish *valentino* mutants have defects in these rhombomeres causing a shortened hindbrain (Moens et al., 1996).

Hox genes activate downstream targets that initiate cell specification and differentiation. The inactivation of murine *Hoxa1* causes a partial loss of rhombomere 4 and 5, a loss that alters facial and cranial neurons of this area (Gavalas et al., 1998; Mark et al., 1993; Studer et al., 1998). Rhombomere-specific mis-expression of *hoxb1* in chick results in altered neuronal identity and behavior where rhombomere 4-derived neurons are born in rhombomere 2 (Bell et al., 1999). Therefore Hox-derived configuration of rhombomere territories is required for organization of cranial nerves and for correct innervation of targets (Chandrasekhar et al., 1997; Moens and Prince, 2002). Further identification of factors downstream of *hox* will be essential in fine-tuning their role in defining neural fate within the hindbrain.

1.1.4 Neural specification and differentiation

Through the process of neurogenesis, proliferative cells of the neural tube are fated to become neurons by triggering cell cycle exit. These cells differentiate into specific neuronal classes depending on anterior-posterior and dorsal-ventral location (Diez del Corral and Storey, 2001). This process occurs in concert with hindbrain segmentation such that neural identity is determined based on a "coordinate system," determined by longitudinal proneural domains and mediolateral bands of segment identity. In zebrafish, the first neurons become post-mitotic just after gastrulation – this allows the fish to be motile at one-day post fertilization (Mendelson, 1986). It is hypothesized that there are two waves of neurogenesis - the first wave, primary neurogenesis, forms neuronal circuits responsible for initial movement and overlays simple neuronal scaffolding which acts as guidance for the neurons born later, during secondary neurogenesis (Kimmel et al., 1990; Maden, 2007).

Within the neural ectoderm, neurogenic regions are defined by the expression of proneural genes, the basic helix-loop-helix transcription factors including *neuroD* and *neurogenin* which promote neural differentiation (Blader and Strahle, 2000). Regions of proneural gene expression are complemented by adjacent expression of neurogenesis inhibiting genes to produce tightly regulated regions of neurogenesis. Over-expression of NeuroD or Neurogenin in Xenopus, results in ectopic formation of neurons (Lee et al., 1995; Ma et al., 1996). In addition, mis-expression of chick Neurogenin1 in non-neural myotome results in activation of neural differentiation markers (Perez et al., 1999).

Within neurogenic regions, lateral inhibition via the Notch signaling pathway is essential in regulating neural differentiation. Proneural gene expression results in the expression of the Notch ligand, Delta, in presumptive neural cells. Delta binds the Notch receptor in neighboring cells – an interaction that promotes expression of repressors of neural differentiation (Diez del Corral and Storey, 2001). In Xenopus neurogenesis,

XDelta1 over-expression inhibits neuron differentiation and interestingly, as XDelta1 acts to activate Notch signaling, over-expression of XNotch1 produces a similar phenotype (Chitnis et al., 1995). An XDelta1 construct lacking the intracellular domain interferes with XDelta activity, producing ectopic neurons comparable to proneural gene over-expression (Chitnis et al., 1995; Ma et al., 1996). This mechanism regulates neural differentiation such that cells within the same region do not differentiate at the same time or acquire the same cell fate.

1.1.5 Branchiomotor neurons arise in a segment-specific manner

Zebrafish have become an increasingly important model for neural development, partly due to the large number of transgenic zebrafish available that allow identification and tracing of individual cell populations. Of particular interest for this work is one class of ventrally located neurons, the branchiomotor neurons, which are beautifully labeled using the Tg(*islet-1:gfp*) transgenic zebrafish line (Figure 1.2 B) (Higashijima et al., 2000). This transgenic was created by isolating branchiomotor neuron specific enhancers upstream of *islet-1*, a LIM-homeobox transcription factor required for motor neuron development (Varela-Echavarria et al., 1996).

Branchiomotor neurons arise in a segment specific manner within the hindbrain and innervate the muscles around the eye, jaw, face, and brachial arches (Chandrasekhar, 2004). Within the zebrafish hindbrain there are three main populations of *islet-1*-positive branchiomotor neurons: the trigeminal, the cranial, and the vagal neurons (Figure 1.2 A) (Higashijima et al., 2000). Trigeminal neurons arise in r2-r3 where they remain, while the facial neurons arise in r4-r5 and migrate posteriorly to occupy r5-r6. These two classes are required for innervation of jaw muscles and support structures within zebrafish. The most posterior class of neurons, located within r7 extending posteriorly into the anterior spinal cord, is the vagal neurons. During development the vagal neurons are born medially and migrate to encompass two lateral domains. In zebrafish the vagals innervate

the gill muscles, whereas they innervate the larynx and pharynx of mice (Chandrasekhar, 2004).

Sonic hedgehog (Shh) is one signaling pathway required for motor neuron induction. Shh mutant mice have complete loss of motor neurons (Chiang et al., 1996; Oh et al., 2009), and in zebrafish, knockdown of multiple Shh proteins causes a severe reduction in motor neurons (Beattie et al., 1997; Bingham et al., 2001). Similarly, activator function of the Shh-transcriptional mediator Gli, is essential for motor neuron induction (Vanderlaan et al., 2005).

As the branchiomotor neurons arise in a segment-specific manner, their identity is highly dependent on *Hox* gene activity and correct A-P patterning. Mutations in murine *Krox20* or *Hoxa1*/*Hoxb1* both cause segmentation and neural defects including loss of trigeminal neurons and mispatterning of posterior cranial nerves (VII-XI), respectively (Studer et al., 1998; Swiatek and Gridley, 1993). In zebrafish, *valentino* mutants have disrupted r5/6 development with corresponding defects in cranial nerves nVII and nIX. Interestingly, this cranial nerve defect is specific to r5/6 as the vagal neuron population within r8 and the spinal cord is unaffected (Chandrasekhar et al., 1997; Moens et al., 1996).

1.2 Retinoic acid signaling

Retinoic Acid (RA) has a variety of functions during embryonic development – most predominantly in AP patterning but it is also involved in neurogenesis, organogenesis, and regulating cell proliferation (Glover et al., 2006). The teratogenic defects associated with RA were identified about 40 years ago through Vitamin A administration to pregnant rats (Morriss, 1972). This was later expanded to mouse studies where, in both cases, increased levels of RA during development caused expansion of rostral hindbrain (Glover et al., 2006; Morriss-Kay et al., 1991; Wood et al., 1994). In addition, exogenous treatment of Xenopus, and later zebrafish, embryos with RA causes severe truncation, with complete loss of anterior head tissue (Durston

et al., 1989; Holder and Hill, 1991). Vitamin A-deficient (VAD) models (predominantly the quail) have greatly helped elucidate the roles of RA. In VAD embryos, the anterior hindbrain develops normally while posterior hindbrain does not differentiate (Gale et al., 1999; White et al., 2000). In fact, posterior regions of the neural tube instead take on a more anterior fate, shown by expansion of anterior forebrain markers. Within zebrafish, VAD phenotypes are created with exogenous RA treatment or using the pharmacological inhibitor of RA synthesis, diethylaminobenzaldehyde (DEAB). Therefore RA acts as a crucial morphogen regulating posterior neural induction – in conjunction with its role in hindbrain patterning and determination of cell fates within rhombomeres via *hox* gene regulation (Moens and Selleri, 2006; Papalopulu et al., 1991).

1.2.1 The RA signaling and metabolism pathway

The main sites of RA action during early developmental stages are within presumptive posterior neural tissue, the hindbrain and spinal cord (Maden, 2002). In simplest terms, retinoic acid begins as retinol (Vitamin A; Figure 1.3 A) – a small molecule that, upon entering a cell, is enzymatically converted into retinal by a retinol dehydrogenase –catalyzed reaction (zebrafish Rdh10a/b). The importance of this oxidation step is illustrated in the lethal Rdh10 mutant mouse, which elicits teratogenic defects characteristic of reduced RA (Sandell et al., 2007). Retinal is metabolized by aldehyde dehydrogenase enzymes (Aldh1a2, Aldh1a3 in zebrafish) to form the biologically active molecule, retinoic acid (RA). Typically, within a cell, RA is bound by a cytoplasmic protein partner that varies depending on cell type. After its synthesis RA can act in an autocrine, via diffusion, or paracrine fashion where it enters the nucleus and interacts with nuclear hormone receptor heterodimers: Retinoic Acid Receptor (RAR) – Retinoid-X Receptor (RXR) (Maden, 2002). Upon ligand activation, the complex binds Retinoic Acid Response Elements (RAREs) within control regions of responsive genes and activates transcription. Alternatively, through the action of cytochrome

p450 oxidase enzymes (Cyp26a1, Cyp26b1, Cyp26c1), RA is metabolized to more polar intermediates before being excreted.

During zebrafish somitogenesis stages and beyond, several synthesis and degradation enzymes are expressed which facilitates complex tissue-specific RA metabolism. For example, RA synthesis enzymes are present within the myotome (*aldh1a2*), ventral eye (*aldh1a2*), dorsal eye (*aldh1a3*), and cells surrounding the lens (*cyp1b1*) (Chambers et al., 2007; Thisse et al., 2004). RA degrading enzymes are expressed in various distinct and overlapping regions within the hindbrain (*cyp26b1* in r2-r3 boundary and within r4-r6, *cyp26c1* in r2-r6), forebrain (*cyp26b1* in the diencephalon, cerebellum, and MHB and *cyp26c1* in the diencephalon, telencephalon, otic vesticle) as well as the pharyngeal arches (*cyp26a1* and *cyp26c1*) and tailbud (*cyp26a1*) (White and Schilling, 2008).

Due to the large degree of redundancy between RA –metabolism genes during somitogenesis stages, RA metabolism during early stages of zebrafish embryogenesis is significantly simpler than later (Figure 1.3 B). During gastrulation, RA levels are regulated by two main enzymes: the anteriorly expressed RA-degrading enzyme Cyp26a1 and the posterior RA-synthesizing enzyme Aldh1a2. The activities of these enzymes produce a "source-and-sink" for RA during embryogenesis whereby higher levels of RA act in the presumptive posterior and lower levels in the anterior.

A popular theory regarding the action of RA in neural development is that it functions as a gradient where the level of RA at specific anterior-posterior locations determines cell identity. Support for this hypothesis is controversial as detection of a morphogen gradient *in vivo* is extremely difficult. Using microbeads to achieve localized increase in RA within transgenic zebrafish, White et al. (2007) demonstrated that RA is diffusible *in vivo* and can elicit long range positional cues. Treatment of chick embryos with sequentially increasing concentrations of pan-RAR-antagonist causes a sequential loss in rhombomeres (from posterior to anterior of the embryo) (Dupe and Lumsden, 2001). While this strongly supports a requirement for a

graded RA levels, instead of a global role it appears that the presumptive hindbrain (between *aldh1a2* and *cyp26a1* expression domains) is most susceptible to an RA gradient (Maden, 2002).

An alternative model of RA signaling states that RA levels within the hindbrain are regulated locally through the combinatorial action of Cyp26a1/b1/c1 degradation enzymes (Hernandez et al., 2007). This hypothesis is supported by the fact that VAD embryos are rescued with uniform exogenous RA treatment, and that *cyp26* genes have dynamic hindbrain expression during development. Additionally, in RARE-LacZ reporter mice there is no gradient detected within the hindbrain. Instead, distinct shifting boundaries of reporter expression are present, which supports regional RA regulation (Rossant et al., 1991; Sirbu et al., 2005). Likely, regulation of RA levels and signaling during embryogenesis exists as a combination of these models.

1.2.2 RA metabolism enzymes are crucial regulators of RA levels

After initial studies on the teratogenic effect of RA, studies in mouse, chick, and more recently zebrafish have focused on how RA levels are modulated during embryonic development. Aldh1a2/Raldh2 is the main RA synthesis enzyme, expressed within paraxial mesoderm during gastrulation and later within the somites. Therefore RA must diffuse to its main sites of action – the hindbrain and spinal cord (Begemann et al., 2001; Molotkova et al., 2005). The murine *Raldh2* mutant is embryonic lethal with defects in heart and limb formation as well as disruption of hindbrain segmentation. Within these mutants, hindbrain tissue is anteriorized such that posterior regions take on rhombomere 4 characteristics (Niederreither et al., 1999; Niederreither et al., 2000). These phenotypes are consistent with anterior expansion seen in VAD embryos. Conversely, the embryonic lethal *Cyp26a1* mutant has posterior expansion of hindbrain, mimicking excess RA (Sakai et al., 2001). Interestingly, these enzymes act to maintain a dynamic balance of RA levels, such that heterozygous disruption of *Raldh2* in a *Cyp26a1* mutant

mouse allows phenotypic rescue (Niederreither et al., 2002). Similarly, in Xenopus, *cyp26a1* over-expression causes an anterior expansion, concurrent with increased RA degradation (Hollemann et al., 1998).

The zebrafish *aldh1a2* mutant (*neckless*) has a surprisingly mild hindbrain phenotype, with minor alterations to the segmental pattern of rhombomeres and primary neurons originating at the hindbrain borders (Begemann et al., 2004). However, these embryos have severe defects in branchiomotor neuron development, with almost complete loss of vagal neurons within the posterior hindbrain and spinal cord (Begemann et al., 2004; Linville et al., 2004). The zebrafish *cyp26a1* mutant (*giraffe)* has relatively normal hindbrain patterning but exhibits a rostral expansion of the spinal cord whereby posterior tissues (including the vagal neurons) develop at the expense of hindbrain (Emoto et al., 2005). G*iraffe* embryos also have defects in lateral plate mesoderm causing incorrect formation of the cardinal vein and pectoral fin. Although considerable research has focused on the enzymatic regulation of RA itself, the factors responsible for initiation and maintenance of RA metabolism genes remain largely unknown.

1.2.3 Transcriptional mediators: RARs/RXRs

To mediate gene transcription, RA interacts with Retinoic-acid receptor (RAR) – Retinoid-X receptor (RXR) nuclear receptor heterodimers within the cell nucleus. While humans and mice have three RARs (α, β, and γ and three RXRs (α, β, and γ), zebrafish have ten receptors in total (four RARs: RARαa/b, RARγa/b; six RXRs: RXRαa/b, RXRβa/b, RXRγa/b). In response to ligand binding, RAR/RXR heterodimers act to recruit intermediary proteins, such as coactivators and chromatin remodelers, to activate RA-responsive gene transcription (Bastien and Rochette-Egly, 2004). In the absence of ligand, RAR:RXR dimers are capable of repressing gene transcription through the recruitment of co-repressors (Minucci and Pelicci, 1999). The vast array of nuclear receptors has made study difficult as they act combinatorally and

in a semi-redundant manner such that single gene knockout/knockdown has little or no phenotype (White and Schilling, 2008).

Single murine mutants, for example RARα or RXRβ, develop normally, while RARα/RXRβ double mutants have eye, skull, heart, and urogenital abnormalities but lack defects in craniofacial and limb development (Lohnes et al., 1994; Mendelsohn et al., 1994). While creation of double mutants is often necessary to obtain defects, these often recapitulate only some aspects of VAD. This suggests that specific RAR:RXR pairs may function within different tissues. However, universal blockage of retinoid receptors using a pan-RAR-antagonist mimics VAD, such that the hindbrain of chick embryos is anteriorized with the posterior hindbrain adopting r4 identity (Dupe and Lumsden, 2001). Additionally, a dominant negative retinoic acid receptor causes anteriorization of posterior rhombomeres in Xenopus (Blumberg et al., 1997; Kolm et al., 1997).

1.2.4 RA regulates *hox* genes in hindbrain segmentation

The relationship between RA and *hox* genes was first discovered in cell culture experiments, where posteriorly expressed *Hox* genes are activated at higher RA concentrations than anterior *Hox* genes (Papalopulu et al., 1991; Simeone et al., 1990; Simeone et al., 1991). Since then, hindbrain segmentation defects associated with VAD embryos have been attributed to RA alterations to *hox* gene expression. Experiments using a pan-RAR-antagonist within chick embryos show that increasing the amounts of RA allow sequential specification of posterior rhombomeres (Dupe and Lumsden, 2001), with similar results found in mouse (Wendling et al., 2001). RA treatment in developing mice causes ectopic *Hoxa2* expression, such that anterior hindbrain segments are altered to an r4 fate (Conlon and Rossant, 1992). In fact, RA is required for initiation of *Hoxa1* and *Hoxb1* transcription within rhombomere 4 (Gavalas et al., 1998; Studer et al., 1998). Alterations to RA signaling levels by altering RA itself, knockdown of synthesis and

degradation enzymes, manipulation of receptor levels, and pharmacological treatments all display a range of hindbrain defects reminiscent of alterations to *hox* (Alexander et al., 2009). This is a direct regulation through RARE elements located within many *Hox* enhancer regions, including murine *Hoxa1, Hoxb1, Hoxa4, Hoxb4*, and *Hoxd4* (Alexander et al., 2009; Studer et al., 1998; Zhang et al., 2000).

1.2.5 RA functions during neurogenesis

RA is thought to act upstream of nearly all neural developmental stages (patterning, neurogenic and differentiation genes) (Franco et al., 1999). Within Xenopus and teleost fish, RA regulates primary neuron development such that increasing RA through exogenous treatment or receptor over-expression increases neuron number (Sharpe and Goldstone, 2000). RA also promotes neural cell fates by upregulating prepattern and neurogenic genes (such as, XNgnr1 and Xdelta1) and downregulating inhibitors of neurogenesis (Zic2, Xshh) (Franco et al., 1999; Papalopulu and Kintner, 1996).

Additionally, RA also promotes neural differentiation. In chick, Raldh2-derived RA from the somites is required for formation of somatic motor neurons in rhombomeres 5-8 as well as lateral motor columns of the spinal cord (Guidato et al., 2003; Swindell et al., 1999). The lateral motor column neurons are located near the hindlimb and are responsible for innervating the limb muscles. Interestingly, later in development, the brachial and lumbar motor neurons themselves synthesize RA through *Raldh2* expression (Sockanathan and Jessell, 1998). Using viral-induced over-expression of *Raldh2*, ectopic motor neurons form implicating the paracrine action of RA in maintenance of spinal neural populations (Ji et al., 2006; Sockanathan and Jessell, 1998). Finally, transplantation of wild-type cells into paraxial mesoderm of *aldh1a2* mutant zebrafish (*neckless*) rescues the branchiomotor neuron defects (Linville et al., 2004). This suggests that

the role of RA in hindbrain patterning and neural differentiation is at least partially separable.

1.2.6 Mechanisms of feedback regulation

RA signaling is a complex pathway with multiple levels of feedback regulation that allow an embryo to compensate for alterations in RA levels. RA can facilitate its own response by upregulating RARs, specifically RARβ (Dobbs-McAuliffe et al., 2004; Niederreither et al., 1997). In addition, RA negatively regulates its own synthesis by repressing *aldh1a2* and similarly, RA facilitates its own degradation by upregulating *cyp26a1* (Hu et al., 2008). Interestingly, some degradation metabolites can themselves activate RAR (Pijnappel et al., 1993).

Recently, essential retinol-independent mechanisms of RA synthesis and signaling have been identified (White and Schilling, 2008). For example, the beta-carotene pathway (catalyzed by beta-carotene 15,15'-monooxygenase 1; Bcox) provides an alternative source of RA via breakdown of beta-carotene stored within the egg (Lampert et al., 2003). Zebrafish morpholino-mediated knockdown of carotene oxygenase causes severe defects within the eyes, pectoral fins, and in cranial facial development - defects characteristic of reduced RA (Niederreither and Dolle, 2008). The existence of multiple independent sources of RA, in addition to feedback regulation of metabolism genes, further emphasizes the importance of maintaining RA levels during development.

1.3 Zinc Finger of the Cerebellum transcription factor family

Zinc Finger of the Cerebellum (Zic) transcription factors were originally identified in the murine cerebellum (Aruga et al., 1994; Yokota et al., 1996). Since then, Zics have been studied in a variety of developmental processes including neural development, myogenesis, cell proliferation, left-right symmetry, and neural crest development (Aruga, 2004).

1.3.1 Zic evolution and protein structure

Zic transcription factors are evolutionarily related to the Drosophila pair-rule gene, *Odd-paired* (*Opa*) – a transcription factor which functions to specify cell fates via interaction with other transcription factors (Benedyk et al., 1994). Evolutionarily, Zics appear to have emerged from a single ancestral gene to form the three ZICs in humans (*ZIC1-3*), five in mice (*Zic1-5*), four in Xenopus (*Zic1-3, 5*), and seven in zebrafish (*zic1/2a/2b/3/4/5/6*). Zic family members are highly conserved across species (~90% amino acid similarity between humans and zebrafish) with higher conservation within their DNA binding domain. Phylogenetic comparison of amino acid sequences shows that Zic2 and Zic3 are most closely related, followed by Zic1 (Figure 1.4 A). Interestingly, as a result of gene duplication, there is a teleost fish specific *zic6* (Keller and Chitnis, 2007). The overall Zic protein structure is characteristic of zinc finger transcription factors containing five tandem C2H2-zinc finger domains at the C-terminal end, which function in DNA binding and protein-protein interaction (Figure 1.4 B) (Koyabu et al., 2001). Other recognizable motifs include an N-terminal transcriptional regulatory ZOC domain (highly conserved Zic-Opa domain) and several single amino acid stretches (an N-terminal poly-alanine and C-terminal poly-glycine region) (Mizugishi et al., 2001).

Chromosomally, *zic* genes are arranged together such that *zic1* and *zic4*, and *zic2* (*zic2a* in zebrafish) and *zic5* are arrayed head to head (Aruga, 2004). The likely sharing of cis-regulatory elements between closely arrayed genes suggests some degree of functional redundancy or compensation between these genes.

1.3.2 Zic family expression patterns

Within vertebrates Zics are expressed in partially overlapping regions indicative of a role in neural development, with distinct regional and temporal regulation. Murine *Zics* are regionally expressed at gastrulation within embryonic mesoderm and neuroectoderm, with *Zic2* enriched in the

headfold region (Merzdorf, 2007). Later in development, *Zic* expression becomes more restricted within the brain, neural tube and trunk. *Zic1/2/4* are broadly expressed in these regions and *Zic5* is notably reduced in trunk tissue and upregulated in the limb buds (Merzdorf, 2007). Interestingly, *Zic3* expression is limited to regions of the brain with little expression in posterior tissues (Nagai et al., 1997). During later organogenesis, these genes are expressed in specialized portions of the brain, spinal cord, retina, and limb buds.

Similarly, zebrafish *zic1/4*, *zic2a/5*, *zic2b*, and *zic3* are initiated by the end of gastrulation in presumptive dorsal tissue and are expressed in remarkably similar domains through somitogenesis. These six genes become localized within the dorsal neural tube, including regions of the forebrain, midbrain, hindbrain and spinal cord – with distinct but overlapping regions. Regions of variation include *zic1/4* enrichment in regions of the forebrain, while *zic2a/5* are expressed within the ventral eye and MHB (Nyholm et al., 2007; Thisse et al., 2004). These expression regions are highly conserved within Xenopus, with *zic5* initiation observed notably later (Aruga, 2004). Expression of teleost specific *zic6* varies significantly from other *zics*, within two small populations of neuroectodermal cells. *zic6* expression is subsequently restricted to two populations of prospective neurogenic cells at the lateral edge of the neural plate (Keller and Chitnis, 2007).

1.3.3 Zic transcription factors in neural development

In concordance with their neural expression, the role of Zics has predominantly been studied in development of the nervous system. Human and murine Zic1 were first identified within the cerebellum; subsequently studies identified a requirement for *Zic1*, *Zic2*, and *Zic3* in cerebellar morphogenesis (Aruga, 2004; Aruga et al., 2002a; Aruga et al., 1998; Nagai et al., 1997). Loss of *Zic1/2/3* causes incorrect formation of cerebellum lobulations due to reduced cerebellar cell proliferation. In fact, human *ZIC1/4* mutations are associated with Dandy-Walker malformation, a defect

characterized by reduced cerebellar size resulting from defective granule cell proliferation (Blank et al., 2011).

All known mutations in murine *Zics* result in some degree of neural tube defects with inadequate neural tube closure at the forebrain in *Zic2* and *Zic5* mutants and the hindbrain in *Zic3* mutants (Aruga et al., 2002a; Klootwijk et al., 2000; Nagai et al., 1997). Mutation in human *ZIC2* causes the most common congenital forebrain defect, Holoprosencephaly (HPE), characterized by incomplete division of cerebral hemispheres and facial deformities (Brown et al., 1998). Notably, the murine *Zic2* mutant has defective neural crest development and hindbrain patterning, in addition to neural tube defects. In this case, *Zic2* is required for maintenance of rhombomere 3 and 5, but not the initial formation of this region (Elms et al., 2003). Human and mouse *Zic3* mutants exhibit left-right symmetry defects associated with X-linked heterotaxy (Grinberg and Millen, 2005).

Zic transcription factors are expressed within the dorsal embryo during specification of neural ectoderm in gastrulation. Over-expression of Xenopus *Zic1-3*, and *Zic5* induces both neural crest and anterior neural markers (Brewster et al., 1998; Mizuseki et al., 1998; Nakata et al., 1997). Interestingly, BMP inhibition is sufficient to induce neural induction and *Zic3* expression is limited by BMPs (Nakata et al., 1997; Yamamoto et al., 2000). These data implicate a possible regulatory mechanism whereby *Zics* aid in neural induction.

Neurogenic regions are established in alternating longitudinal stripes by proneural factors that activate or repress neurogenesis. *Zic2* is one such factor that has been studied in defining neurogenic regions during Xenopus primary neurogenesis (Brewster et al., 1998). *Zic2*, expressed in alternating stripes with Gli transcription factors, represses neural differentiation by restricting expression of *Xneurog1* (Brewster et al., 1998; Franco et al., 1999).

In zebrafish, studies have focused predominantly on the role of Zics in forebrain patterning, ventricular morphogenesis and cell proliferation. Morpholino-mediated depletion of Zic2a causes specific defects within the

prethalamic region of the diencephalon (Sanek and Grinblat, 2008). *zic2a* and *six3*, expressed in neighboring regions of the forebrain, are both activated by Shh (Sanek et al., 2009). Interestingly, in prethalamus formation, *zic2a* acts in a non-cell-autonomous manner to limit *six3* expression (Sanek et al., 2009). Human mutations in *SHH*, *SIX3*, and *ZIC2* all result in HPE; suggesting that forebrain defects may result from disruption of a regulatory mechanism between these genes (Dubourg et al., 2004). The chromosomally linked pair, *zic1* and *zic4*, act together in hindbrain ventricular morphogenesis whereby *zic1/4* knockdown prevents ventricle opening and reduces cell proliferation within the dorsal hindbrain (Elsen et al., 2008). Another chromosomally linked pair, *zic2a* and *zic5*, act downstream of Wnt signaling and are required for cell proliferation within the midbrain (Nyholm et al., 2007). Although zebrafish Zics are expressed very early in development, their role in neural induction or their potential as regulators of neural cell fates has yet to be investigated.

1.3.4 Zics, members of the Gli transcription factor superfamily

Zics are members of the Gli (human glioma) superfamily of transcription factors. Glis are most commonly known for their role as transcriptional mediators of Shh signaling, acting both as activators and repressors of target genes (Koebernick and Pieler, 2002). Structurally, Glis, like Zics, have 5 tandem zinc finger domains that are involved in DNA binding (Koyabu et al., 2001). In fact, Zics and Glis can bind each other via their zinc finger domains *in vitro* and are able to modulate each other's transcriptional activity. Functionally, Glis can be translocated into the nucleus by co-expressed Zics in cell culture (Koyabu et al., 2001). Due to strong similarity within their DNA binding domains, Zics are able to bind the same regulatory sequence as Glis, a nonamer sequence 5'-TGGGTGGTC-3', in gel shift assays, albeit at a lower affinity (Aruga, 2004; Aruga et al., 1994). When expressed together Zics and Glis synergistically enhance or mutually repress transcription, depending on the cell type (Koyabu et al., 2001). Interestingly,

the activation and repression actions of Glis are controlled by proteolytic processing and by subcellular localization – implicating a potential functional interaction between Glis and co-expressed Zics to mediate Shh signaling *in vivo.*

While there are many regions of co- or neighboring expression, there is little evidence that Zics and Glis function together. Within zebrafish both Zics (*zic2a*) and Shh signaling (mediated by Glis) are important for prethalamus development, however they act in parallel pathways (Sanek et al., 2009). In murine forebrain development, Gli3 and Zic2 could be an important mechanism in defining regions of Shh signaling by modulating each other's activity, however direct evidence for this is lacking. As mentioned previously, Zic2 and Glis oppose each other's function during Xenopus neurogenesis, but transcriptional opposition has yet to be shown (Brewster et al., 1998). However, Shh over-expression reduces Zic transcript levels within the dorsal neural tube of zebrafish and chick (Aruga et al., 2002b; Rohr et al., 1999). Moreover, Zic2 expression extends throughout the neural tube in Shh mutant mice (Brown et al., 2003). This provides a potential mechanism for Zic expression within the spinal cord – resulting from positive regulation by dorsal (BMP) factors and negative regulation by ventral (Shh) factors.

1.4 Zic2a2b and RA metabolism

The role and requirement of RA metabolism genes in regulating RA levels during embryogenesis has been extensively studied in many model organisms, however the factors acting to initiate and maintain expression of these genes remain largely unknown. Zic transcription factors function in several stages of neural developmental including formation of the neural tube and defining neurogenic cell populations. However, the role of zebrafish Zics in early neural induction has yet to be investigated. There is some evidence suggesting a connection between Zic transcription factors and the RA signaling pathway: first, previous work in our lab has identified a link

between Holoprosencephaly and aberrant RA signaling (Gongal and Waskiewicz, 2008). Second, Maurus and Harris (2009) identified a regulatory interaction between Zic1 and RA-degradation enzyme, *cyp26a1*, at zebrafish somitogenesis stages. Interestingly, during development of the forebrain, *zic2a* functions in a cell-non-autonomous fashion; this suggests that Zic2a acts through an extracellular or secreted signaling molecule. We provide evidence that during zebrafish neural development, this secreted molecule acts upstream of RA and present a novel regulatory interaction between Zic2a2b transcription factors and the RA synthesizing gene, *aldh1a2*.

‘

1.5 Figures

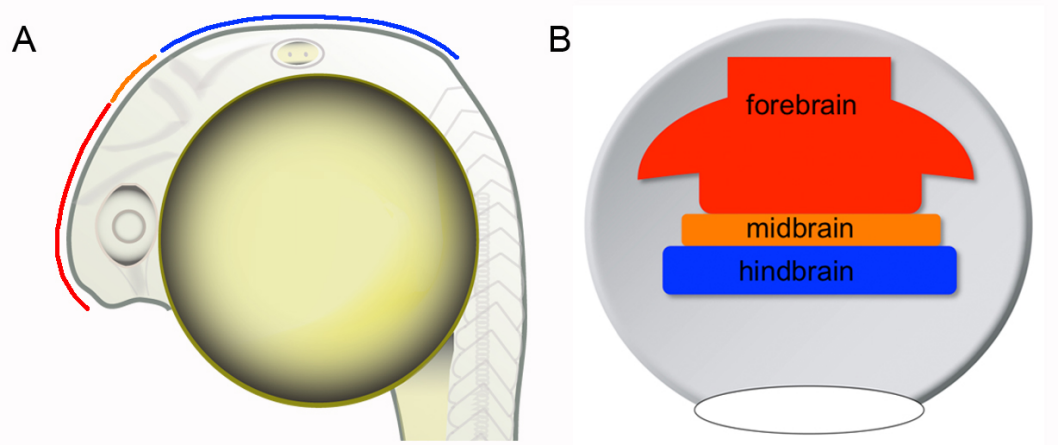

Figure 1.1: Regionalization of the zebrafish neural tube during development.

Fate map studies have determined that the overall architecture of the nervous system (26hpf; A) is present by the end of gastrulation (75% epiboly; B) such that the presumptive forebrain (red), midbrain (orange), and hindbrain (blue) are in correct anterior-posterior locations.

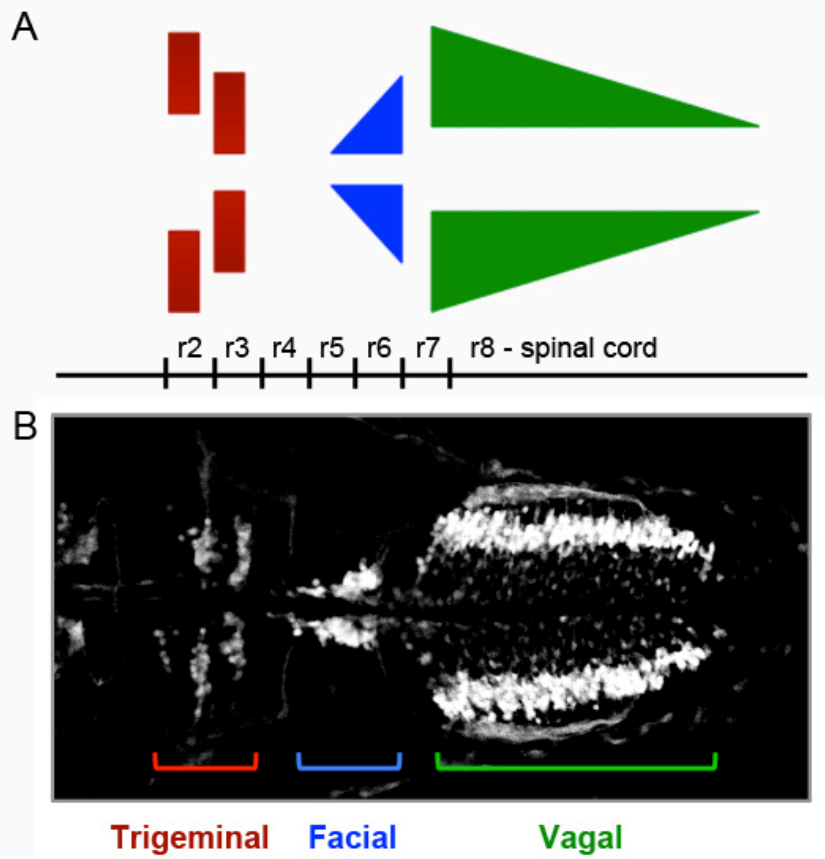

Figure 1.2: Branchiomotor neurons arise in a segment-specific manner.

Specific classes of branchiomotor neurons are born within characteristic hindbrain rhombomeres (r). (A) Diagram showing trigeminal motor neurons within r2/3 (red), facial motor neurons in r5/6 (blue), and vagal motor neurons in the posterior HB extending down the spinal cord (green). The *islet1:gfp* transgenic zebrafish allows visualization of these neurons by fluorescent microscopy (B; 48hpf; dorsal view).

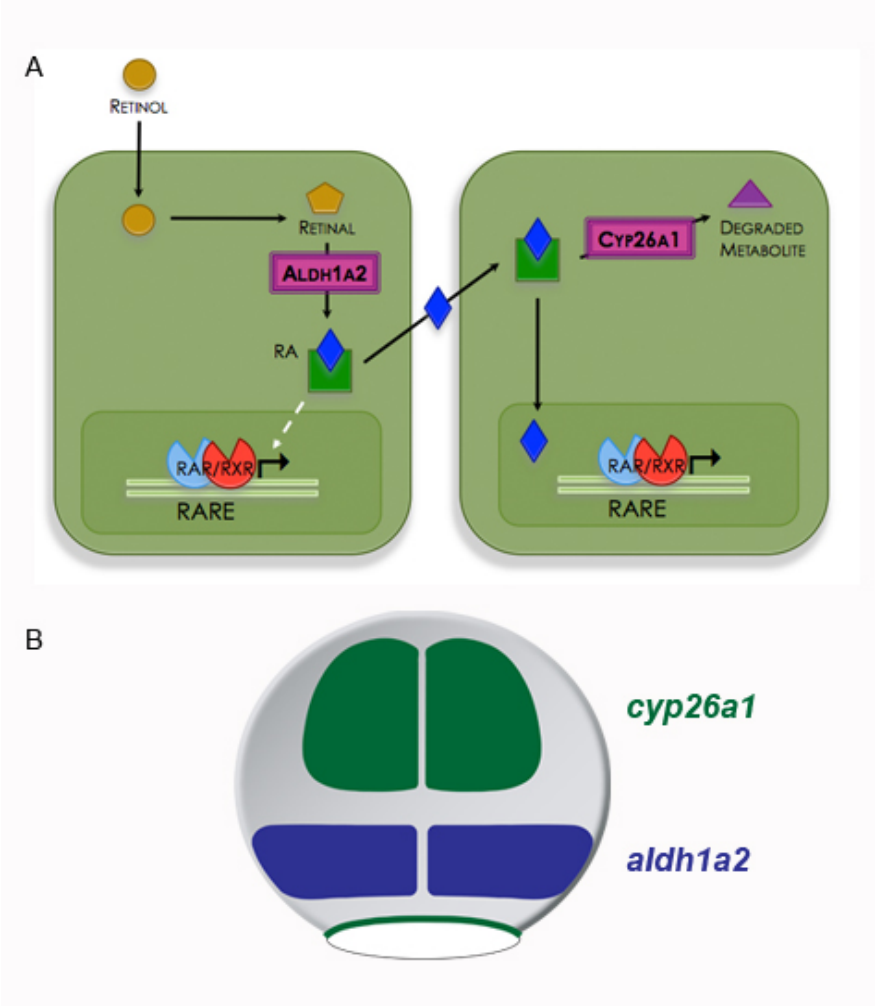

Figure 1.3: Retinoic acid signaling in early zebrafish development.

Retinol (Vitamin A; beige circle) enters into a cell where enzymes of the retinol dehydrogenase family (Rdh10a/b) act to convert it into retinal. Retinal is acted on by aldehyde dehydrogenase enzymes (Aldh1a2) and converted into the active metabolite, retinoic acid (RA; blue diamond). RA is bound by a cytoplasmic protein partner (green square) and can act within its cell of synthesis or diffuse to neighboring cells. In the nucleus, RA interacts with Retinoic Acid Receptor (RAR): Retinoid-X Receptor (RXR) heterodimer nuclear proteins to activate gene transcription via Retinoic Acid Response Elements (RAREs) within DNA (A). At 75% epiboly RA metabolism enzymes are expressed in regionally restricted domains – *cyp26a1* (green) is expressed anteriorly and *aldh1a2* (blue) within the lateral mesoderm (B).

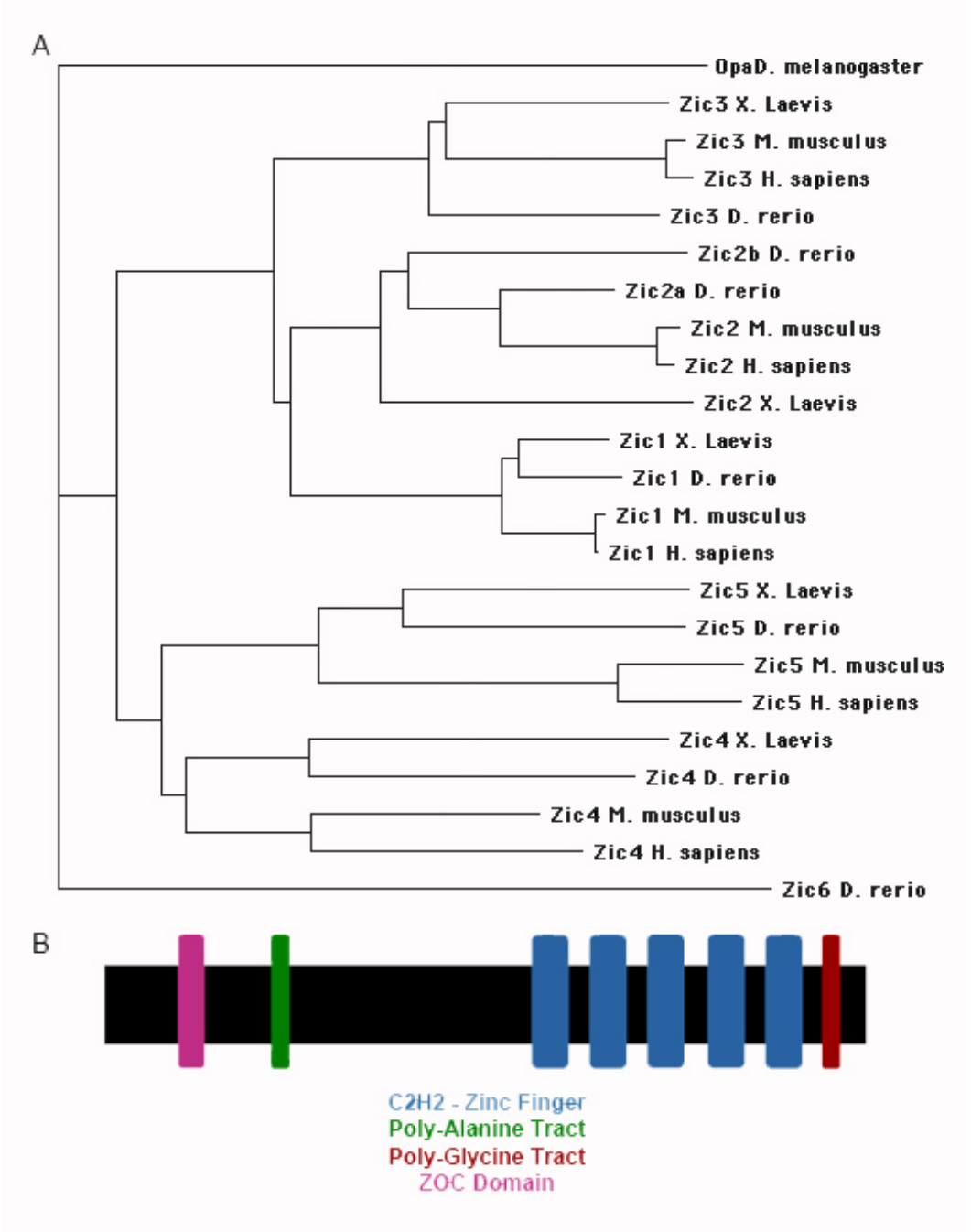

Figure 1.4: Zic transcription factor phylogenetic tree and protein motifs.

Phylogenetic tree compares amino acid sequences of Zics in zebrafish, mouse, human, frog, and drosophila (A). All Zics have similar protein structure with five C2H2-zinc finger domains (blue rectangles), an N-terminal ZOC domain (Zic-Opa conserved domain; pink rectangle) and poly-alanine tract (green rectangle) and C-terminal poly-glycine tract (B; red rectangle).

1.6 Literature Cited

Alexander, T., Nolte, C., and Krumlauf, R. (2009). Hox genes and segmentation of the hindbrain and axial skeleton. Annu Rev Cell Dev Biol *25*, 431-456.

Amaya, E., Musci, T.J., and Kirschner, M.W. (1991). Expression of a dominant negative mutant of the FGF receptor disrupts mesoderm formation in Xenopus embryos. Cell *66*, 257-270.

Appel, B. (2000). Zebrafish neural induction and patterning. Dev Dyn *219*, 155-168.

Aruga, J. (2004). The role of Zic genes in neural development. Mol Cell Neurosci *26*, 205-221.

Aruga, J., Inoue, T., Hoshino, J., and Mikoshiba, K. (2002a). Zic2 controls cerebellar development in cooperation with Zic1. J Neurosci *22*, 218-225.

Aruga, J., Minowa, O., Yaginuma, H., Kuno, J., Nagai, T., Noda, T., and Mikoshiba, K. (1998). Mouse Zic1 is involved in cerebellar development. J Neurosci *18*, 284-293.

Aruga, J., Tohmonda, T., Homma, S., and Mikoshiba, K. (2002b). Zic1 promotes the expansion of dorsal neural progenitors in spinal cord by inhibiting neuronal differentiation. Dev Biol *244*, 329-341.

Aruga, J., Yokota, N., Hashimoto, M., Furuichi, T., Fukuda, M., and Mikoshiba, K. (1994). A novel zinc finger protein, zic, is involved in neurogenesis, especially in the cell lineage of cerebellar granule cells. J Neurochem *63*, 1880-1890.

Bastien, J., and Rochette-Egly, C. (2004). Nuclear retinoid receptors and the transcription of retinoid-target genes. Gene *328*, 1-16.

Beattie, C.E., Hatta, K., Halpern, M.E., Liu, H., Eisen, J.S., and Kimmel, C.B. (1997). Temporal separation in the specification of primary and secondary motoneurons in zebrafish. Dev Biol *187*, 171-182.

Begemann, G., Marx, M., Mebus, K., Meyer, A., and Bastmeyer, M. (2004). Beyond the neckless phenotype: influence of reduced retinoic acid signaling on motor neuron development in the zebrafish hindbrain. Dev Biol *271*, 119-129.

Begemann, G., Schilling, T.F., Rauch, G.J., Geisler, R., and Ingham, P.W. (2001). The zebrafish neckless mutation reveals a requirement for raldh2 in mesodermal signals that pattern the hindbrain. Development *128*, 3081-3094.

Bell, E., Wingate, R.J., and Lumsden, A. (1999). Homeotic transformation of rhombomere identity after localized Hoxb1 misexpression. Science *284*, 2168-2171.

Benedyk, M.J., Mullen, J.R., and DiNardo, S. (1994). odd-paired: a zinc finger pair-rule protein required for the timely activation of engrailed and wingless in Drosophila embryos. Genes Dev *8*, 105-117.

Bingham, S., Nasevicius, A., Ekker, S.C., and Chandrasekhar, A. (2001). Sonic hedgehog and tiggy-winkle hedgehog cooperatively induce zebrafish branchiomotor neurons. Genesis *30*, 170-174.

Blader, P., and Strahle, U. (2000). Zebrafish developmental genetics and central nervous system development. Hum Mol Genet *9*, 945-951.

Blank, M.C., Grinberg, I., Aryee, E., Laliberte, C., Chizhikov, V.V., Henkelman, R.M., and Millen, K.J. (2011). Multiple developmental programs are altered by loss of Zic1 and Zic4 to cause Dandy-Walker malformation cerebellar pathogenesis. Development *138*, 1207-1216.

Blumberg, B., Bolado, J., Jr., Moreno, T.A., Kintner, C., Evans, R.M., and Papalopulu, N. (1997). An essential role for retinoid signaling in anteroposterior neural patterning. Development *124*, 373-379.

Brewster, R., Lee, J., and Ruiz i Altaba, A. (1998). Gli/Zic factors pattern the neural plate by defining domains of cell differentiation. Nature *393*, 579-583.

Brown, L.Y., Kottmann, A.H., and Brown, S. (2003). Immunolocalization of Zic2 expression in the developing mouse forebrain. Gene Expr Patterns *3*, 361-367.

Brown, S.A., Warburton, D., Brown, L.Y., Yu, C.Y., Roeder, E.R., Stengel-Rutkowski, S., Hennekam, R.C., and Muenke, M. (1998). Holoprosencephaly

due to mutations in ZIC2, a homologue of Drosophila odd-paired. Nat Genet *20*, 180-183.

Chambers, D., Wilson, L., Maden, M., and Lumsden, A. (2007). RALDH-independent generation of retinoic acid during vertebrate embryogenesis by CYP1B1. Development *134*, 1369-1383.

Chandrasekhar, A. (2004). Turning heads: development of vertebrate branchiomotor neurons. Dev Dyn *229*, 143-161.

Chandrasekhar, A., Moens, C.B., Warren, J.T., Jr., Kimmel, C.B., and Kuwada, J.Y. (1997). Development of branchiomotor neurons in zebrafish. Development *124*, 2633-2644.

Chiang, C., Litingtung, Y., Lee, E., Young, K.E., Corden, J.L., Westphal, H., and Beachy, P.A. (1996). Cyclopia and defective axial patterning in mice lacking Sonic hedgehog gene function. Nature *383*, 407-413.

Chitnis, A., Henrique, D., Lewis, J., Ish-Horowicz, D., and Kintner, C. (1995). Primary neurogenesis in Xenopus embryos regulated by a homologue of the Drosophila neurogenic gene Delta. Nature *375*, 761-766.

Conlon, R.A., and Rossant, J. (1992). Exogenous retinoic acid rapidly induces anterior ectopic expression of murine Hox-2 genes in vivo. Development *116*, 357-368.

Diez del Corral, R., and Storey, K.G. (2001). Markers in vertebrate neurogenesis. Nat Rev Neurosci *2*, 835-839.

Dobbs-McAuliffe, B., Zhao, Q., and Linney, E. (2004). Feedback mechanisms regulate retinoic acid production and degradation in the zebrafish embryo. Mech Dev *121*, 339-350.

Draper, B.W., Stock, D.W., and Kimmel, C.B. (2003). Zebrafish fgf24 functions with fgf8 to promote posterior mesodermal development. Development *130*, 4639-4654.

Dubourg, C., Lazaro, L., Pasquier, L., Bendavid, C., Blayau, M., Le Duff, F., Durou, M.R., Odent, S., and David, V. (2004). Molecular screening of SHH, ZIC2, SIX3, and TGIF genes in patients with features of holoprosencephaly

spectrum: Mutation review and genotype-phenotype correlations. Hum Mutat *24*, 43-51.

Dupe, V., and Lumsden, A. (2001). Hindbrain patterning involves graded responses to retinoic acid signalling. Development *128*, 2199-2208.

Durston, A.J., Timmermans, J.P., Hage, W.J., Hendriks, H.F., de Vries, N.J., Heideveld, M., and Nieuwkoop, P.D. (1989). Retinoic acid causes an anteroposterior transformation in the developing central nervous system. Nature *340*, 140-144.

Elms, P., Siggers, P., Napper, D., Greenfield, A., and Arkell, R. (2003). Zic2 is required for neural crest formation and hindbrain patterning during mouse development. Dev Biol *264*, 391-406.

Elsen, G.E., Choi, L.Y., Millen, K.J., Grinblat, Y., and Prince, V.E. (2008). Zic1 and Zic4 regulate zebrafish roof plate specification and hindbrain ventricle morphogenesis. Dev Biol *314*, 376-392.

Emoto, Y., Wada, H., Okamoto, H., Kudo, A., and Imai, Y. (2005). Retinoic acid-metabolizing enzyme Cyp26a1 is essential for determining territories of hindbrain and spinal cord in zebrafish. Dev Biol *278*, 415-427.

Fekany, K., Yamanaka, Y., Leung, T., Sirotkin, H.I., Topczewski, J., Gates, M.A., Hibi, M., Renucci, A., Stemple, D., Radbill, A.*, et al.* (1999). The zebrafish bozozok locus encodes Dharma, a homeodomain protein essential for induction of gastrula organizer and dorsoanterior embryonic structures. Development *126*, 1427-1438.

Franco, P.G., Paganelli, A.R., Lopez, S.L., and Carrasco, A.E. (1999). Functional association of retinoic acid and hedgehog signaling in Xenopus primary neurogenesis. Development *126*, 4257-4265.

Gale, E., Zile, M., and Maden, M. (1999). Hindbrain respecification in the retinoid-deficient quail. Mech Dev *89*, 43-54.

Gavalas, A., Studer, M., Lumsden, A., Rijli, F.M., Krumlauf, R., and Chambon, P. (1998). Hoxa1 and Hoxb1 synergize in patterning the hindbrain, cranial nerves and second pharyngeal arch. Development *125*, 1123-1136.

Glover, J.C., Renaud, J.S., and Rijli, F.M. (2006). Retinoic acid and hindbrain patterning. J Neurobiol *66*, 705-725.

Gongal, P.A., and Waskiewicz, A.J. (2008). Zebrafish model of holoprosencephaly demonstrates a key role for TGIF in regulating retinoic acid metabolism. Hum Mol Genet *17*, 525-538.

Griffin, K., Patient, R., and Holder, N. (1995). Analysis of FGF function in normal and no tail zebrafish embryos reveals separate mechanisms for formation of the trunk and the tail. Development *121*, 2983-2994.

Griffin, K.J., and Kimelman, D. (2003). Interplay between FGF, one-eyed pinhead, and T-box transcription factors during zebrafish posterior development. Dev Biol *264*, 456-466.

Grinberg, I., and Millen, K.J. (2005). The ZIC gene family in development and disease. Clin Genet *67*, 290-296.

Grinblat, Y., Gamse, J., Patel, M., and Sive, H. (1998). Determination of the zebrafish forebrain: induction and patterning. Development *125*, 4403-4416.

Guidato, S., Prin, F., and Guthrie, S. (2003). Somatic motoneurone specification in the hindbrain: the influence of somite-derived signals, retinoic acid and Hoxa3. Development *130*, 2981-2996.

Hernandez, R.E., Putzke, A.P., Myers, J.P., Margaretha, L., and Moens, C.B. (2007). Cyp26 enzymes generate the retinoic acid response pattern necessary for hindbrain development. Development *134*, 177-187.

Higashijima, S., Hotta, Y., and Okamoto, H. (2000). Visualization of cranial motor neurons in live transgenic zebrafish expressing green fluorescent protein under the control of the islet-1 promoter/enhancer. J Neurosci *20*, 206-218.

Holder, N., and Hill, J. (1991). Retinoic acid modifies development of the midbrain-hindbrain border and affects cranial ganglion formation in zebrafish embryos. Development *113*, 1159-1170.

Hollemann, T., Chen, Y., Grunz, H., and Pieler, T. (1998). Regionalized metabolic activity establishes boundaries of retinoic acid signalling. EMBO J *17*, 7361-7372.

Hu, P., Tian, M., Bao, J., Xing, G., Gu, X., Gao, X., Linney, E., and Zhao, Q. (2008). Retinoid regulation of the zebrafish cyp26a1 promoter. Dev Dyn *237*, 3798-3808.

Ji, S.J., Zhuang, B., Falco, C., Schneider, A., Schuster-Gossler, K., Gossler, A., and Sockanathan, S. (2006). Mesodermal and neuronal retinoids regulate the induction and maintenance of limb innervating spinal motor neurons. Dev Biol *297*, 249-261.

Keller, M.J., and Chitnis, A.B. (2007). Insights into the evolutionary history of the vertebrate zic3 locus from a teleost-specific zic6 gene in the zebrafish, Danio rerio. Dev Genes Evol *217*, 541-547.

Keller, R. (1991). Early embryonic development of Xenopus laevis. Methods Cell Biol *36*, 61-113.

Keller, R.E. (1975). Vital dye mapping of the gastrula and neurula of Xenopus laevis. I. Prospective areas and morphogenetic movements of the superficial layer. Dev Biol *42*, 222-241.

Keller, R.E. (1976). Vital dye mapping of the gastrula and neurula of Xenopus laevis. II. Prospective areas and morphogenetic movements of the deep layer. Dev Biol *51*, 118-137.

Kim, C.H., Oda, T., Itoh, M., Jiang, D., Artinger, K.B., Chandrasekharappa, S.C., Driever, W., and Chitnis, A.B. (2000). Repressor activity of Headless/Tcf3 is essential for vertebrate head formation. Nature *407*, 913-916.

Kimmel, C.B., Warga, R.M., and Schilling, T.F. (1990). Origin and organization of the zebrafish fate map. Development *108*, 581-594.

Klootwijk, R., Franke, B., van der Zee, C.E., de Boer, R.T., Wilms, W., Hol, F.A., and Mariman, E.C. (2000). A deletion encompassing Zic3 in bent tail, a mouse model for X-linked neural tube defects. Hum Mol Genet *9*, 1615-1622.

Koebernick, K., and Pieler, T. (2002). Gli-type zinc finger proteins as bipotential transducers of Hedgehog signaling. Differentiation *70*, 69-76.

Kolm, P.J., Apekin, V., and Sive, H. (1997). Xenopus hindbrain patterning requires retinoid signaling. Dev Biol *192*, 1-16.

Koshida, S., Shinya, M., Mizuno, T., Kuroiwa, A., and Takeda, H. (1998). Initial anteroposterior pattern of the zebrafish central nervous system is determined by differential competence of the epiblast. Development *125*, 1957-1966.

Koyabu, Y., Nakata, K., Mizugishi, K., Aruga, J., and Mikoshiba, K. (2001). Physical and functional interactions between Zic and Gli proteins. J Biol Chem *276*, 6889-6892.

Kudoh, T., Wilson, S.W., and Dawid, I.B. (2002). Distinct roles for Fgf, Wnt and retinoic acid in posteriorizing the neural ectoderm. Development *129*, 4335-4346.

Lampert, J.M., Holzschuh, J., Hessel, S., Driever, W., Vogt, K., and von Lintig, J. (2003). Provitamin A conversion to retinal via the beta,beta-carotene-15,15'-oxygenase (bcox) is essential for pattern formation and differentiation during zebrafish embryogenesis. Development *130*, 2173-2186.

Lee, J.E., Hollenberg, S.M., Snider, L., Turner, D.L., Lipnick, N., and Weintraub, H. (1995). Conversion of Xenopus ectoderm into neurons by NeuroD, a basic helix-loop-helix protein. Science *268*, 836-844.

Lekven, A.C., Thorpe, C.J., Waxman, J.S., and Moon, R.T. (2001). Zebrafish wnt8 encodes two wnt8 proteins on a bicistronic transcript and is required for mesoderm and neurectoderm patterning. Dev Cell *1*, 103-114.

Lewis, E.B. (1978). A gene complex controlling segmentation in Drosophila. Nature *276*, 565-570.

Linville, A., Gumusaneli, E., Chandraratna, R.A., and Schilling, T.F. (2004). Independent roles for retinoic acid in segmentation and neuronal differentiation in the zebrafish hindbrain. Dev Biol *270*, 186-199.

Lohnes, D., Mark, M., Mendelsohn, C., Dolle, P., Dierich, A., Gorry, P., Gansmuller, A., and Chambon, P. (1994). Function of the retinoic acid receptors (RARs) during development (I). Craniofacial and skeletal abnormalities in RAR double mutants. Development *120*, 2723-2748.

Londin, E.R., Niemiec, J., and Sirotkin, H.I. (2005). Chordin, FGF signaling, and mesodermal factors cooperate in zebrafish neural induction. Dev Biol *279*, 1-19.

Ma, Q., Kintner, C., and Anderson, D.J. (1996). Identification of neurogenin, a vertebrate neuronal determination gene. Cell *87*, 43-52.

Maden, M. (2002). Retinoid signalling in the development of the central nervous system. Nat Rev Neurosci *3*, 843-853.

Maden, M. (2007). Retinoic acid in the development, regeneration and maintenance of the nervous system. Nat Rev Neurosci *8*, 755-765.

Mark, M., Lufkin, T., Vonesch, J.L., Ruberte, E., Olivo, J.C., Dolle, P., Gorry, P., Lumsden, A., and Chambon, P. (1993). Two rhombomeres are altered in Hoxa-1 mutant mice. Development *119*, 319-338.

Maurus, D., and Harris, W.A. (2009). Zic-associated holoprosencephaly: zebrafish Zic1 controls midline formation and forebrain patterning by regulating Nodal, Hedgehog, and retinoic acid signaling. Genes Dev *23*, 1461-1473.

Mendelsohn, C., Lohnes, D., Decimo, D., Lufkin, T., LeMeur, M., Chambon, P., and Mark, M. (1994). Function of the retinoic acid receptors (RARs) during development (II). Multiple abnormalities at various stages of organogenesis in RAR double mutants. Development *120*, 2749-2771.

Mendelson, B. (1986). Development of reticulospinal neurons of the zebrafish. II. Early axonal outgrowth and cell body position. J Comp Neurol *251*, 172-184.

Merzdorf, C.S. (2007). Emerging roles for zic genes in early development. Dev Dyn *236*, 922-940.

Minucci, S., and Pelicci, P.G. (1999). Retinoid receptors in health and disease: co-regulators and the chromatin connection. Semin Cell Dev Biol *10*, 215-225.

Mizugishi, K., Aruga, J., Nakata, K., and Mikoshiba, K. (2001). Molecular properties of Zic proteins as transcriptional regulators and their relationship to GLI proteins. J Biol Chem *276*, 2180-2188.

Mizuseki, K., Kishi, M., Matsui, M., Nakanishi, S., and Sasai, Y. (1998). Xenopus Zic-related-1 and Sox-2, two factors induced by chordin, have distinct activities in the initiation of neural induction. Development *125*, 579-587.

Moens, C.B., and Prince, V.E. (2002). Constructing the hindbrain: insights from the zebrafish. Dev Dyn *224*, 1-17.

Moens, C.B., and Selleri, L. (2006). Hox cofactors in vertebrate development. Dev Biol *291*, 193-206.

Moens, C.B., Yan, Y.L., Appel, B., Force, A.G., and Kimmel, C.B. (1996). valentino: a zebrafish gene required for normal hindbrain segmentation. Development *122*, 3981-3990.

Molotkova, N., Molotkov, A., Sirbu, I.O., and Duester, G. (2005). Requirement of mesodermal retinoic acid generated by Raldh2 for posterior neural transformation. Mech Dev *122*, 145-155.

Morriss, G.M. (1972). Morphogenesis of the malformations induced in rat embryos by maternal hypervitaminosis A. J Anat *113*, 241-250.

Morriss-Kay, G.M., Murphy, P., Hill, R.E., and Davidson, D.R. (1991). Effects of retinoic acid excess on expression of Hox-2.9 and Krox-20 and on morphological segmentation in the hindbrain of mouse embryos. EMBO J *10*, 2985-2995.

Nagai, T., Aruga, J., Takada, S., Gunther, T., Sporle, R., Schughart, K., and Mikoshiba, K. (1997). The expression of the mouse Zic1, Zic2, and Zic3 gene suggests an essential role for Zic genes in body pattern formation. Dev Biol *182*, 299-313.

Nakata, K., Nagai, T., Aruga, J., and Mikoshiba, K. (1997). Xenopus Zic3, a primary regulator both in neural and neural crest development. Proc Natl Acad Sci U S A *94*, 11980-11985.

Niederreither, K., Abu-Abed, S., Schuhbaur, B., Petkovich, M., Chambon, P., and Dolle, P. (2002). Genetic evidence that oxidative derivatives of retinoic acid are not involved in retinoid signaling during mouse development. Nat Genet *31*, 84-88.

Niederreither, K., and Dolle, P. (2008). Retinoic acid in development: towards an integrated view. Nat Rev Genet *9*, 541-553.

Niederreither, K., McCaffery, P., Drager, U.C., Chambon, P., and Dolle, P. (1997). Restricted expression and retinoic acid-induced downregulation of the retinaldehyde dehydrogenase type 2 (RALDH-2) gene during mouse development. Mech Dev *62*, 67-78.

Niederreither, K., Subbarayan, V., Dolle, P., and Chambon, P. (1999). Embryonic retinoic acid synthesis is essential for early mouse post-implantation development. Nat Genet *21*, 444-448.

Niederreither, K., Vermot, J., Schuhbaur, B., Chambon, P., and Dolle, P. (2000). Retinoic acid synthesis and hindbrain patterning in the mouse embryo. Development *127*, 75-85.

Nieuwkoop, P. D., and Others. (1952). Activation and organization of the central nervous system in amphibians. Part II. Differentiation and organization. Journal of Experimental Zoology *120*: 33–81.

Nyholm, M.K., Wu, S.F., Dorsky, R.I., and Grinblat, Y. (2007). The zebrafish zic2a-zic5 gene pair acts downstream of canonical Wnt signaling to control cell proliferation in the developing tectum. Development *134*, 735-746.

Oh, S., Huang, X., Liu, J., Litingtung, Y., and Chiang, C. (2009). Shh and Gli3 activities are required for timely generation of motor neuron progenitors. Dev Biol *331*, 261-269.

Papalopulu, N., Clarke, J.D., Bradley, L., Wilkinson, D., Krumlauf, R., and Holder, N. (1991). Retinoic acid causes abnormal development and

segmental patterning of the anterior hindbrain in Xenopus embryos. Development *113*, 1145-1158.

Papalopulu, N., and Kintner, C. (1996). A posteriorising factor, retinoic acid, reveals that anteroposterior patterning controls the timing of neuronal differentiation in Xenopus neuroectoderm. Development *122*, 3409-3418.

Perez, S.E., Rebelo, S., and Anderson, D.J. (1999). Early specification of sensory neuron fate revealed by expression and function of neurogenins in the chick embryo. Development *126*, 1715-1728.

Pijnappel, W.W., Hendriks, H.F., Folkers, G.E., van den Brink, C.E., Dekker, E.J., Edelenbosch, C., van der Saag, P.T., and Durston, A.J. (1993). The retinoid ligand 4-oxo-retinoic acid is a highly active modulator of positional specification. Nature *366*, 340-344.

Rohr, K.B., Schulte-Merker, S., and Tautz, D. (1999). Zebrafish zic1 expression in brain and somites is affected by BMP and hedgehog signalling. Mech Dev *85*, 147-159.

Rossant, J., Zirngibl, R., Cado, D., Shago, M., and Giguere, V. (1991). Expression of a retinoic acid response element-hsplacZ transgene defines specific domains of transcriptional activity during mouse embryogenesis. Genes Dev *5*, 1333-1344.

Sakai, Y., Meno, C., Fujii, H., Nishino, J., Shiratori, H., Saijoh, Y., Rossant, J., and Hamada, H. (2001). The retinoic acid-inactivating enzyme CYP26 is essential for establishing an uneven distribution of retinoic acid along the anterio-posterior axis within the mouse embryo. Genes Dev *15*, 213-225.

Sandell, L.L., Sanderson, B.W., Moiseyev, G., Johnson, T., Mushegian, A., Young, K., Rey, J.P., Ma, J.X., Staehling-Hampton, K., and Trainor, P.A. (2007). RDH10 is essential for synthesis of embryonic retinoic acid and is required for limb, craniofacial, and organ development. Genes Dev *21*, 1113-1124.

Sanek, N.A., and Grinblat, Y. (2008). A novel role for zebrafish zic2a during forebrain development. Dev Biol *317*, 325-335.

Sanek, N.A., Taylor, A.A., Nyholm, M.K., and Grinblat, Y. (2009). Zebrafish zic2a patterns the forebrain through modulation of Hedgehog-activated gene expression. Development *136*, 3791-3800.

Saude, L., Woolley, K., Martin, P., Driever, W., and Stemple, D.L. (2000). Axis-inducing activities and cell fates of the zebrafish organizer. Development *127*, 3407-3417.

Sharpe, C., and Goldstone, K. (2000). The control of Xenopus embryonic primary neurogenesis is mediated by retinoid signalling in the neurectoderm. Mechanisms of Development *91*, 69-80.

Shih, J., and Fraser, S.E. (1996). Characterizing the zebrafish organizer: microsurgical analysis at the early-shield stage. Development *122*, 1313-1322.

Simeone, A., Acampora, D., Arcioni, L., Andrews, P.W., Boncinelli, E., and Mavilio, F. (1990). Sequential activation of HOX2 homeobox genes by retinoic acid in human embryonal carcinoma cells. Nature *346*, 763-766.

Simeone, A., Acampora, D., Nigro, V., Faiella, A., D'Esposito, M., Stornaiuolo, A., Mavilio, F., and Boncinelli, E. (1991). Differential regulation by retinoic acid of the homeobox genes of the four HOX loci in human embryonal carcinoma cells. Mech Dev *33*, 215-227.

Sirbu, I.O., Gresh, L., Barra, J., and Duester, G. (2005). Shifting boundaries of retinoic acid activity control hindbrain segmental gene expression. Development *132*, 2611-2622.

Sockanathan, S., and Jessell, T.M. (1998). Motor neuron-derived retinoid signaling specifies the subtype identity of spinal motor neurons. Cell *94*, 503-514.

Studer, M., Gavalas, A., Marshall, H., Ariza-McNaughton, L., Rijli, F.M., Chambon, P., and Krumlauf, R. (1998). Genetic interactions between Hoxa1 and Hoxb1 reveal new roles in regulation of early hindbrain patterning. Development *125*, 1025-1036.

Studer, M., Lumsden, A., Ariza-McNaughton, L., Bradley, A., and Krumlauf, R. (1996). Altered segmental identity and abnormal migration of motor neurons in mice lacking Hoxb-1. Nature *384*, 630-634.

Swiatek, P.J., and Gridley, T. (1993). Perinatal lethality and defects in hindbrain development in mice homozygous for a targeted mutation of the zinc finger gene Krox20. Genes Dev *7*, 2071-2084.

Swindell, E.C., Thaller, C., Sockanathan, S., Petkovich, M., Jessell, T.M., and Eichele, G. (1999). Complementary domains of retinoic acid production and degradation in the early chick embryo. Dev Biol *216*, 282-296.

Toivonen, S., Saxen, L. (1968) Morphogenetic interaction of presumptive neural and mesodermal cells mixed in different ratios. Science *159*: 539.

Thisse, B., Heyer, V., Lux, A., Alunni, V., Degrave, A., Seiliez, I., Kirchner, J., Parkhill, J.P., and Thisse, C. (2004). Spatial and temporal expression of the zebrafish genome by large-scale in situ hybridization screening. Methods Cell Biol *77*, 505-519.

Trevarrow, B., Marks, D.L., and Kimmel, C.B. (1990). Organization of hindbrain segments in the zebrafish embryo. Neuron *4*, 669-679.

Vanderlaan, G., Tyurina, O.V., Karlstrom, R.O., and Chandrasekhar, A. (2005). Gli function is essential for motor neuron induction in zebrafish. Dev Biol *282*, 550-570.

Varela-Echavarria, A., Pfaff, S.L., and Guthrie, S. (1996). Differential expression of LIM homeobox genes among motor neuron subpopulations in the developing chick brain stem. Mol Cell Neurosci *8*, 242-257.

Wendling, O., Ghyselinck, N.B., Chambon, P., and Mark, M. (2001). Roles of retinoic acid receptors in early embryonic morphogenesis and hindbrain patterning. Development *128*, 2031-2038.

White, J.C., Highland, M., Kaiser, M., and Clagett-Dame, M. (2000). Vitamin A deficiency results in the dose-dependent acquisition of anterior character and shortening of the caudal hindbrain of the rat embryo. Dev Biol *220*, 263-284.

White, R.J., Nie, Q., Lander, A.D., and Schilling, T.F. (2007). Complex regulation of cyp26a1 creates a robust retinoic acid gradient in the zebrafish embryo. PLoS Biol *5*, e304.

White, R.J., and Schilling, T.F. (2008). How degrading: Cyp26s in hindbrain development. Dev Dyn *237*, 2775-2790.

Wilson, P.A., Lagna, G., Suzuki, A., and Hemmati-Brivanlou, A. (1997). Concentration-dependent patterning of the Xenopus ectoderm by BMP4 and its signal transducer Smad1. Development *124*, 3177-3184.

Woo, K., and Fraser, S.E. (1998). Specification of the hindbrain fate in the zebrafish. Dev Biol *197*, 283-296.

Wood, H., Pall, G., and Morriss-Kay, G. (1994). Exposure to retinoic acid before or after the onset of somitogenesis reveals separate effects on rhombomeric segmentation and 3' HoxB gene expression domains. Development *120*, 2279-2285.

Yamamoto, T.S., Takagi, C., and Ueno, N. (2000). Requirement of Xmsx-1 in the BMP-triggered ventralization of Xenopus embryos. Mech Dev *91*, 131-141.

Yokota, N., Aruga, J., Takai, S., Yamada, K., Hamazaki, M., Iwase, T., Sugimura, H., and Mikoshiba, K. (1996). Predominant expression of human zic in cerebellar granule cell lineage and medulloblastoma. Cancer Res *56*, 377-383.

Zhang, F., Nagy Kovacs, E., and Featherstone, M.S. (2000). Murine hoxd4 expression in the CNS requires multiple elements including a retinoic acid response element. Mech Dev *96*, 79-89.

Zhang, M., Kim, H.J., Marshall, H., Gendron-Maguire, M., Lucas, D.A., Baron, A., Gudas, L.J., Gridley, T., Krumlauf, R., and Grippo, J.F. (1994). Ectopic Hoxa-1 induces rhombomere transformation in mouse hindbrain. Development *120*, 2431-2442.

Chapter 2. Materials and Methods

2.1 Zebrafish care and lines

All fish were grown in embryo media (EM) at 28.5°C, 25°C, or 33°C and maintained according to recorded standards (Westerfield, 2000; Table 2.1). Embryos older than 24 hpf were grown in EM + 0.003% 1-phenyl 2-thiourea (PTU; Sigma, Markham, Ontario, Canada) to prevent pigment formation. Embryos were staged following standard morphological features described by (Kimmel et al., 1995). Wild-type AB strain of zebrafish was used unless otherwise stated, in addition the Retinoic Acid Response Element (RARE) transgenic Tg(12XRARE-*ef1a:gfp*)sk71 (Feng et al., 2010; Waxman and Yelon, 2011) and Tg(*isl1:gfp*) on Wik background (Higashijima et al., 2000) were used.

2.2 mRNA *in situ* hybridization

mRNA *in situ* hybridization procedure was based on previously published methods and is described here (Gongal and Waskiewicz, 2008; Thisse et al., 2004). Probes were synthesized via probe plasmids or a PCR-based approach with primers designed to amplify the targets 3' untranslated regions (Table 2.2, 2.3).

Embryos of desired stage were fixed in 4% paraformaldehyde (PFA) and subsequently removed using five PBST washes (1X PBS/0.1% Tween-20; 5 minutes each). After manual chorion removal, embryos were permeabilized in Proteinase K (10μg/ml) for varying times depending on embryonic stage: 30 seconds (10-12 hfp), 1 minute (12-14 hfp), 4 minutes (18-24 hpf), 20 minutes (48 hpf), 40 minutes (72 hpf). Embryos were then re-fixed in 4% PFA for 20 minutes followed by five PBST washes (5 minutes each).

The pre-hybridization (pre-hyb), hybridization (hyb), and high stringency wash steps were carried out in a 65°C waterbath. Embryos were incubated for at least two hours in warmed pre-hyb solution (50% deionized formamide, 5X SSC, 0.1% Tween 20, 50 μg/ml of heparin, 500 μg/ml of

RNase-free tRNA, pH 6.0 by adding citric acid) followed by overnight incubation in hyb (pre-hyb solution including probe RNA; 1/200 – 1/400 dilution). Embryos then undergo a series of five minute washes (66% hyb/33% 2X SSC; 33% hyb/66% 2X SSC; 2X SSC) followed by three 20-minute high stringency washes (0.2X SSC + 0.1% Tween-20; 0.1X SSC + 0.1% Tween-20; 0.1X SSC + 0.1% Tween-20). At room temperature embryos were transferred to PBST by sequential five minute washes in 66% 0.2X SSC/33% PBST, 33% 0.2X SSC/ 33% PBST, and finally into PBST.

Detection of the RNA probe is dependent on antibody labeling of the digoxigenin (DIG) label on the RNA probe. Embryos were first incubated in Blocking Solution (2% Sheep Serum + 2 mg/ml Bovine Serum Albumin in PBST) for one hour at room temperature, or 4^{o}C overnight, before transfer into primary antibody (Blocking Solution + 1/5000 dilution of sheep anti-DIG-AP-FAB fragments antibody; Roche, Mississauga, Ontario, Canada) for two hours at room temperature, or 4^{o}C overnight. Embryos were then washed in five PBST washes (15 minutes each).

The coloration reaction was performed with either nitro-blue tetrazolium (NBT)/bromo-4-chloro-3-indolyl phosphate (BCIP) stock (embryos older than 2-Somite stage) in Coloration Buffer or with BM purple (embryos between 50% epiboly and 2S; Roche, Mississauga, Ontario, Canada). For NBT/BCIP protocol, embryos were washed four times in Coloration Buffer (5 minutes each) before incubation in 500 μl of Coloration Solution (Coloration Buffer + 45μl NBT + 35 μl BCIP). Embryos were left at room temperature in the dark for coloration reaction to occur. To stop coloration, embryos were rinsed four times in Stop Solution (5 minutes each), followed by two additional Stop Solution washes (15 minutes each). Alternatively, to stop the coloration reaction embryos were washed twice in 100% methanol/0.1% Tween-20. For BM purple coloration, embryos were transferred from PBST into sterile water (two-ten minute and one-fifteen

minute washes) before incubation in 500 μl of BM purple in the dark. Coloration was stopped by washing in 100% methanol/0.1% Tween-20.

Embryos were prepared for imaging by directly transferring to PBST (from Stop Solution) or through a series of five-minute re-hydration washes (75% MeOH/25% PBST; 50% MeOH/50% PBST; 25% MeOH/75% PBST). Deyolked embryos were dehydrated in 50% glycerol, then 70% glycerol before mounting. Images were taken with a Zeiss Axio Imager.Z1 using Axovision SE64 Rel.4.8 software. Embryos in early development (6-14 hpf) or with yolk attached were photographed using an Olympus SZX12 stereoscope using QImaging micropublisher camera.

2.3 Gene knockdown analysis – morpholinos

Morpholino oligonucleotides (MO) are a common tool in zebrafish used to knockdown target RNA levels (Nasevicius and Ekker, 2000). Zic1MO (Maurus and Harris, 2009), Zic2aMO (Nyholm et al., 2007), Zic2bMO, Zic3MO, Aldh1a2MO (Alexa et al., 2009; Begemann et al., 2001), Cyp26a1MO (Kudoh et al., 2002), and p53MO morpholinos were designed to produce a non- or partially-functional protein product (Gene-Tools, Table 2.4).

Due to aberrant activation of the p53 apoptotic pathway, morpholinos can cause non-specific effects including neural tube defects, necrosis, and neural cell death. The addition of p53MO to the morpholino cocktail counteracts this effect and was used in our experiments as noted in figure legends (Table 2.5) (Robu et al., 2007). Of note, in early experiments Zic2aMO, Zic2bMO, and Zic3MO were used to obtain combinatorial knockdown. This high dose of morpholino was detrimental to embryo health and, upon discovery that Zic3MO was dispensable for our observed phenotypes, Zic3MO was removed from the cocktail.

2.4 Retinoic acid manipulation

Methods of manipulating RA levels included pharmacological treatment, MO-mediated gene knockdown, and exogenous RA treatment. Because RA is a small diffusible molecule, addition of RA directly to embryo media increased endogenous RA levels. Embryos at approximately 50% epiboly were treated with RA in DMSO (1 nM, 5 nM, or 10 nM in embryo media; Sigma, Markham, Ontario, Canada). This range of RA concentration is similar to physiological levels, estimated to be 3 nM (Maden et al., 1998; Ohishi et al., 1995). Conversely, to reduce embryonic RA levels the pharmacological inhibitor of RA-synthesis called diethylaminobenzaldehyde (DEAB; Sigma, Markham, Ontario, Canada) was used. DEAB blocks aldehyde dehydrogenase enzymatic activity, thus preventing the conversion of retinal to RA. Embryos were treated at approximately 50% epiboly DEAB in DMSO (1 μM, 5 μM, or 10 μM in embryo media). Embryos were manually dechorionated at 26 hpf and, maintaining treatment concentration, media was changed once per day. If necessary, 60 mg/ml PTU was added to media after 24 hpf to prevent pigment formation. All treatments were carried out at 28.5^{o}C in 5 mL petri dishes, each containing approximately 40 embryos grown.

Indirectly manipulating RA levels was accomplished through MO-mediated gene knockdown of relevant RA metabolism genes, *cyp26a1* and *aldh1a2*. Deficiency of *cyp26a1* theoretically increases RA levels due to loss of RA-degradation (White et al., 2007). Similarly, *aldh1a2*-deficiency reduces RA levels due to reduced RA synthesis (Begemann et al., 2001).

2.5 Total RNA extraction

Live embryos of the desired stage were manually dechorionated and RNA was extracted using Ambion RNAqueous RNA extraction as described here (Streetsville, Ontario, Canada). Approximately 50 embryos were collected in a 1.7 ml tube and 10-12 times volume of Lysis Binding Solution

was added. This mixture was vortexed thoroughly to homogenize. An equal volume of 64% ethanol was added followed by another 30-second vortex. The solution was transferred to a carbon collection tube (included with kit) and centrifuged at 14,800 rpm for one minute. Flow-through was discarded and 700 μl of Wash Solution #1 was added to collection tube before centrifuging at 14,800 rpm for one minute. Flow through was discarded before the final two wash steps: [500 μl of Wash Solution #2/3 was added to the collection tube, one minute centrifugation at 14,800 rpm, and removal of flow-through] completed twice. The filter was transferred to a new RNAse-free collection tube and 40 μl of Elution Buffer (heated to 70°C) was dispensed onto the filter. After sitting for one minute, the tube was centrifuged for 30 seconds at 14,800 rpm to remove RNA from the filter. An additional elution step was carried out with the application of another 30 μl of Elution Buffer to the filter. After sitting for one minute, the final centrifugation (30 seconds at 14,800 rpm) allows isolation of 70 μl total RNA. RNA samples were stored at -80°C.

2.6 mRNA overexpression

2.6.1 cDNA synthesis and RT-PCR

Primers used to generate mRNA overexpression constructs for *zic2a* and *aldh1a2* were designed based on previous protocols (Table 2.6). Primer design was based on the following requirements: forward and reverse primers flank the entire coding region of the gene of interest, melting temperature of both primers equals approximately 66°C, primers must have a G-C clamp (ending with one, or several G nucleotides), the G-C content of primers ranges from 40%-60%, and a length of 23-27 nucleotides. Primers were designed using the MacVector program with additional sequence added: four nucleotides (CACA) at the 5' end followed by a different restriction enzyme cut site within the forward and reverse primer. Restriction sites were selected based on the following: first, the sites must be

appropriate for cloning into pCS2+ vector and they must not cut within the gene of interest. For this purpose, BamHI (cut site G|GATCC) and EcoRI (cut site G|AATTC) were used. The forward primer also contained a kozak sequence (ACCAUGG), which allows initiation of translation. This sequence was placed upstream of the 23-27 nucleotide sequence designed by the MacVector program (Figure 2.1).

Complementary DNA (cDNA) was synthesized using SuperScript III First Strand Synthesis kit (Invitrogen, Burlington, Ontario, Canada) using the following procedure. In an RNAse-free PCR tube, a 10 μl solution was prepared consisting of: 4 μl total RNA, 1 μl 50 μM oligo dT, 1 μl 10 μM dNTPs, 4 μl diethylpyrocarbonate (DEPC) -treated H_2O water. The mixture was incubated in a thermocycler at 65°C for five minutes and then left on ice for at least one minute. The cDNA synthesis mixture (2 μl 10X reaction buffer, 4 μl 25 mM $MgCl_2$, 2 μl 0.1 M DTT, 1 μl 40 units/μl RNAse-OUT, 1 μl 200 units/μl SuperScript III reverse transcriptase) was the added to the RNA and incubated at 50°C for 50 minutes. The reaction was terminated by incubation for five minutes at 85°C and 5 minutes on ice. Final removal of RNA from the cDNA was accomplished by addition of 1 μl RNAse-H and incubation at 37°C for 20 minutes. The cDNA product was stored at -20°C or used immediately for Phusion PCR.

2.6.2 Phusion high fidelity PCR and TOPO cloning

The coding sequence of the gene of interest (*zic2a*/*aldh1a2*) was amplified using High Fidelity Phusion PCR (Fisher Scientific, Ottawa, Ontario, Canada). Reactions were set up in PCR tubes on ice containing: 24.5 μl MilliQ water, 10 μl 5XHF buffer, 4 μl 2.5 nM dNTPs, 5 μl 5 μM forward primer, 5 μl 5 μM reverse primer, 0.5 μl Phusion DNA Polymerase, using the following the thermocycler program:

Initial	Denaturation	98°C for 30 seconds
35X	Denaturation	98°C for 10 seconds

Annealing	63°C for 30 seconds
Elongation	72°C for 75 seconds
Final Extension	72°C for 5 minutes

Thermocycler program parameters were optimized for each primer set by setting the annealing temperature +3°C above the lowest melting point primer. Elongation was 15 seconds per kilobase length of DNA. PCR products were confirmed by visualization in a 1% agarose gel and desired product was isolated by gel extraction (Qiagen, Toronto, Ontario, Canada).

Blunt-ended cloning was required to transfer PCR products, *zic2a* and *aldh1a2* coding sequences, into the pCR4-TOPO vector (*zic2a*) or directly into pCS2+ (*aldh1a2*) (Invitrogen, Burlington, Ontario, Canada). First, dATP was added to the blunt-ended PCR product using the following conditions: 16.5 μl Phusion PCR product, 2 μl 10X ExTaq Buffer, 0.5 μl 10 mM dATP (or 1 μl 10 mM dNTPs), 1 μl sterile water. This reaction was incubated for 10 minutes at 72°C in the thermocycler and was used immediately for ligation and transformation. For ligation into pCR4-TOPO, 1 μl PCR product + 0.25 μl pCR4-TOPO vector + 1.25 μl sterile water were mixed and incubated at room temperature for 5 minutes (for *aldh1a2* ligation directly into pCS2+ out, see below). The ligation product was transformed into TOP-10 cells by incubating 10 μl TOP-10 cells with 2.5 μl ligation product on ice for 20 minutes. Cells were heat shocked at 42°C for 30-45 seconds, followed by incubation on ice for 2 minutes. Five times cell volume of SOC (LB media + glucose) or LB media was added and incubated at 37°C for 30-45 minutes. Cells were suspended in 100 μl of LB/SOC medium and plated on LB containing 50 μg/ml carbenicillin for growth overnight at 37°C. To isolate pCR4-TOPO containing insert (TOPO-zic2a), plasmid DNA was isolated using standard mini-prep procedure (Qiagen, Toronton, Ontario, Canada). To clone the insert into pCS2+, pCR4-TOPO vector (or *aldh1a2* PCR product) underwent restriction enzyme digestion (BamHI/EcoRI; Promega, Madison, Wisconsin, USA). pCS2+ was linearized (BamHI/EcoRI) and ligation reaction

was performed (2 μl insert, 1 μl linear pCS2+, 3 μl 10X ligation buffer, 2 μl T4 DNA ligase (Promega, Madison, Wisconsin, USA), to 30 μl with MilliQ water) overnight at 4°C followed by bacterial transformation and plasmid preparation.

2.6.3 mMessage mMachine mRNA synthesis

pCS2+ plasmid containing the coding sequence of interest (*zic2a*, *aldh1a2*) was linearized using NotI restriction enzyme digestion (10 μg plasmid, 1.5 μl Buffer D (Promega, Madison, Wisconsin, USA), 2.5 μl NotI (Promega, Madison, Wisconsin, USA), and DEPC-treated H_2O to 40μl) at 37°C for 2.5 hours. A portion (1 μl) of the digested product was ran on 1% agarose gel to confirm complete linearization. Residual RNAse and enzyme was removed with SDS/Proteinase K treatment. To each 40 μl reaction, 5μl 1 μg/ul ProtK, 1.25 μl 20% SDS, and 4.75 μl DEPC-treated H_2O water was added and incubated at 50°C for 30 minutes. Phenol-Chloroform extraction was performed by first adding 150 μl DEPC-treated H_2O to 50 μl linearized DNA to generate a 200 μl volume. An equal volume of Phenol:Chloroform (Fisher BioReagents) was added, vortexed for 20 seconds, and centrifuged at 14,800 rpm for 5 minutes. The upper layer was transferred to new 1.7 ml tube and an equal volume of Chloroform (Fisher BioReagents) was added, followed by vortexing and centrifugation as in previous step. The upper aqueous layer was transferred to a new tube and the purified DNA was ethanol precipitated. One-tenth volume of 3M NaOAc was added along with 3 times volume of 100% RNAse-free ethanol. The solution was mixed and left on ice for at least 15 minutes, followed by centrifugation at 14,800 rpm for 15 minutes at 4°C. The ethanol was removed leaving DNA pellet undisturbed. The DNA pellet was the washed with 100 μl of 70% RNAse-free ethanol followed by centrifugation at 14,800 rpm for 15 minutes at 4°C. The ethanol was removed and the pellet was air dried before re-suspension in 6-8 μl of DEPC-treated H_2O.

The linearized, purified product was used for RNA transcription using mMessage mMachine (Ambion, Streetsville, Ontario, Canada). Reaction was prepared at room temperature and components added in the following order: 10 μl 2X NTP/CAP, 2 μl 10X Reaction Buffer, 1 μg linear template, 2 μl enzyme mix, filled to 20 μl with nuclease-free water. After incubation for 2 hours at 37°C, 1 μl TURBO DNAse (Ambion, Streetsville, Ontario, Canada) was added and incubated at 37°C for 15 minutes. RNA product was isolated using Amicon Microcom Columns with addition of 480 μl DEPC. The total 500 μl solution was transferred into an Amicon Column and centrifuged at 3000 rpm for 15 minutes. Flow-through was discarded and another 400 μl DEPC-treated H_2O was added to column before being centrifuged at 3,000 rpm for 16 minutes. The Amicon Column was inverted into a new 1.7 ml tube and centrifuged at 3000 rpm for 3 minutes (leaving the concentrate in the 1.7 ml tube). The concentrate was transferred into a new Amicon Column, and filled to 500 μl with DEPC-treated H_2O. After centrifugation at 3,000 rpm for 25 minutes the Amicon column was inverted into a new 1.7 ml tube and centrifuged at 3,000 rpm for 3 minutes to obtain mRNA. mRNA was stored at -80°C.

2.7 Transgenic zebrafish and confocal microscopy

Visualization of hindbrain branchiomotor neurons was accomplished using the Tg(*isl1:gfp*) transgenic zebrafish line (Higashijima et al., 2000). Additionally, Tg(12XRARE-*ef1a:gfp*)sk71 transgenics allow visualization of RA-signaling levels by assaying fluorescence (or *in situ* hybridization for *gfp*) (Feng et al., 2010; Waxman and Yelon, 2011). For fluorescent analysis, embryos were grown as described previously (to 48 hpf) and fixed with 4% PFA for 4 hours at room temperature. Yolks were removed manually and embryos were dehydrated in 50% and 70% glycerol before mounting. Imaging was done using Zeiss Axio Imager.Z1 and Zeiss Zen software. Image preparation and analysis (quantification of vagal neuron fluorescent area and

length of vagal domain) was completed with ImageJ software. To calculate vagal area, Z-stacked images were converted to 8-bit color and scale was set to correspond with that of the image (pixel length 1024 or 2048, length of field of view 319.93 μm). The image threshold was set (70-255 units) – this threshold captured the greatest number of neurons while keeping noise low. Finally using the Measure tool and the "magic wand" for area or "line tool" for length, individual regions of fluorescence were selected and calculated. All numerical information was transferred to Microsoft Excel – where totals and averages were calculated. Significant differences among treatments in Figure 3.10 were determined through analyses of variance (ANOVA) and using post-hoc Tukey's Honestly Significant Difference test using R (http://r-project.org). In Figure 3.12 statistical differences were calculated using unpaired t-test.

2.8 Zn-5 antibody

The Zn-5 antibody (ZIRC; Table 2.7) was used to label hindbrain commissural neurons and neurons of the cerebellum. Two-day old embryos were fixed in 4% PFA for four hours followed by four PBST washes (5 minutes each). Permeabilization was achieved with a ten minute incubation in 10 μg/ml Proteinase K in PBST before re-fixing embryos for 20 minutes in 4% PFA. Embryos were removed from fix with four PBST washes (5 minutes each) before incubation in Block Solution (2% Goat Serum + 2 mg/ml Bovine Serum Albumin + 0.1% Triton in PBST) for one hour at room temperature. The primary Zn-5 antibody (1:250 dilution; Table 2.7) was added to the same Blocking Solution and incubated overnight at 4^{o}C. After removal of primary antibody, embryos undergo five PBSDTT washes (1XPBS + 1% DMSO + 1% Tween-20 + 1% Triton-X; 30 minutes each) washes at room temperature. Subsequent reblocking involves a one hour incubation in PBSDTT + 1% Goat Serum at room temperature. Secondary antibody was added directly to reblocking solution (1:750 dilution of goat anti-mouse AlexaFluor-568;

Invitrogen) and incubated overnight at 4°C, or for five hours at room temperature. Embryos were washed out of antibody using six PBSDTT washes (15 minutes each). All washes and incubations were carried out on a nutator in the dark. Embryos were deyolked and mounted as described in the *in situ* hybridization procedure and prepared for confocal imaging.

2.9 Anti-activated caspase-3 antibody

The Anti-Activated Caspase-3 antibody (Table 2.7; BD Biosciences, Mississauga, Ontario, Canada) immunofluorescence was used to detect cells that are undergoing apoptosis. Two-day old embryos were fixed in 4% PFA, then rinsed three times in 1XPBS (20 minutes each). This was followed by a series of washes: five minutes in water + 1% Tween-20, seven minutes in Acetone (chilled to -20°C), five minutes in water + 1% Tween-20, and five minutes in 1X PBS (Table 2.1). Embryos were blocked in PBSDTT + 10% Goat Serum for 60 minutes at room temperature. Primary antibody (1:400 dilution α-rabbit activated caspase-3 in PBSDTT + 2% Goat Serum) was added for a two-hour incubation at room temperature, or 4°C overnight. Primary antibody was removed and retained for additional use, while embryos were rinsed twice in PBSDTT, followed by 2 X 20 minute PBSDTT washes at room temperature. Secondary antibody (1:1000 goat anti-rabbit AlexaFluor 568 in PBSDTT + 2% Goat Serum; Invitrogen, Burlington, Ontario, Canada) was added for a two-hour incubation at room temperature (in the dark), or 4°C overnight. Embryos were removed from antibody with two PBSDTT rinses, followed by four PBSDTT washes (15 minutes each). All washes and incubations were carried out on a nutator in the dark. Embryos were deyolked and put directly into 70% glycerol for mounting and confocal imaging.

2.10 Quantitative real-time PCR

Quantitative Real-Time PCR was used to quantify *in vivo* mRNA levels to ascertain gene knockdown in morphants. DNA probes were designed using Roche Universal Probe Library for Zebrafish. Gene sequences were inputted into the program (*zic2a* ENSDART00000010774, *zic2b* ENSDART00000054066, *zic3* ENSDART00000105761, *cyp26a1* ENSDART00000041728), which chooses intron-spanning oligonucleotides that produce a product approximately 100 nucleotides in length (Table 2.8).

After RNA isolation (Ambion RNAqueous, Streetsville, Ontario, Canada), DNA was digested with DNAseI (19 μl DEPC-treated H_2O, 10 μl 10X DNAseI buffer, 1 μl DNAseI (Ambion)) for 30 minutes at 37°C. RNA was further purified with addition of 350 μl RLT lysis buffer to each sample, followed by vortexing and the addition of 250 μl 100% RNAse-free ethanol. The entire solution was transferred to a Qiagen RNeasy column and centrifuged at 10,000 rpm for 15 seconds. In a new collection tube, 500 μl RPE wash buffer was added before centrifugation at 10,000 rpm for 15 seconds. Another 500 μl of RPE wash buffer was added followed by centrifugation at 10,000 rpm for 2 minutes. To remove excess wash solution, the column was centrifuged for an additional minute at 14,800 rpm. RNA is eluted with addition of 15 μl DEPC-treated H_2O to the column and centrifugation at 10,000 rpm for 1 minute. RNA was stored at -80°C.

The cDNA was synthesized from RNA using AffinityScript qPCR cDNA Synthesis kit (Ambion, Streetsville, Ontario, Canada) using the following protocol. In an RNAse-free PCR tube, added in order: 3 μl RNAse-free water, 10 μl 2X Master Mix, 3 μl random hexamers, 1 μl RT/RNAse block enzyme mix, 3 μl RNA (~3 μg). PCR reaction was as follows:

Primer Annealing	25°C for 5 minutes
cDNA synthesis	42°C for 30 minutes
Reaction Termination	95°C for 5 minutes

An additional PCR reaction was carried out to confirm successful cDNA synthesis by mixing in a PCR tube: 2 μl 1/20 dilution cDNA, 5 μl 10X ExTaq buffer, 1 μl 50 nM dNTPs, 1 μl 5 μM EF1α forward primer, 1 μl 5 μM EF1α reverse primer, 1 μl ExTaq, 3 μl sterile water. PCR reaction was as follows:

Initial Denaturation		94 °C for 2 minutes
40X	Denaturation	94 °C for 15 seconds
	Annealing	55 °C for 15 seconds
	Elongation	72 °C for 30 seconds
Final Elongation		72 °C for 2 minutes

A 2% agarose gel was used to analyze band size and consistency of products.

Quantitative RT-PCR and primer validation was carried out as previously described (Livak and Schmittgen, 2001; Pillay et al., 2010). For primer validation, control (AB) cDNA was used to create a 2-fold dilution series: 1/8, 1/16, 1/32, 1/64, 1/128, 1/256. Ambion Brilliant II qPCR kit was used to make 96-well reactions containing: 2.937 μl MilliQ H_2O, 5 μl 2X SYBR Master Mix, 0.3 μl 5 μM forward primer (EF1αF), 0.3 μl 5 μM reverse primer (EF1αR), 0.003 μl Rox, 2 μl cDNA. All reactions were set up using master mix solutions to ensure accuracy between wells, with each reaction carried out in triplicate. Thermocycler program was as follows:

Activation		95 °C for 10 minutes
40X	Denaturation	95 °C for 30 seconds
	Annealing/Fluorescent Reading	55 °C for 1 minute
	Extension	72 °C for 30 seconds

The resulting Standard Curve and Melting Curve data allows validation of primer pair by plotting the linear regression curve. Validated primer pairs include: aldh1a2 (previously completed), zic2a-2 (linear regression slope of -3.5, coefficient of determination (R^2) of 0.99), zic2b-2 (linear regression slop of -3.4, R^2 of 0.99), cyp26a1-2 (linear regression slope of -4.1, R^2 of 0.97).

Relative gene expression level was determined using the comparative Ct method ($2^{-\Delta\Delta Ct}$ method) and unpaired t-test calculations for significance. Reactions were generated as described above, using cDNA isolated from control p53MO -injected and experimental Zic2a2bMO + p53MO –injected embryos (1/16 dilution of cDNA in DEPC –treated H_2O; 7-8 technical replicates). EF1α was used as the endogenous control.

2.11 Figures and Tables

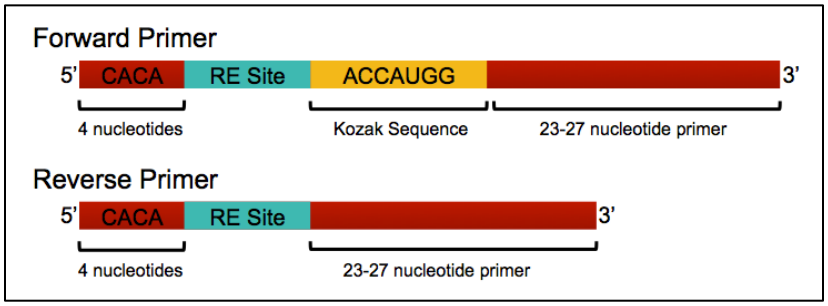

Figure 2.1: mRNA over-expression primer design.

20X Embryo Media		**Embryo Media**		**PBS (1X phosphate buffered saline)**	
17.5 g	NaCl	50 ml	20X EM	80 g	NaCl
0.75 g	KCl	2 ml	500X $NaHCO_3$	2 g	KCl
2.9 g	$CaCl\text{-}2H_2O$	to 1 litre	MilliQ	14.4 g	Na_2HPO_4 (dibasic anhydrous)
0.41 g	KH_2PO_4	10ml/L	penicillin-streptomycin	2.4 g	KH_2PO_4 (monobasic anhydrous)
0.142 g	Na_2HPO_4 anhydrous	60mg/L	PTU	to 1 litre	MilliQ
4.9 g	$MgSO_4\text{-}7H_2O$			pH 7.4	
to 1 litre	MilliQ				

Table 2.1: Solution recipes.

Target	RNA Pol		Primer Sequence	Product
zic1	T7	F	5' - TTT GCT TTT GGG AAG AGT GCG G - 3'	1142
		R	5' - CAG ACT GGA CTG GAG ACG AAA TGT TGT AAT ACG ACT CAC TAT AGG G - 3'	
zic2a	T3	F	5' - CCA ACA ACC ACA GCA GTT TAT CGT C - 3'	1292
		R	5 '- GCC AGA GTC AAG TTC AAG TTC ACG GCA TTA ACC CTC ACT AAA GGG AA - 3'	
zic2b	T7	F	5' - TAT CAC CAG GTG CCC AAT ACG C - 3'	1053
		R	5' - CAA ACA TCG TAA CTT GAC CCG ACG TAA TAC GAC TCA CTA TAG GG - 3'	
zic3	T7	F	5' - CAA GCA GAC TCT CAA ATG GTG GAC C - 3'	1159
		R	5' - TAA TAC GAC TCA CTA TAG GGA ACA CTG TCA CAC GGT TTC AAA GTT G - 3'	
neurog1	T3	F	5' - TCG CTC ACA ACT ACA TCT GGG C - 3'	638
		R	5' - CAT TAA CCC TCA CTA AAG GGA ATT TTT CAC GCT CGT TTT TCA GC -3'	
isl1	T7	F	5' - ATG TCC TCG CAA CTG CCA GAT AC - 3'	832
		R	5' - TAA TAC GAC TCA CTA TAG GGG CTG CCA TAC CCT TAT TTG TGA GC - 3'	
meis3	T7	F	5' - ATT GCC TTT CTT GCC TTG CCT C - 3'	735
		R	5' - TAA TAC GAC TCA CTA TAG GGA TGA CGG GAC GCA CCA GTC - 3'	
vhnf-1	T7	F	5' - AAA GAT GGA GCG GGA AGA CCT G - 3'	947
		R	5' - TAA TAC GAC TCA CTA TAG GGA GGG TTA GGA GTA AGG GAA AGG GC - 3'	

Table 2.2: mRNA *in situ* hybridization probe primer sequences.

Gene	Vector	Antibiotic	Linearize	RNA Pol
otx2		Amp	NotI	T7
hoxa2		Amp	Asp718	T3
wnt1	pCR4-TOPO	Amp	NotI	T3
myod		Amp	XbaI	T7
hoxb4		Amp	KpnI	T3
cyp26a1	pBluescript KS+	Carb	SalI	T7
krox20			PstI	T3
dlx2a			XbaI	T7
hoxd4a		Carb	EcoR1	T7

Table 2.3: mRNA *in situ* hybridization probe constructs.

Target	Sequence	Type	Previously Published
Zic2a	CTC ACC TGA GAA GGA AAA CAT CAT A	splice-blocking	Nyholm et al. 2007
Zic2b	CAC GAA TTG AAA TAA TTA CCA GTG T	splice-blocking	n/a
Zic3	GGA ATT TAA TTT CCT TAC CTG TGT G	splice-blocking	n/a
Cyp26a1	CGC GCA ACT GAT CGC CAA AAC GAA A	translation-blocking	Kudoh et al 2002
Aldh1a2	GCA GTT CAA CTT CAC TGG AGG TCA T	translation-blocking	Begemann et al., 2001
p53	GAC CTC CTC TCC ACT AAA CTA CGAT	translation-blocking	Robu et al., 2007

Table 2.4: Morpholino oligonucleotide sequences.

Morpholino(s)	Concentration	Control
Zic1MO	2ng/nl	un-injected
Zic2aMO	2ng/nl	un-injected
Zic2bMO	2ng/nl	un-injected
Zic3MO	3ng/nl	un-injected
Zic2a2b3MO	2ng/nl:2ng/nl:3ng/nl	un-injected
Zic2a2b3MO (+p53MO)	2ng/nl:2ng/nl:3ng/nl:1ng/nl	1ng/nl p53MO
Zic2a2b (+p53MO)	2ng/nl:2ng/nl:1ng/nl	1ng/nl p53MO
Cyp26a1MO	2ng/nl	1ng/nl p53MO
Aldh1a2MO	2ng/nl	1ng/nl p53MO

Table 2.5: Morpholino concentrations.

Target	Vector	Direction	Enzyme	Primer Sequence
Zic2a	pCS2+	F	BamHI	5' - CAC AGG ATC CAC CAT GTT ACT GGA CGC AGG GCA TCA G - 3'
		R	EcoRI	5' - CAC AGA ATT CCT GTT TTC TTT ATC GGG TCC TCC TG - 3'
Aldh1a2	pCS2+	F	BamHI	5’ - CAC AGG ATC CAC CAT GGG ATG ACC TCC AGT GAA GTT GAA CTG - 3’
		R	EcoRI	5’ - CAC AGA ATT CCC CAC CAA AGG ATA ACG GCT AAC - 3’

Table 2.6: mRNA over-expression primer sequences.

Primary Antibody	Host Organism	Immunogen Organism	Dilution	Company
zn5/zn8 Anti-Alcam MC	Mouse	Zebrafish	1/250	ZIRC
rmo44 Anti-160 kD NF-M MC	Mouse	Rat	1/250	Sigma
6-11B-1 Anti-Acetylated Tubulin MC	Mouse	Chlamydomonas	1/500	Sigma
PE Rabbit Anti-Active Caspase-3	Rabbit	Goat	1/400	BD Pharmigen

Table 2.7: Description of antibodies.

Primer	Sequence
Zic2a RTP-L1	5' - CCA GCT CTC TTC GAA AGC AT - 3'
Zic2a RTP-R1	5' - GAG GAC TCA TAA CCA GAA CTT GC - 3'
Zic2a RTP-L2	5' - AGA TAC ACA AAA GAA CAC ACA CAG G - 3'
Zic2a RTP-R2	5' - ATG GTT TGT CTG ACG TGT GG - 3'
Zic2b RTP-L1	5' - GGA GAA TTT GAA AAT ACA CAA ACG - 3'
Zic2b RTP-R1	5' - TTC GAA TTC ACA CAG GAA CG - 3'
Zic2b RTP-L2	5' - TGC GAC AAG TCC TAC ACA CAC - 3'
Zic2b RTP-R2	5' - TAT TGG AGC CTG ATC CTC GT - 3'
Zic3 RTP-L1	5' - ATT CAC AAA AGA ACT CAC ACA GGT - 3'
Zic3 RTP-R1	5' - GTC GCA GCC ATC GAA CTC - 3'
Zic3 RTP-L2	5' - TGC AAA GTG TGT GAC AAG TCC - 3'
Zic3 RTP-R2	5' - TCT GAG CCT TGT GAT TCG TG - 3'
Cyp26a1 RTP - L2	5' - CCA ATG TCC ATG GAG TTC AA - 3'
Cyp26a1 RTP - R2	5' - TCA CCT CCT GCT GGA TCA C - 3'
Aldh1a2 – F	5’ – AAC CAC TGA ACA CGG ACC TC – 3’
Aldh1a2 – R	5’ – ATG AGC TCC AGC ACA CGT 3 – 3’
EF1α-F	5’ – CCT TCG TCC CAA TTT CAG G – 3’
EF1α-R	5’ – CCT TGA ACC AGC CCA TGT – 3’

Table 2.8: Real-time PCR primers.

2.12 Literature Cited

Alexa, K., Choe, S.K., Hirsch, N., Etheridge, L., Laver, E., and Sagerstrom, C.G. (2009). Maternal and zygotic aldh1a2 activity is required for pancreas development in zebrafish. PLoS One *4*, e8261.

Begemann, G., Schilling, T.F., Rauch, G.J., Geisler, R., and Ingham, P.W. (2001). The zebrafish neckless mutation reveals a requirement for raldh2 in mesodermal signals that pattern the hindbrain. Development *128*, 3081-3094.

Feng, L., Hernandez, R.E., Waxman, J.S., Yelon, D., and Moens, C.B. (2010). Dhrs3a regulates retinoic acid biosynthesis through a feedback inhibition mechanism. Dev Biol *338*, 1-14.

Gongal, P.A., and Waskiewicz, A.J. (2008). Zebrafish model of holoprosencephaly demonstrates a key role for TGIF in regulating retinoic acid metabolism. Hum Mol Genet *17*, 525-538.

Higashijima, S., Hotta, Y., and Okamoto, H. (2000). Visualization of cranial motor neurons in live transgenic zebrafish expressing green fluorescent protein under the control of the islet-1 promoter/enhancer. J Neurosci *20*, 206-218.

Kimmel, C.B., Ballard, W.W., Kimmel, S.R., Ullmann, B., and Schilling, T.F. (1995). Stages of embryonic development of the zebrafish. Dev Dyn *203*, 253-310.

Kudoh, T., Wilson, S.W., and Dawid, I.B. (2002). Distinct roles for Fgf, Wnt and retinoic acid in posteriorizing the neural ectoderm. Development *129*, 4335-4346.

Livak, K.J., and Schmittgen, T.D. (2001). Analysis of relative gene expression data using real-time quantitative PCR and the 2(-Delta Delta C(T)) Method. Methods *25*, 402-408.

Maden, M., Sonneveld, E., van der Saag, P.T., and Gale, E. (1998). The distribution of endogenous retinoic acid in the chick embryo: implications for developmental mechanisms. Development *125*, 4133-4144.

Maurus, D., and Harris, W.A. (2009). Zic-associated holoprosencephaly: zebrafish Zic1 controls midline formation and forebrain patterning by regulating Nodal, Hedgehog, and retinoic acid signaling. Genes Dev *23*, 1461-1473.

Nasevicius, A., and Ekker, S.C. (2000). Effective targeted gene 'knockdown' in zebrafish. Nat Genet *26*, 216-220.

Nyholm, M.K., Wu, S.F., Dorsky, R.I., and Grinblat, Y. (2007). The zebrafish zic2a-zic5 gene pair acts downstream of canonical Wnt signaling to control cell proliferation in the developing tectum. Development *134*, 735-746.

Ohishi, K., Nishikawa, S., Nagata, T., Yamauchi, N., Shinohara, H., Kido, J., and Ishida, H. (1995). Physiological concentrations of retinoic acid suppress the osteoblastic differentiation of fetal rat calvaria cells in vitro. Eur J Endocrinol *133*, 335-341.

Pillay, L.M., Forrester, A.M., Erickson, T., Berman, J.N., and Waskiewicz, A.J. (2010). The Hox cofactors Meis1 and Pbx act upstream of gata1 to regulate primitive hematopoiesis. Dev Biol *340*, 306-317.

Robu, M.E., Larson, J.D., Nasevicius, A., Beiraghi, S., Brenner, C., Farber, S.A., and Ekker, S.C. (2007). p53 activation by knockdown technologies. PLoS Genet *3*, e78.

Thisse, B., Heyer, V., Lux, A., Alunni, V., Degrave, A., Seiliez, I., Kirchner, J., Parkhill, J.P., and Thisse, C. (2004). Spatial and temporal expression of the zebrafish genome by large-scale in situ hybridization screening. Methods Cell Biol *77*, 505-519.

Waxman, J.S., and Yelon, D. (2011). Zebrafish retinoic acid receptors function as context-dependent transcriptional activators. Dev Biol *352*, 128-140.

Westerfield, M. (2000). The zebrafish book. A guide for laboratory use of zebrafish (Danio rerio). Univ. of Oregan Press., Eugene, OR.

White, R.J., Nie, Q., Lander, A.D., and Schilling, T.F. (2007). Complex regulation of cyp26a1 creates a robust retinoic acid gradient in the zebrafish embryo. PLoS Biol *5*, e304.

Chapter 3: Results and Discussion

Retinoic acid (RA) signaling is essential in anterior-posterior patterning of the neural tube and functions to define regional identity of hindbrain segments (Glover et al., 2006). As severe teratogenic defects result from aberrant RA levels, a considerable amount of research has focused on the mechanisms of RA regulation. Enzymes involved in RA metabolism, including Aldh1a2 (RA -synthesis) and Cyp26a1 (RA -degradation) are key in controlling RA levels. Mutation of either gene causes severe truncation or expansion of posterior tissue, respectively, and results in murine embryonic lethality (Niederreither et al., 1999; Niederreither et al., 2000; Sakai et al., 2001). While the requirement for RA metabolism enzymes is apparent, the factors acting upstream to initiate and maintain metabolism gene expression are largely unknown. This chapter will evaluate the hypothesis that Zic transcription factors play a key role in initiation and maintenance of RA metabolism gene expression during zebrafish embryogenesis.

3.1 Zic transcription factors are expressed in largely overlapping regions during embryonic development

To ascertain which Zic transcription factors could regulate embryonic initiation of RA metabolism, we first examined which of the seven zebrafish *zics* are expressed in regions correlating with RA metabolism genes. During gastrulation the main enzymes regulating RA levels are cytochrome p450 oxidase, Cyp26a1, responsible for RA hydroxylation (targeting its degradation), and aldehyde dehydrogenase 1a2, Aldh1a2, which synthesizes RA from retinal. *cyp26a1* transcription is initiated early in zebrafish embryogenesis, expressed in presumptive neural ectoderm at 50% epiboly (Thisse et al., 2004). During early somitogenesis (2 – 15 somites, S), *cyp26a1* mRNA is found in the forebrain, midbrain, and part of the tailbud. *cyp26a1* expression becomes restricted to parts of the retina, caudal notochord, and tailbud by late somitogenesis stages (15S-24S) (Thisse et al., 2004). *aldh1a2*

transcription is also initiated early in development, and is found in the embryonic margin at 50% epiboly and later in lateral plate mesoderm (75% epiboly) (Maves and Kimmel, 2005). Subsequently, *aldh1a2* expression is restricted to the eyes and somites beginning at 18S.

Using *in situ* hybridization in conjunction with known expression data, we determined that *zic1, zic2a*, *zic2b,* and *zic3* are the best candidates for initiation of RA metabolism genes because they are expressed at the earliest stages of development (Elsen et al., 2008; Nyholm et al., 2007; Thisse et al., 2004). Although *zic1* is not yet expressed at 50% epiboly, *zic2a*, *zic2b,* and *zic3* are all expressed broadly at this developmental stage (Figure 3.1 A, F, K, P). By 75% epiboly and tailbud stage, *zic1* and *zic2a* are expressed in discrete regions consistent with the anterior neural ectoderm and the domain of *cyp26a1* expression (Figure 3.1 B-D, G-I). *zic2b* and *zic3* maintain broad dorsal expression domains at 75% epiboly, in regions that overlap with both the anterior *cyp26a1* expression and the dorsal domain of *aldh1a2* (Figure 3.1 L, Q).

As development continues, the overlapping regions of expression between *zics* and *aldh1a2* or *cyp26a1* become less obvious. Shown here, *zic1*, *zic2a*, *zic2b*, and *zic3* are expressed within the dorsal hindbrain and extend down the spinal cord (Figure 3.1 E, J, O, T). However, the level and degree of spinal cord expression differs, with *zic1* and *zic2b* expressed strongly and extending further posteriorly than *zic2a* and *zic3* (Figure 3.1 E, J, M-O, R-T). At 18S, *aldh1a2* is expressed in the somites, located lateral to the neural tube expression of *zics* (Maves and Kimmel, 2005). Therefore if Zics mediate *aldh1a2* expression at this stage – they must act in a cell non-autonomous fashion. Interestingly, similar to *cyp26a1* expression, *zic2b* and *zic3* are expressed in a region consistent with caudal notochord (Figure 3.1 O, T) (Thisse et al., 2004).

There is evidence suggesting a regulatory interaction between Zic1 and the RA degrading enzyme, *cyp26a1* (Maurus and Harris, 2009). We have found considerable expression overlap between the earliest expressed Zic

transcription factors and *cyp26a1* and *aldh1a2*, especially within early epiblast and dorsal embryonic tissue during gastrulation. Based on these data, we chose to focus first on *zic2a*, *zic2b*, and *zic3* as these candidates are expressed at early stages indicative of initiation of RA metabolism.

3.2 Zics act upstream of early retinoic acid metabolism genes, *cyp26a1* and *aldh1a2*

Zebrafish embryos lacking Zic1 have defects in maintenance of anterior *cyp26a1* expression, and display increased RA signaling in the forebrain (Maurus and Harris, 2009). These studies did not address the question of whether *zic* genes initiate RA metabolism gene expression. To address this further, we determined whether *zic* genes are candidates for initiation of *cyp26a1* and *aldh1a2* – the main metabolism genes expressed during gastrulation. Due to the propensity for redundancy, we chose to look at all three transcription factors (Zic2a, Zic2b, and Zic3) by gene knockdown analysis. Splice-blocking morpholinos were designed to knockdown translation of Zic2a (Nyholm et al., 2007), Zic2b, and Zic3 to assay whether they regulate *cyp26a1* and *aldh1a2* expression. Upon examining resulting phenotypes we determined that Zic3 is dispensable and was removed from the cocktail.

We found that embryos injected with both Zic2a and Zic2b morpholinos (hereafter known as Zic2a2bMO) display a reduction in *cyp26a1* and *aldh1a2* expression at 65% epiboly (Figure 3.2). While both *cyp26a1* expression level and domain appears reduced (Figure 3.2 A, B), *aldh1a2* levels appear normal with a reduced domain size (Figure 3.2 C, D). We confirmed the reduction of *aldh1a2* using Quantitative Real-Time PCR and found that in Zic2a2b-depleted embryos *aldh1a2* expression is reduced 30% (p-value<0.0001) compared to control expression levels (Figure 3.2 E).

Our attempts to rescue morphant phenotypes using Zic2a mRNA over-expression resulted in 95% embryonic lethality. This difficulty has been

noted by other groups, and is attributed to a requirement for Zics during early mechanisms of gastrulation (Maurus and Harris, 2009; Sanek and Grinblat, 2008).

Of note, *zic2a* is not expressed within the lateral mesoderm (*aldh1a2*-positive domain), however contributes to reduction in *aldh1a2* transcription within Zic2a2b morphants. As *zic2a* and *zic2b* are both expressed before 50% epiboly, it is possible that knockdown of Zic2a2b is affecting early embryonic events within pluripotent epiblast cells of the blastula. Alternatively, previous work has identified non-cell-autonomous regulatory functions of Zic2a in repressing the transcription factor *six3b* within the forebrain (Sanek et al., 2009). It is possible that a similar non-cell autonomous mechanism is occurring during early embryogenesis.

Embryonic depletion of Zic2a2b results in reduced expression of RA synthesis (*aldh1a2*) and RA degradation (*cyp26a1*) genes. We next carried out a series of experiments to determine whether the reduction in RA metabolism genes causes alterations to RA responsive signaling levels or hindbrain segmentation in Zic2a2b morphants.

3.3 Zic-depletion causes mild alterations to RA-responsive genes and hindbrain patterning

Within Zic2a2b morphants there is a reduction in both RA synthesis, *aldh1a2*, and degradation, *cyp26a1*, gene expression (Figure 3.3 A). Reduction of *cyp26a1* alone results in increased levels of RA signaling due to a loss of RA degradation, while reduction of *aldh1a2* results in reduced RA signaling due to loss of synthesis. To ascertain the overall level of RA signaling in Zic2a2b3-depleted embryos, we carried out *in situ* hybridization for the RA-responsive genes *variant hepatic nuclear factor 1 (vhnf1), hoxb1a, hoxd4,* and *myeloid ecotropic retroviral integration site-3* (*meis3).* These genes are known to be downstream of RA signaling such that with increased RA, there is upregulation and with reduced RA these genes are

downregulated (Figure 3.3 B) (Hernandez et al., 2004; Huang et al., 2002; Kudoh et al., 2002; Moroni et al., 1993; Zhang et al., 2000). In Zic2a2b3-depleted embryos, there is a strong reduction in *meis3* and a mild reduction in *hoxd4* expression within the presumptive hindbrain (Figure 3.3 C, D, G, H). However, there is no significant change in *vhnf1* or *hoxb1a* expression (Figure 3.3 E, F, I, J). Although these effects were milder than anticipated, these data are consistent with a mild reduction in RA signaling in Zic2a2b3 morphants.

The anterior neural marker *otx2* is also downregulated in Zic2a2b3 morphants (Figure 3.3 C, D). Interestingly, *cyp26a1*-depleted embryos have reduced *otx2* expression levels (Kudoh et al., 2002) - suggesting a potential regulatory mechanism whereby Zic2a2b3 function upstream of both *cyp26a1* and *otx2* in defining early neural regions.

The predominant role for RA is in mediating hindbrain segmentation through regulation of *hox* gene expression (Glover et al., 2006). *Hox* genes exhibit concentration dependent activation by RA (Simeone et al., 1991). Increased RA levels, by exogenous treatment or mutation of degradation genes (*Cyp26a1*), cause embryonic posteriorization resulting from expansion of posterior *Hox* expression (Niederreither and Dolle, 2008; Sakai et al., 2001; Simeone et al., 1991). RA-deficiency through mutation of synthesis genes (*Aldh1a2*) causes truncations with loss of posterior *Hox* expression domains (Durston et al., 1989; Niederreither and Dolle, 2008; Niederreither et al., 2000).

We asked whether the reduction in RA metabolism gene expression in Zic2a2b morphants causes defects in hindbrain patterning. *In situ* hybridization for hindbrain markers (*krox20*, *val*, *hoxb4*, *hoxb1a, egfl6*) was used to examine hindbrain segmentation and rhombomere morphology. We found that overall hindbrain segmentation is overtly normal, as all rhombomeres are successfully formed, however rhombomeres (r) 3 and 5 (*krox20*) are reduced in size (Figure 3.4 C, D) and there is reduced *hoxa2* expression within r2-r6 (Figure 3.4 A, B). Notably, the *hoxb4* expression domain within the posterior hindbrain and spinal cord is reduced in size

(Figure 3.4 C, D). Other regions within the hindbrain appear normal: r4 (*hoxb1a*; Figure 3.4 E, F), r5 and r6 (*val*; Figure 3.4 G, H), and r2, r4, and r6-7 (*egfl6*; Figure 3.4 I-L). This suggests that there is a reduction in posterior neural domain (*hoxb4* within posterior hindbrain and spinal cord), however the reduction in RA-signaling in Zic2a2b3 morphants is not sufficient to cause a complete loss of posterior regions. Of note, the zebrafish *neckless* (*aldh1a2*) mutants show a non-cell autonomous reduction in *hoxb4* expression within the hindbrain, similar to Zic2a2b3-depleted embryos (Begemann et al., 2001). Additionally, the reduction of *krox20*-expressing rhombomeres (3/5) is consistent with murine data, where Zic2 is involved in size determination of rhombomeres 3 and 5 (Elms et al., 2003). Regulation of *hoxa2* within the hindbrain remains poorly understood, although its expression is upregulated in response to exogenous RA in the rat lung (Cardoso et al., 1996). The reduction in *hoxa2* could result from reduced RA signaling levels, or alternatively, it could be a RA-independent transcriptional target (direct or indirect) of Zic2a2b.

The requirement for Zic2a2b in regulating the domain of *hoxb4*-expression was analyzed by comparing hindbrain *wnt1*/*krox20*/*hoxb4* expression in embryos injected with morpholino combinations - Zic1, Zic2a, Zic2a2b, Zic12a2b, Zic2a2b3. While, Zic1MO-injection cause no alteration to hindbrain patterning (Figure 3.5 A, B), the *hoxb4* expression domain is reduced in Zic2a-depleted embryos (Figure 3.5 C). An even greater reduction in length is observed with Zic2a2bMO-, Zic12a2bMO-, and Zic2a2b3MO-injection (Figure 3.5 D, E, F). Therefore, of the co-expressed *zics*, Zic2a2b appear most important in specification of posterior hindbrain and the spinal cord identity.

Mouse studies have shown that both *Cyp26* and *Raldh2* are necessary for embryonic development, with mutations in each gene resulting in anterior-posterior patterning defects and embryonic lethality (Niederreither et al., 1999; Sakai et al., 2001). Interestingly, heterozygous loss of *Raldh2* in a *Cyp26* mutant rescues embryonic lethality and many patterning defects,

suggesting dynamic interplay between these two enzymes during development (Niederreither et al., 2002). This suggests that the interplay between enzyme activities is crucial. Thus, the RA level itself may not be as important as the variations of RA levels within adjacent tissues. Therefore it is possible that in Zic2a2b3 morphants, loss of both *cyp26a1* and *aldh1a2* allows acquisition of a similar equilibrium.

3.4 Zic2a2b-depletion reduces retinoic acid signaling during somitogenesis

Thus far, we have studied alterations in RA signaling in Zic-depleted embryos using indirect assays such as RA-responsive gene expression and hindbrain patterning. The murine *RARE:LacZ* reporter strain has been useful in determining areas and levels of RA signaling during mouse development (Rossant et al., 1991). However, in zebrafish there are surprisingly few reagents available to study levels and regions of RA signaling *in vivo*. To accomplish this we obtained the transgenic zebrafish Tg(12xRARE-ef1a:gfp)sk71 (*RARE:gfp*) which contains twelve Retinoic Acid Response Elements (RAREs) upstream of a ubiquitous promoter linked to *gfp* (Figure 3.6 A) (Feng et al., 2010; Waxman and Yelon, 2011). Using such a reporter facilitates the identification of regions with active RA signaling as detected by fluorescence or *gfp* mRNA *in situ* hybridization. The sensitivity of this transgenic line was examined by assaying its response to alterations in RA levels.

In control DMSO treated embryos at 48 hpf and 26 hpf, the predominant region of RA signaling, as demarcated by the 12xRARE transgenic line, is within the posterior hindbrain and spinal cord (Figure 3.6 B, E, H, K, N). This region is close to the main site of RA synthesis, the somites, and the most responsive to alterations in RA (Begemann et al., 2001; Molotkova et al., 2005). Interestingly, at 48 hpf there is a second RA signaling center detectable by fluorescence and *in situ* hybridization within the ventral eye (Figure 3.6 H', K). An additional region in the dorsal eye is only

detectable by *in situ* hybridization because this assay is more sensitive to low *gfp* signal (Figure 3.6 K). *In situ* hybridization also identifies *RARE:gfp* signal within the yolk syncitial layer, ventral to the hindbrain (48 hpf, 26 hpf; Figure 3.6 K, N).

The fluorescence domain increases at both stages in response to 5nM RA treatment - expanding further anteriorly into the hindbrain and posteriorly down the spinal cord (Figure 3.6 C, F, I, L, O). There is likely a complex mechanism regulating RA signaling within the eye, as exogenous addition of RA causes loss of the dorsal *gfp*-positive region while the ventral region is maintained (Figure 3.6 I', L). The eye is morphologically smaller with RA treatment, suggesting that the dorsal domain may be completely lost or mis-specified. Blocking RA synthesis with 5 μM DEAB treatment results in loss of all RA signaling – no fluorescence or *in situ* coloration is visible at 26 hpf or 48 hpf (Figure 3.6 D, G, J, J', M, P).

The Tg(12xRARE-ef1a:gfp)sk71 transgenic line displayed fluorescence indicative of RA signaling consistent with previous RARE transgenics, however variations in the minimal promoter and number of RARE elements alters strength and regions of expression. Perz-Edwards et al. (2001) described four 3xRARE transgenic lines they created: all had ventral eye and neural tube fluorescence; however, additional regions including the notochord, dorsal eye, heart, and pronephric ducts were also present. Of note, although using *in situ* hybridization allows earlier detection of *gfp* as compared to fluorescence, we are unable to accurately detect the transgene before 24 hpf. This limitation prevents analysis of RA signaling levels at early embryonic stages that would better reflect when RA metabolism genes are first transcribed. Further, *aldh1a2* is expressed within the developing eye by 20 hpf and shortly after its initiation, RA is synthesized within the eye. There is a delay in *gfp* detection in the transgenic zebrafish, as RA signaling within this region is still not visible at 26 hpf (Figure 3.6 N).

As the *RARE:gfp* transgenic line labels posterior RA-signaling regions, we asked whether the early reduction in RA metabolism genes corresponds

to an alteration in later embryonic RA signaling levels. As compared to control *gfp* levels (Figure 3.7 A, B), there is a strong reduction in *gfp* expression in 74.5% of the Zic2a2b-morphant embryos (Figure 3.7 C, D, E; p-value=0.0004). This suggests that, while early RA-dependent processes may compensate for alterations to RA levels, there is in fact a reduction in RA signaling within Zic2a2b-depleted embryos.

To test the hypothesis that the reduction in RA signaling within Zic2a2b morphants is a result of reduced *aldh1a2* expression, we compared RA signaling in Aldh1a2-depleted and Cyp26a1-depleted embryos. Strikingly, there is a comparable reduction in RA signaling levels with Zic2a2b and Aldh1a2 knockdown, with strong reduction of *gfp* transcript (Figure 3.8 B, C) as compared to controls (Figure 3.8 A). *gfp* levels appear unaltered in Cyp26a1MO-injected embryos (Figure 3.8 D).

We have identified a novel regulatory mechanism whereby Zic2a2b regulates RA levels, likely by regulating *aldh1a2* transcription. While early RA-dependent processes are mildly defective in Zic2a2b-depleted embryos, alteration in RA signaling levels at 26 hpf suggests a later developmental defect. In fact, during neural tube development, 26 hpf is a key time-point for specification and differentiation of hindbrain neural classes (Chandrasekhar, 2004).

3.5 Vagal neurons are sensitive to alterations in retinoic acid levels

Although Zic2a2b knockdown results in reduced RA signaling levels at 26 hpf, there are only mild effects on early RA-responsive gene expression and hindbrain patterning. To determine the developmental consequence of the reduction in RA signaling, we chose to look at a later RA-dependent process: development of vagal motor neurons within the posterior hindbrain and spinal cord (Linville et al., 2004). Using the *islet-1:gfp* transgenic line, we sought to analyze development of hindbrain branchiomotor neurons in response to Zic2a2b depletion (Higashijima et al., 2000).

Several classes of hindbrain branchiomotor neurons are easily visualized by confocal microscopy of the transgenic zebrafish *islet-1:gfp.* Trigeminal neuron cell bodies are located within rhombomeres 2 and 3, facial neurons within rhombomere 5 and 6 and the vagal neuron domain extends from the posterior hindbrain down the spinal cord (DMSO; Figure 3.9 A, D, G) (Higashijima et al., 2000). Using ImageJ software we quantified the area and length of vagal neuron domain within DMSO-treated control embryos and found the average area to be 5481 μm^2 (SD = 321 μm^2; Figure 3.9 H, J) and anterior-posterior length to be 165 μm (SD = 4.5 μm; Figure 3.9 I, J). Upon 5 nM RA treatment, the vagal domain is greatly expanded with more neural cell bodies visible (Figure 3.9 B, E, G). Both the area, at 10,353 μm^2 (SD = 1448 μm^2; Figure 3.9 H, J; p-value≤0.005), and length, at 214 μm (SD = 11 μm; Figure 3.9 I, J; p-value≤0.003), of the domain is significantly increased. Alternatively, treatment with 5 μM diethylaminobenzaldehyde (DEAB), a pharmacological inhibitor of RA synthesis, significantly alters embryonic patterning such that all posterior rhombomeres are lost. The vagal domain is almost undetectable in these embryos (Figure 3.9 C, F, G). DEAB treatment also results in mispatterning of anterior branchiomotor neuron classes such that it is difficult to identify trigeminal, facial, and possible remnants of vagal neuron populations. The area of vagal neurons in DEAB treated embryos is 1683 μm^2 (SD = 1264 μm^2; Figure 3.9 H, J; p-value≤0.005) with a length of 65 μm (SD = 20 μm; Figure 3.9 I, J; p-value≤0.003). While alterations to the vagal neurons are easily visible with the high treatment concentrations used here, it is important to note that slight alterations in RA levels would result in milder defects.

3.6 Zic2a2b knockdown causes loss of vagal neurons

Zic2a2b-depleted embryos have reduced RA signaling levels within the posterior hindbrain and spinal cord. To ascertain whether this reduction in RA signaling causes a concomitant defect in vagal motor neurons, Zic2a2b knockdown was introduced in *islet-1:gfp* transgenics. Embryos were grown in DMSO or treated with exogenous RA (5 nM) or DEAB (5 μM) to determine if RA supplementation could rescue phenotypes. Zic -depleted embryos have significantly reduced vagal neuron area (6555 μm^2, SD = 415 μm^2; p-value≤0.05) and length (147 μm, SD = 9.5 μm; p-value≤0.05) as compared to control embryos in the DMSO treatment (area of 8947 μm^2, SD = 174 μm^2; length of 168 μm, SD = 1.4 μm; Figure 3.10 A, D, M, N, O). This reduction in vagal neuron domain would be expected with a mild reduction in RA levels. In many cases the medial-lateral width of each vagal population was increased in morphants – suggesting a possible migrational error as vagal neurons are born medially and migrate laterally during development (Chandrasekhar et al., 1997).

With treatment of 5 nM RA, the vagal neuron domain in control embryos is increased as noted previously (Figure 3.10 B, E, H, K). Interestingly, the vagal neuron defects in Zic-depleted embryos are rescued with this concentration of RA. Both the area (10,571 μm^2, SD = 1408 μm^2; p-value≤0.05) and the length of vagal domain (234 μm, SD = 17 μm; p-value≤0.05) are increased to control values (12,536 μm^2, SD = 412 μm^2; 224 μm, SD = 13 μm; Figure 3.10 M, N, O). Finally, further reducing RA levels using 5 μM DEAB treatment causes a significant reduction, or almost complete loss, of vagal neurons in both control and Zic2a2b-depleted embryos (Figure 3.10 C, F, I, L, M, N, O).

The physiological level of RA is hypothesized to be 3 nM (Maden et al., 1998; Ohishi et al., 1995). Therefore treatment with above physiological levels (5 nM RA) is expected to promote posterior fates in both control and Zic –depleted embryos. This was observed as the expansion of vagal neuron

domain in both cases. Due to reduced RA levels in Zic –depleted embryos, we postulate that supplementation with below physiological levels (1 nM) of RA, a concentration that causes no significant alteration to control embryos, may be sufficient to rescue the neural phenotype.

As noted previously, there is a significant reduction in the vagal neuron area with Zic-depletion, at 4979 μm^2 (DMSO; SD = 1443 μm^2), as compared to controls (DMSO; area of 7382 μm^2, SD = 377 μm^2; p-value≤0.01). Additionally, reduction in the length of the vagal domain is observed in Zic morphants, at 126 μm (SD = 14 μm; control length of 177 μm, SD = 11 μm; Figure 3.11 A, D, G-I).

There is as a mild, but not statistically significant, increase in vagal neuron area and length in control embryos in response to 1 nM RA treatment. Strikingly, with low dose treatment of RA, the vagal neuron area of Zic -depleted embryos, at 8616 μm^2 (SD = 1929 μm^2), is rescued to values similar to control embryos (8964 μm^2, SD = 1139 μm^2). There is a significant increase in the length of vagal domain in morphants treated with RA (156 μm, SD = 16 μm) compared to morphants in DMSO treatment (126 μm, SD = 14 μm; p-value≤0.05). Interestingly, while the resulting length is similar to control embryos (DMSO treatment), this length is still significantly reduced compared to control RA treated embryos (191 μm, SD = 9 μm; Figure 3.11 G, H, I). By further reducing RA levels with DEAB treatment, there is a roughly equivalent loss of vagal neuron domain in both Zic2a2b morphants and control embryos (Figure 3.11 C, F, G, H, I).

In summary, the posterior-most class of branchiomotor neurons, the vagal neurons, is sensitive to alterations in RA such that increased RA causes expansion of area and length of this neuron population. Conversely, reduction in RA reduces this population. The reduction in RA signaling levels in Zic2a2b-depleted embryos elicits a reduction in size of the vagal neuron domain – a reduction that is completely rescued with RA treatment.

3.7 Vagal neuron defect in Zic2a2b morphants is reminiscent of *aldh1a2* depletion

Our data is consistent with a model whereby Zic2a and Zic2b act upstream of RA metabolism by activating transcription of *aldh1a2*. This model is supported by the early reduction in *aldh1a2* transcript levels in Zic2a2b morphants. Additionally, the reduction in RA signaling levels within *RARE:gfp* transgenics is almost identical in Zic2a2b and Aldh1a2-depleted embryos. Further, the reduction of vagal neurons in Zic2a2b morphants is rescued by treatment with the product of the Aldh1a2 catalyzed reaction, RA.

We next asked whether the reduction of vagal neuron domain within Zic2a2b morphants is identical to that observed upon Aldh1a2-depletion. To reduce *aldh1a2* levels we used morpholino-mediated knockdown and analyzed vagal neurons via fluorescent visualization of *islet-1:gfp*. The reduction in vagal domain within Aldh1a2-depleted and Zic2a2b-depleted embryos is morphologically similar (Figure 3.12 A-C). Additionally, there is a significant reduction in length of vagal domain within Aldh1a2-depleted (129 μm, SD = 16 μm; p-value=0.01) and Zic2a2b-depleted (136 μm, SD = 14 μm; -value=0.01) embryos compared to controls (173 μm, SD = 1 μm). Notably, these lengths are not significantly different from each other (Figure 3.12 D, E). The comparable reduction in vagal neuron length supports the hypothesis that Zic2a2b act upstream of *aldh1a2*. While the zebrafish *neckless* mutant has a complete loss of vagal neurons, due to a combination of possible factors (incomplete knockdown by morpholinos, compensation by later-expressed Zics, feedback regulation, or other *aldh1a2* regulators) the phenotype in Zic2a2b morphants is consistent with a reduction, not complete loss, of *aldh1a2* (Begemann et al., 2004).

3.8 Conclusions

We have identified a novel regulatory mechanism between Zic2a2b transcription factors and early RA signaling levels. We propose a model

whereby Zic2a and Zic2b act either directly or indirectly upstream of both RA synthesis (*aldh1a2*) and degradation (*cyp26a1)* genes in an early embryo. Due to stage limitations of the *RARE:gfp* transgenic zebrafish, we were unable to ascertain alterations to RA levels at stages indicative of initiation of RA metabolism. However, there is a persistent reduction in RA signaling in Zic2a2b morphants at 26 hpf; this reduction is indistinguishable from that observed in embryos depleted of the main RA synthesis enzyme, Aldh1a2. Consistent with reduced RA levels, Zic2a2b knockdown causes reduced vagal motor neurons within the posterior hindbrain and spinal cord, a phenotype nearly identical to Aldh1a2-depleted embryos. Strikingly, this defect is rescued by exogenous RA treatment.

While the role and requirement for RA metabolism genes has been thoroughly studied, little is known about the upstream regulators of these factors. During mouse development, Hoxa1-Pbx1 (Pre-B-cell leukemia homeobox 1) complexes directly regulate Raldh2 transcription within mesodermal tissue (Vitobello et al., 2011). Additionally, deficiencies in zebrafish Tgif and Hmx4 cause defects associated with reduced RA levels and morpholino -mediated knockdown of Tgif or Hmx4 results in reduced *aldh1a2* transcription (Gongal et al., 2008; Gongal et al., 2011). Interestingly, Tgif –depletion results in a concomitant reduction in *cyp26a1* mRNA levels, similar to defects observed in Zic -depleted embryos. Further illustrating the relationship between RA metabolism genes, the Cyp26a1 murine mutant has defects associated with increased RA levels (Sakai et al., 2001). Notably, rescue of these defects is observed with heterozygous disruption of *Aldh1a2* in a *Cyp26a1* murine mutant, suggesting co-dependency between these genes; less RA degradation is necessary when RA synthesis is reduced (Niederreither et al., 2002). Together, these findings suggest an elegant method of regulating RA levels during early embryogenesis, whereby transcription factors (such as Zic2a and Zic2b) regulate expression of both RA synthesis and degradation genes. Future experiments will investigate Tgif, Hmx4, and Zics to examine shared regulatory mechanisms.

3.9 Figures

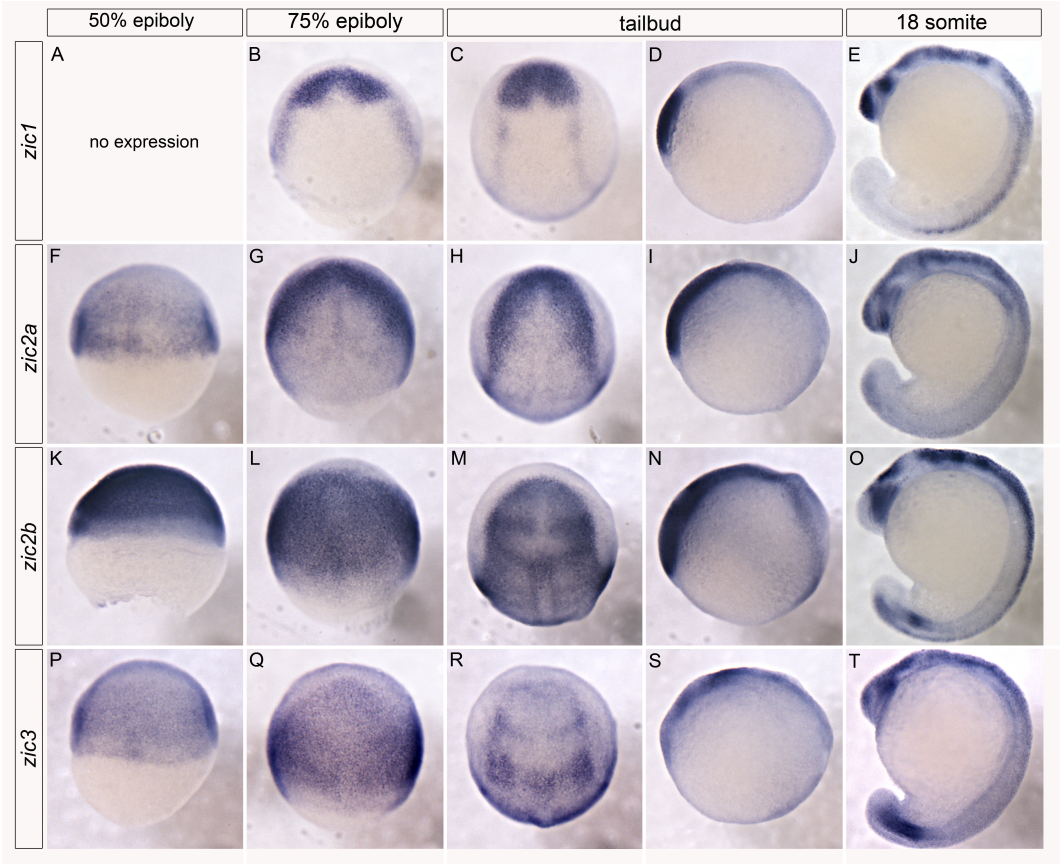

Figure 3.1: Expression of *zic1*, *zic2a*, *zic2b*, and *zic3* transcription factors.
Comparison of domains of the earliest-expressed Zic transcription factors: *zic1*, *zic2a*, *zic2b*, and *zic3* as detected by *in situ* hybridization. *zic1* is not visible until 75% epiboly where it is expressed within the presumptive anterior neural tissue (A, B). This region is maintained at tailbud stage (C, D) and by 18-somites (S) *zic1* is expressed strongly in the telencephalon, midbrain-hindbrain boundary (MHB), dorsal hindbrain (HB) and dorsal spinal cord (SC; E). *zic2a* initiates earlier, at 50% epiboly, and becomes restricted as a chevron-shaped domain at 75% epiboly and tailbud (G, H, I). By 18S, *zic2a* transcript is found in the anterior forebrain, ventral eye, dorsal HB and SC (J). *zic2b* is expressed in a broad domain (K, L; 50%, 75% epiboly). At the tailbud stage expression is strongest within the eye, MHB, and HB (M, N). At 18S, *zic2b* is strongly expressed within the eye, MHB, dorsal HB and SC, and a small region in the tailbud (O). *zic3* mRNA is broadly expressed at 50% and 75% epiboly (P, Q). At tailbud, *zic3* mRNA is expressed within the MHB and HB (R, S). *zic3* transcript is within the telencephalon, posterior forebrain, MHB and dorsal HB, and within the tailbud overlapping with *zic2b* mRNA at 18S (T). Images are dorsal views with anterior to top (A-C, F-G, J-L, O-Q) or lateral views with anterior to left (D, E, I, J, N, O, S, T).

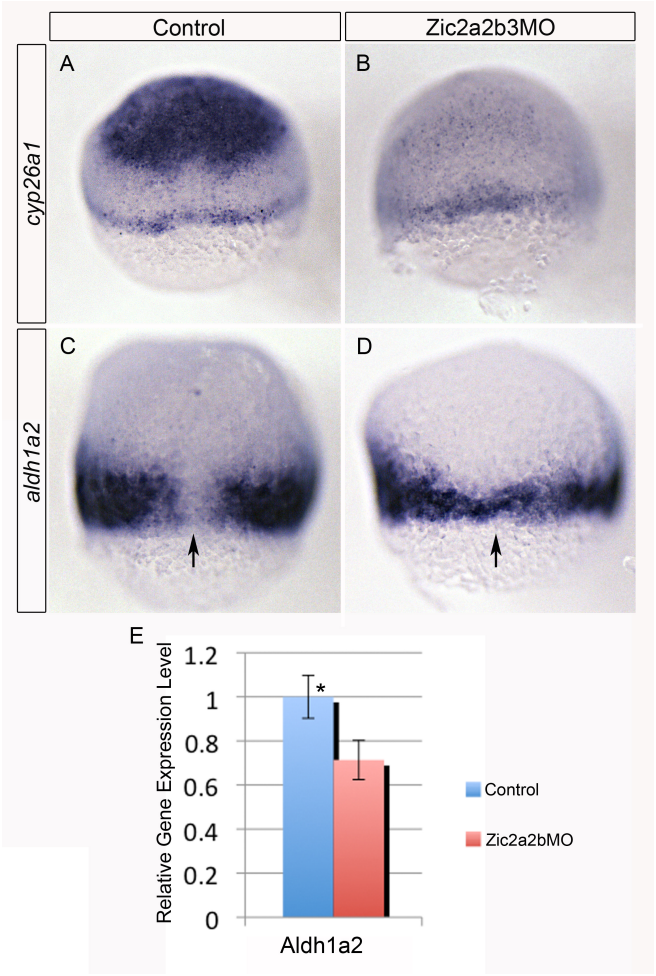

Figure 3.2: Zic2a2b3 depletion causes down-regulation of RA-metabolism genes, *cyp26a1* and *aldh1a2*, during early embryogenesis.

mRNA *in situ* hybridization reveals *cyp26a1* (A, B) and *aldh1a2* (C, D) expression in control p53MO injected embryos (A, C) compared to Zic2a2bp53MO embryos (B, D). Quantitative real-time PCR shows a significant reduction in *aldh1a2* mRNA transcript levels, at 0.71 (SD=0.07) compared to control 1.00 (SD=0.11; p-value<0.0001). qRT-PCR data depicts one biological replicate (7 technical replicates per primer pair) using RNA isolated from 50 embryos. Significance was calculated using unpaired t-test. All images are of 65% epiboly, dorsal view with anterior to top.

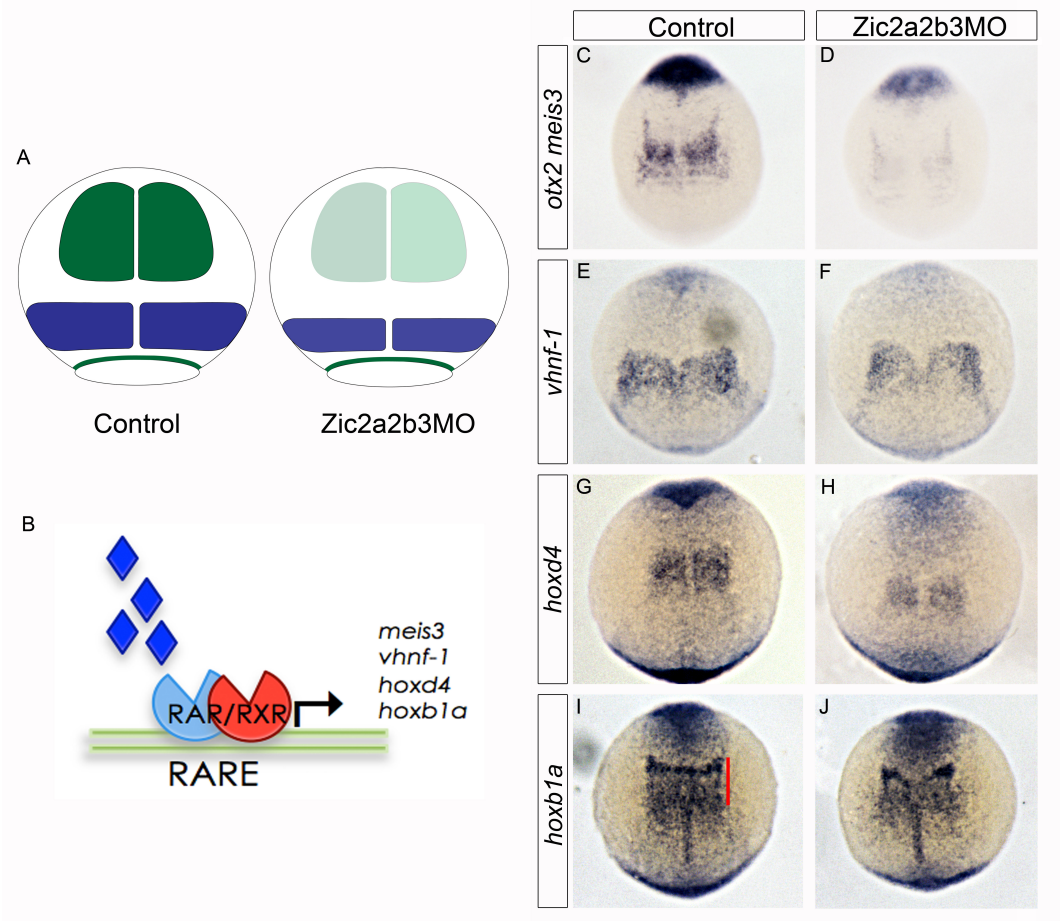

Figure 3.3: RA-responsive gene expression in Zic2a2b3 morphants suggests a reduction in RA signaling levels.

Zic2a2b morphants have reduced RA degradation (*cyp26a1*, green) and reduced RA synthesis (*aldh1a2*, blue; A) gene expression. Genes regulated by RA signaling such as *meis3*, *vhnf-1*, *hoxd4*, and *hoxb1a*, were used to examine alterations to RA-responsive signaling levels (RA, blue triangle; B). Transcript levels of presumptive hindbrain markers *meis3* (C, D), *vhnf-1* (E, F), *hoxd4* (G, H), and *hoxb1a* (I, J' red bar denotes length of domain in control) were compared in control un-injected (C, E, G, I) and Zic2a2b3MO-injected embryos (D, F, H, J). All images are of tailbud to 2S stage, dorsal view is shown with anterior to top.

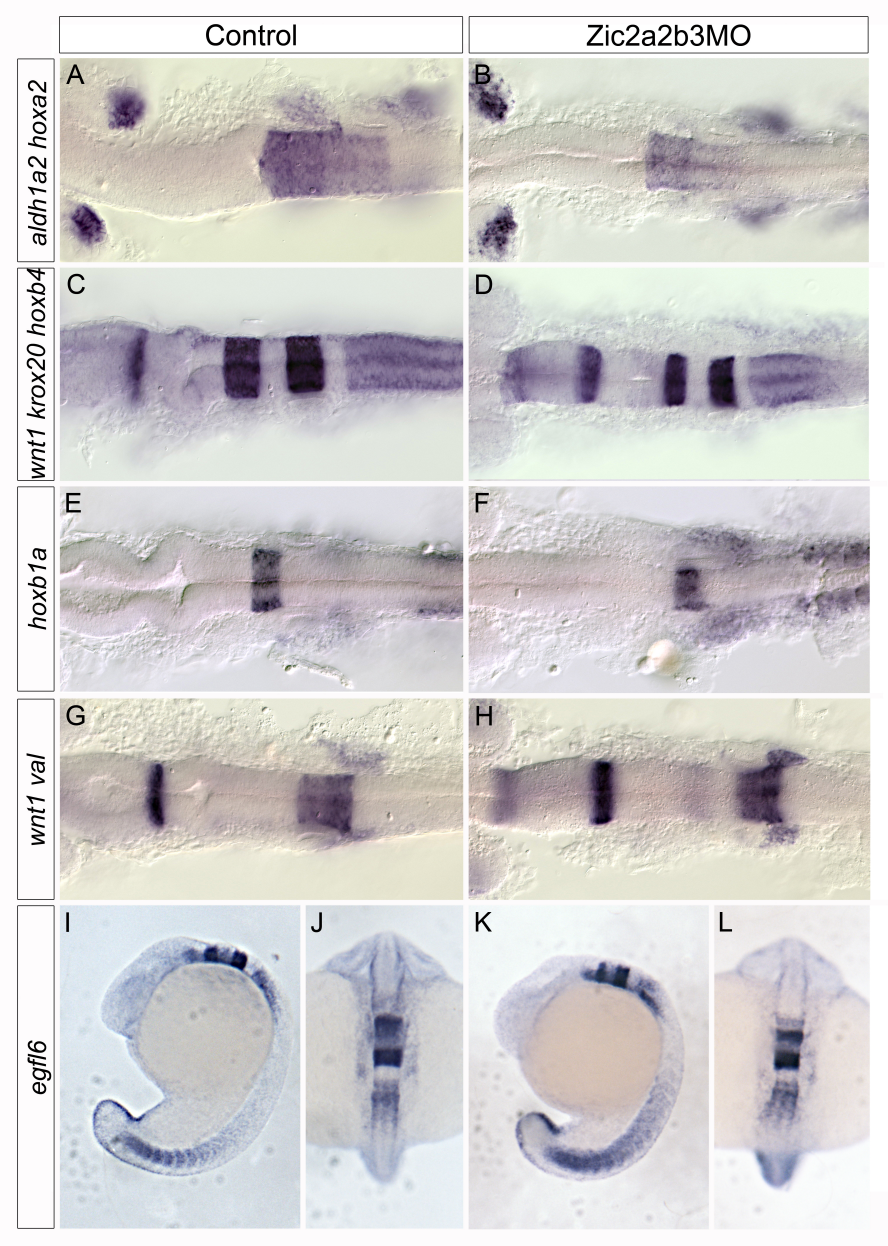

Figure 3.4: Hindbrain patterning is mildly affected in Zic2a2b3 morphants.

Markers within various regions of the hindbrain were examined: *aldh1a2* (eye) and *hoxa2* (r2-6) (A, B), *wnt1* (midbrain-hindbrain boundary, MHB) and *krox20* (r3/5) and *hoxb4* (r8-SC) (C, D), *hoxb1a* (r4) (E, F), *wnt1* (MHB) and *val* (r5-6), and *egfl6* (r2, r4, r6-7) (I-L). Images are of 24 hpf control un-injected (A, C, E, G, J) or Zic2a2b3MO-injected (B, D, F, H, K, L) embryos mounted dorsally with anterior to left (A-H). Images I/J and K/L are of the same embryos oriented laterally with anterior to left (I, K) or dorsally with anterior to top (J, L).

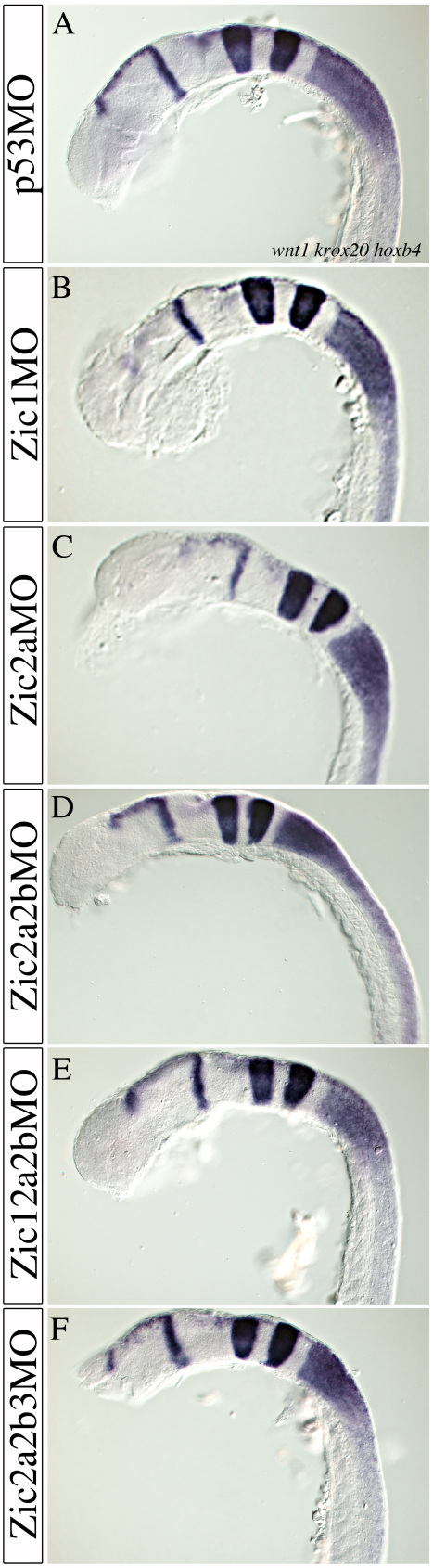

Figure 3.5: Posterior reduction of *hoxb4* expression with combination knockdown of Zic1, Zic2a, Zic2b, and Zic3.

mRNA *in situ* hybridization for MHB (*wnt1*), rhombomeres 3 and 5 (*krox20*), and rhombomere 7 down the spinal cord (*hoxb4*) is used to visualize hindbrain patterning in embryos injected with p53MO (1 ng; A), Zic1MO (2 ng; B), Zic2aMO (2 ng; C), Zic2a2b (2:2 ng; D), Zic12a2bMO (2:2:2 ng; E), and Zic2a2b3MO (2:2:3 ng; F). All experimental injections included 1 ng p53MO. Images are of 24 hpf embryos, laterally mounted with anterior to left.

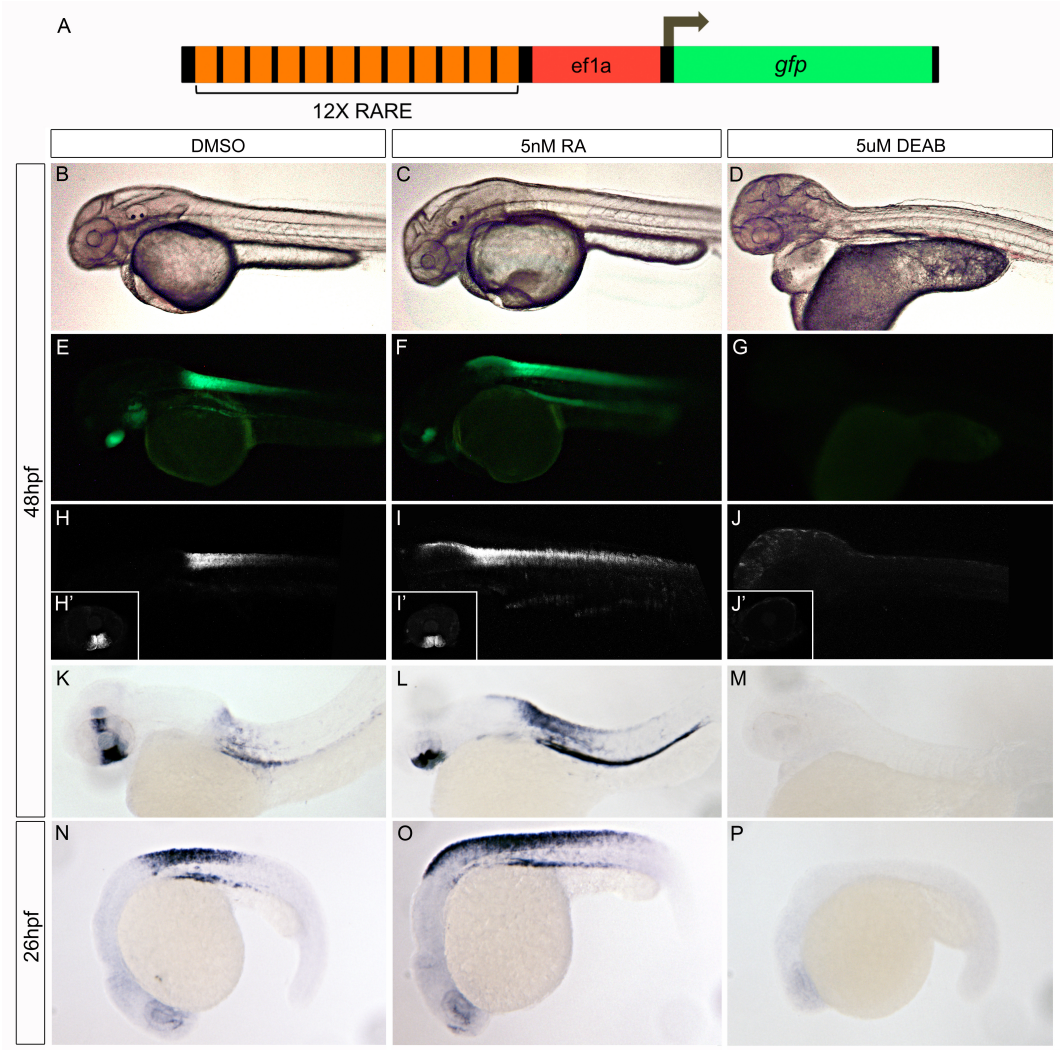

Figure 3.6: *RARE:gfp* transgenic zebrafish show alterations in RA signaling. Tg(12XRARE-*ef1a:gfp*)sk71 transgenic zebrafish contain 12 RARE elements upstream of the ubiquitous ef1α promoter controlling *gfp* expression (A). Embryos were treated with 5 nM RA or 5 μM DEAB at ~50% epiboly to the time of fixation. DMSO-treated embryos show areas of RA signaling based on *gfp* fluorescence within the ventral eye, posterior HB and anterior SC (B, E, H, H'; 48 hpf). mRNA *in situ* hybridization shows additional expression within the dorsal eye and yolk syncitial layer (YSL; K). At 26 hpf, *gfp* is apparent within the posterior HB, SC, and YSL (N). Treatment with 5 nM RA extends *RARE:gfp* into HB and posteriorly down the SC (C, F, I, I', L; 48 hpf, O; 26 hpf). DEAB treatment results in complete loss of *RARE:gfp* fluorescence and *gfp* transcripts (D, G, J, J', M; 48 hpf, P; 26 hfp). Images B-J' are of 48 hpf embryos using light stereomicroscopy (B-D, K-P), fluorescent stereomicroscopy (E-G), and confocal microscopy of full embryos (H-J) or the eye (H'-J'). All images are lateral views with anterior to left.

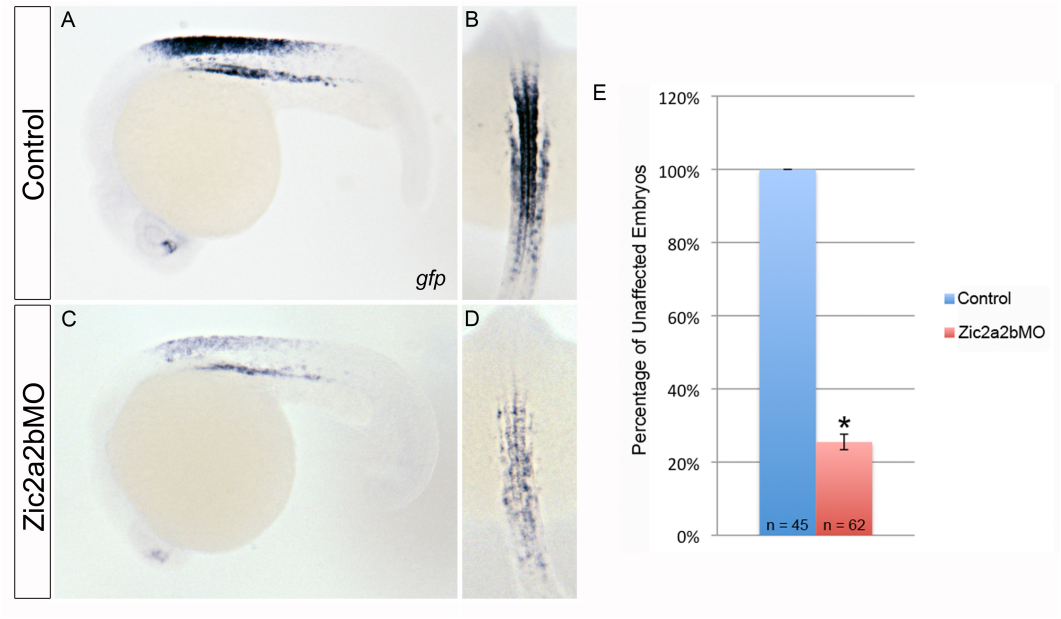

Figure 3.7: Zic2a2b-depletion reduces RA-signaling levels.

Tg(12XRARE-ef1α:gfp)sk71 transgenic embryos were used to examine level of RA-signaling by *in situ* hybridization for *gfp* in control p53MO-injected (1 ng; A, B) and Zic2a2bp53MO-injected embryos (2:2:1 ng; C, D). Reduction in *RARE:gfp* in Zic2a2bp53 morphants is displayed graphically with reduced *gfp* expression in 75% of embryos (p-value=0.0004 calculated using unpaired t-test; standard deviation (SD) of 2.1%). Images are of 26 hpf embryos in lateral (A, C) and dorsal (B, D) views with anterior to top and left, respectively.

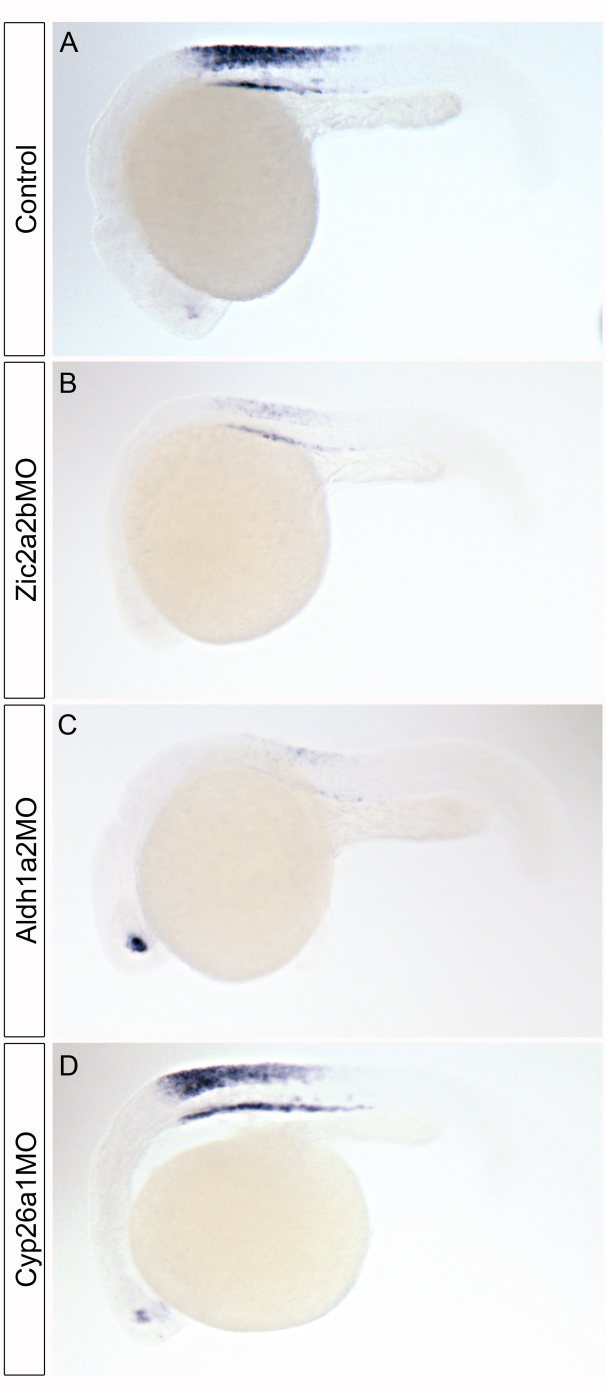

Figure 3.8: Alterations to RA-signaling levels resulting from Zic2a2b, Aldh1a2, and Cyp26a1 knockdown.

Analysis of *gfp* transcript levels in *RARE:gfp* embryos injected with morpholinos for p53 (1 ng; A), Zic2a2bp53 (2:2:1 ng; B), Aldh1a2 (2 ng; C), or Cyp26a1 (2ng; D). All images are of 26 hpf embryos, lateral view with anterior to left.

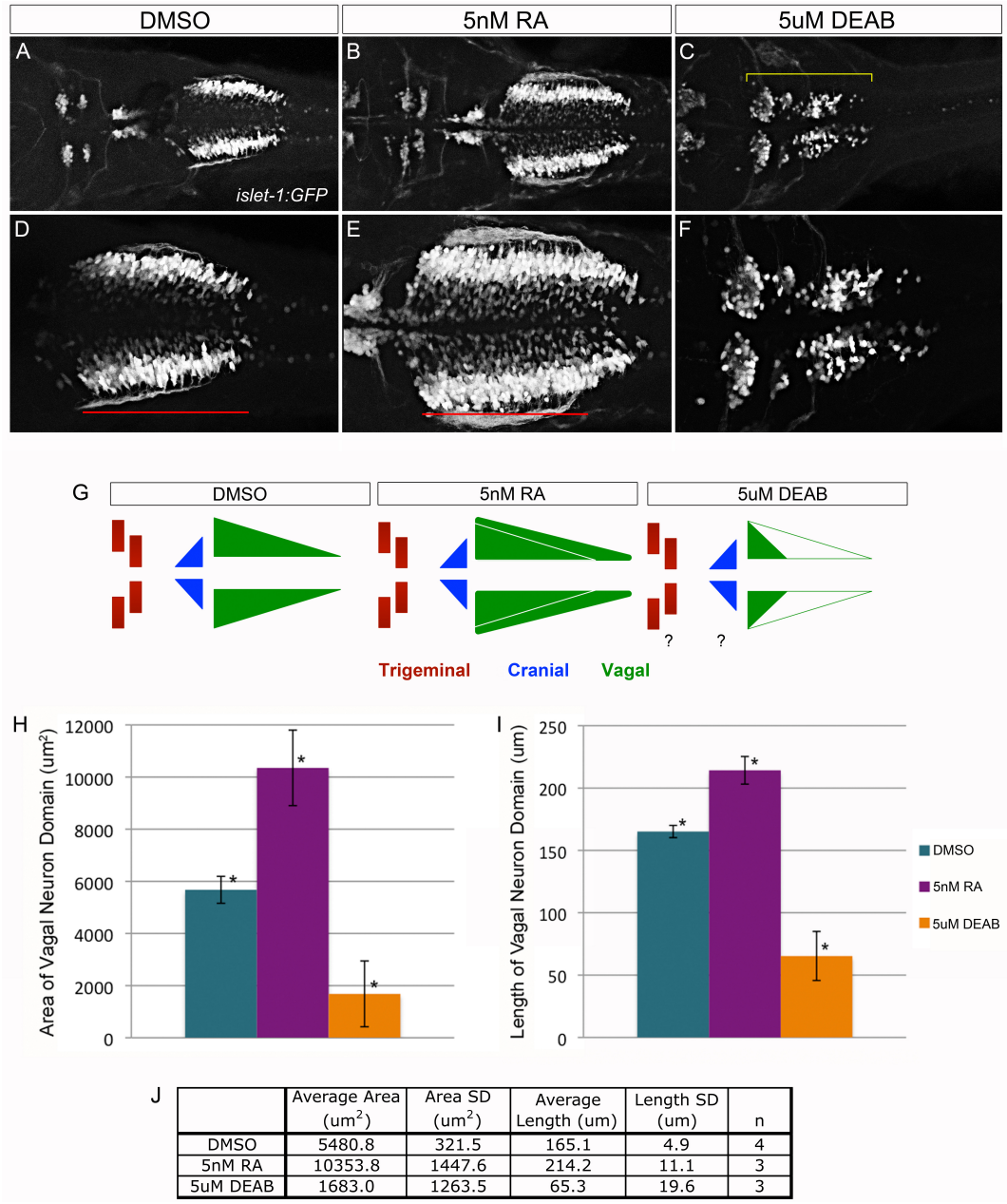

J

	Average Area (um^2)	Area SD (um^2)	Average Length (um)	Length SD (um)	n
DMSO	5480.8	321.5	165.1	4.9	4
5nM RA	10353.8	1447.6	214.2	11.1	3
5uM DEAB	1683.0	1263.5	65.3	19.6	3

Figure 3.9: Vagal neurons are sensitive to alterations in RA levels.

Islet1:gfp transgenic zebrafish are used to visualize alterations to branchiomotor neurons in response to DMSO (A, D), 5 nM RA (B, E), or 5 µM DEAB (C, F) treatment. Images are dorsal views of 48hpf embryo hindbrain at 20X (A-C) or 40X (D-F) magnification. Red line denotes length of vagal neuron domain in DMSO treatment; yellow bracket denotes area imaged at higher magnification. (G) Diagrammatic representation of motor neuron defects in response to treatments. The area (H, J) and length (I, J) of vagal neuron domain is quantified and displayed graphically (significance calculated using ANOVA and Post-Hoc Tukey's HSD test *p-value≤0.005).

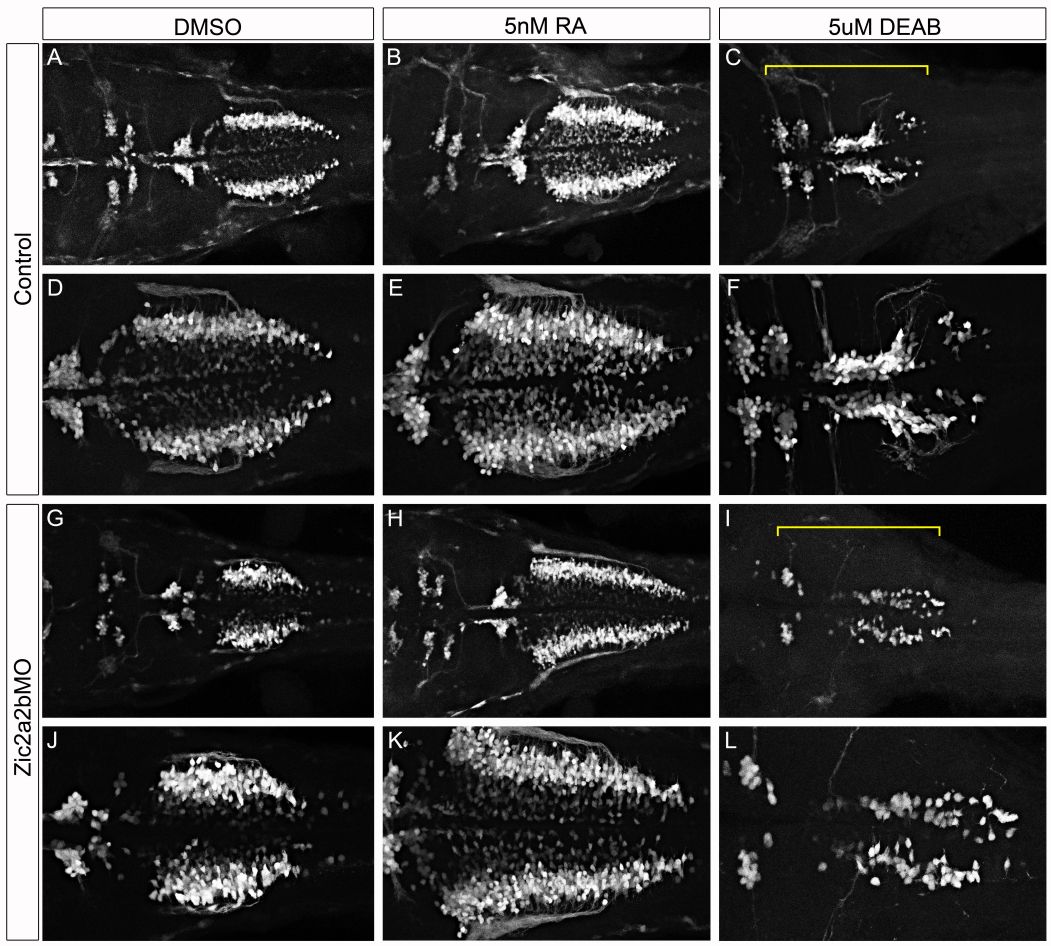
DMSO
5nM RA
5uM DEAB
Control
Zic2a2bMO
A
B
C
D
E
F
G
H
I
J
K
L

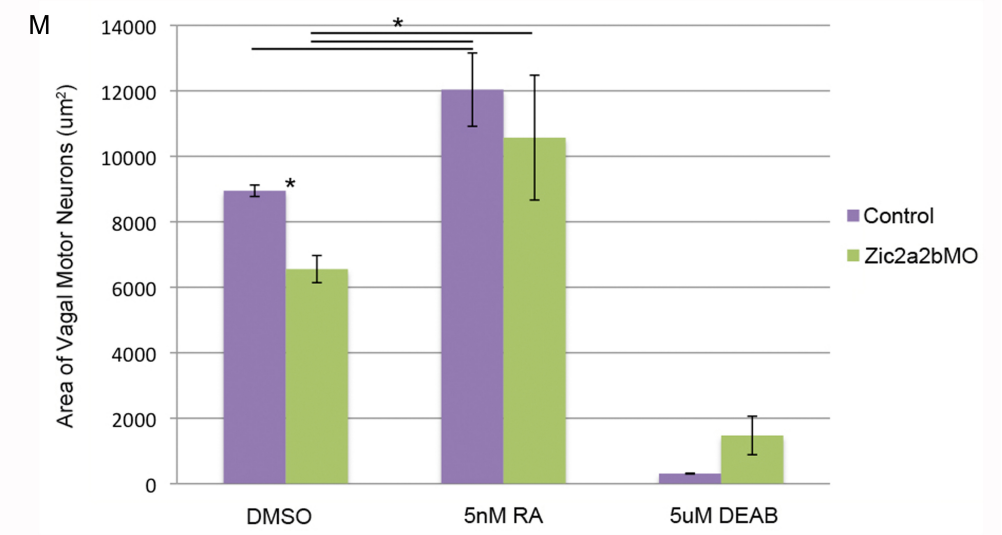

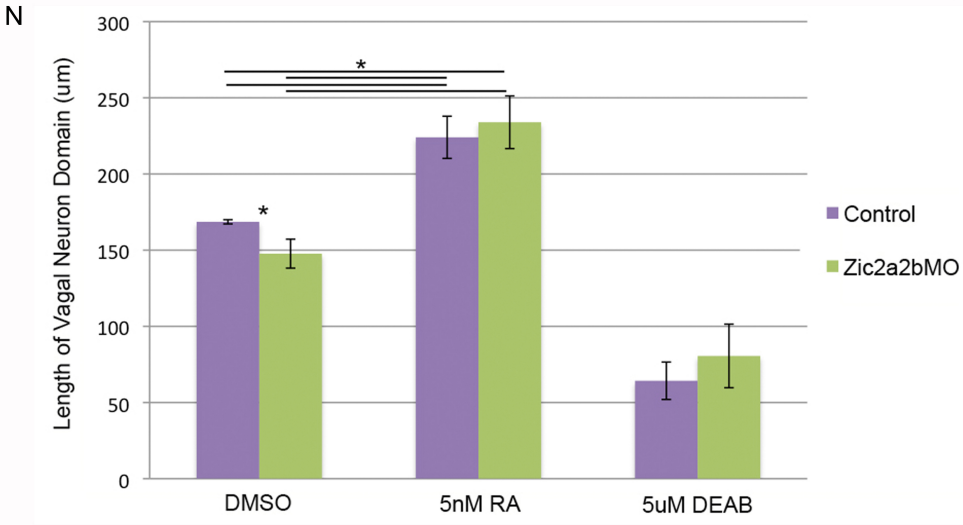

O

		Average Area (um^2)	Area SD (um^2)	Average Length (um)	Length SD (um)	n
DMSO	Control	8947.4	174.4	168.6	1.4	2
	Zic2a2bMO	6555.4	414.7	147.7	9.5	6
5nM RA	Control	12536.2	412.0	224.1	13.9	2
	Zic2a2bMO	10570.7	1408.3	234.0	17.3	6
5uM DEAB	Control	308.8	13.3	64.3	12.3	2
	Zic2a2bMO	1473.0	587.7	80.6	20.9	6

Figure 3.10: Vagal neuron domain in Zic2a2b-depleted embryos is reduced, but with RA treatment.

Vagal motor neurons are visualized using *islet1:gfp* transgenic embryos injected with p53MO (1ng; A-F) or Zic2a2bp53MO (2:2:1ng; G-L) and treated with DMSO (A, D, G, J), 5nM RA (B, E, H, K), or 5uM DEAB (C, F, I, L). Images are dorsal views of 48 hpf embryo HB at 20X (A-C, G-I; yellow bracket denotes region imaged at 40X) and 40X magnification (D-F, J-L). Area (M, O) and length (N, O) were quantified and are displayed. Significance is calculated using ANOVA and Post-Hoc Tukey's HSD test (*p-value≤0.05).

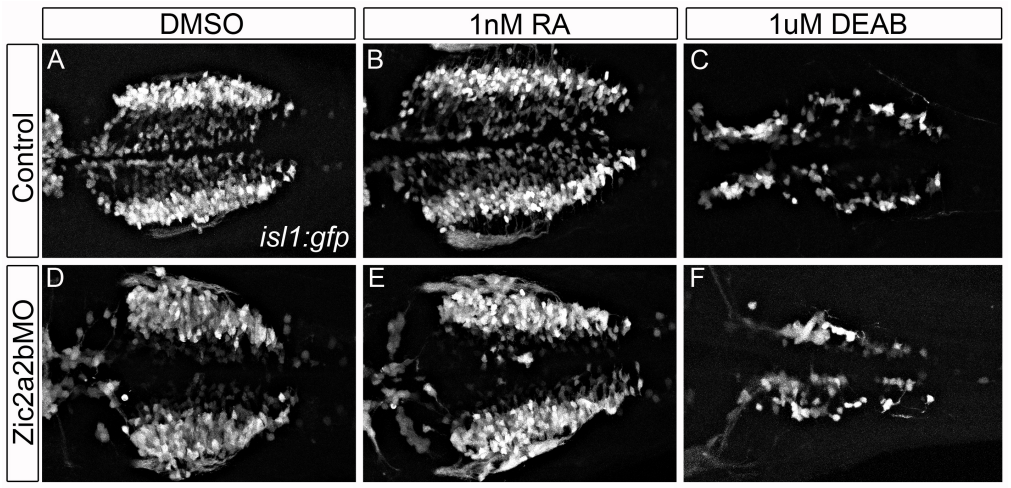

G

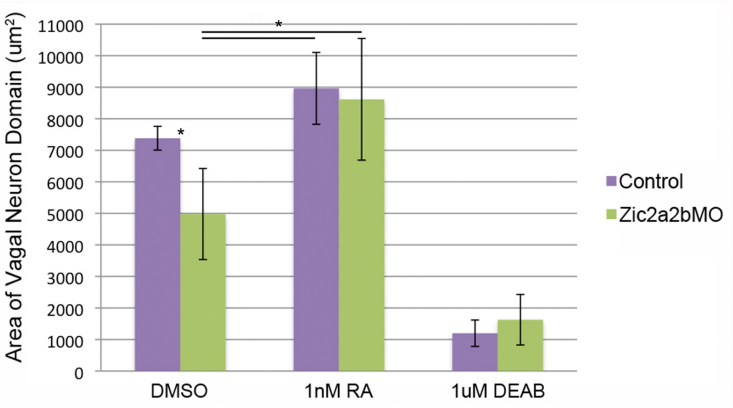

H

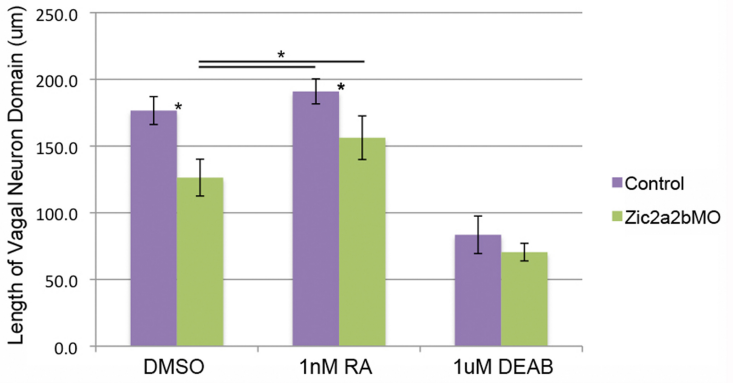

I

		Average Area (um^2)	Area SD (um^2)	Average Length (um)	Length SD (um)	n
DMSO	Control	7382.5	377.2	176.6	10.5	8
	Zic2a2bMO	4979.3	1443.0	126.4	13.8	7
1nM RA	Control	8963.8	1139.1	191.0	9.4	7
	Zic2a2bMO	8616.4	1929.3	156.3	16.3	7
1uM DEAB	Control	1199.8	418.3	83.5	14.1	6
	Zic2a2bMO	1628.0	800.9	70.5	6.6	4

Figure 3.11: Vagal neuron domain in Zic2a2b morphants is rescued with low doses of RA. Vagal motor neurons (*islet1:gfp* trangenics) are visualized in p53MO-injected (1 ng; A-C) and Zic2a2bp53MO-injected (2:2:1 ng; D-F) embryos treated with DMSO (A, D), 1 nM RA (B, E), or 1 µM DEAB (C, F). Images are dorsal views of 48 hpf embryos, 40X magnification of vagal neuron domain. Area (G, I) and length (H, I) of vagal neuron domain is quantified and shown

graphically. Significance is calculated using ANOVA and Post-Hoc Tukey's HSD test (*p-value≤0.01).

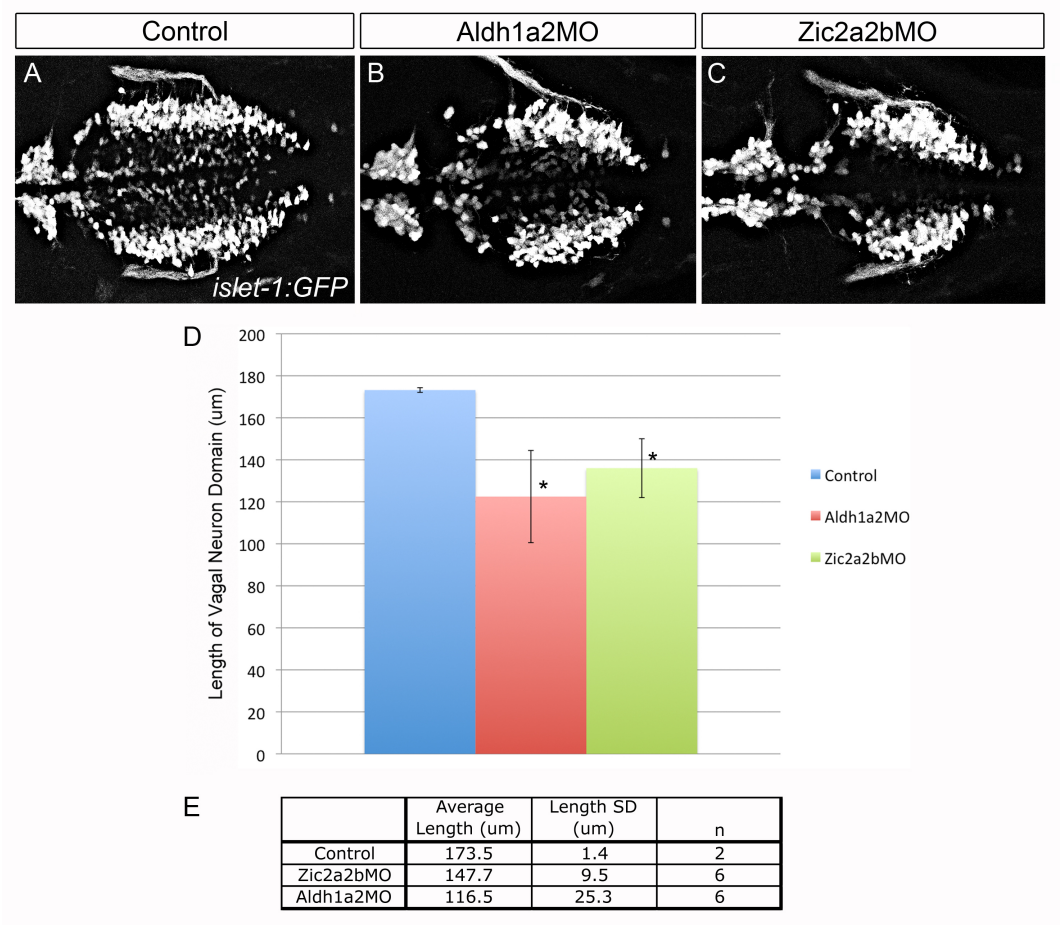

E

	Average Length (um)	Length SD (um)	n
Control	173.5	1.4	2
Zic2a2bMO	147.7	9.5	6
Aldh1a2MO	116.5	25.3	6

Figure 3.12: Reduction in vagal neuron domain in Zic2a2b morphants is reminiscent of *aldh1a2*-depletion.

Analysis of vagal motor neurons within p53MO-injected (1 ng; A), Aldh1a2MO-injected (2 ng; B), or Zic2a2bp53MO-injected (2:2:1ng; C) *islet-1:gfp* transgenic embryos. Images are of 48hpf embryos dorsally mounted with anterior to left, 40X magnification. The length of vagal domain was quantified (E) and is displayed graphically (D). Significance is calculated using unpaired t-test comparing morphant groups to control (*p-value=0.01).

3.10 Literature Cited

Begemann, G., Marx, M., Mebus, K., Meyer, A., and Bastmeyer, M. (2004). Beyond the neckless phenotype: influence of reduced retinoic acid signaling on motor neuron development in the zebrafish hindbrain. Dev Biol *271*, 119-129.

Begemann, G., Schilling, T.F., Rauch, G.J., Geisler, R., and Ingham, P.W. (2001). The zebrafish neckless mutation reveals a requirement for raldh2 in mesodermal signals that pattern the hindbrain. Development *128*, 3081-3094.

Cardoso, W.V., Mitsialis, S.A., Brody, J.S., and Williams, M.C. (1996). Retinoic acid alters the expression of pattern-related genes in the developing rat lung. Dev Dyn *207*, 47-59.

Chandrasekhar, A. (2004). Turning heads: development of vertebrate branchiomotor neurons. Dev Dyn *229*, 143-161.

Chandrasekhar, A., Moens, C.B., Warren, J.T., Jr., Kimmel, C.B., and Kuwada, J.Y. (1997). Development of branchiomotor neurons in zebrafish. Development *124*, 2633-2644.

Durston, A.J., Timmermans, J.P., Hage, W.J., Hendriks, H.F., de Vries, N.J., Heideveld, M., and Nieuwkoop, P.D. (1989). Retinoic acid causes an anteroposterior transformation in the developing central nervous system. Nature *340*, 140-144.

Elms, P., Siggers, P., Napper, D., Greenfield, A., and Arkell, R. (2003). Zic2 is required for neural crest formation and hindbrain patterning during mouse development. Dev Biol *264*, 391-406.

Elsen, G.E., Choi, L.Y., Millen, K.J., Grinblat, Y., and Prince, V.E. (2008). Zic1 and Zic4 regulate zebrafish roof plate specification and hindbrain ventricle morphogenesis. Dev Biol *314*, 376-392.

Feng, L., Hernandez, R.E., Waxman, J.S., Yelon, D., and Moens, C.B. (2010). Dhrs3a regulates retinoic acid biosynthesis through a feedback inhibition mechanism. Dev Biol *338*, 1-14.

Glover, J.C., Renaud, J.S., and Rijli, F.M. (2006). Retinoic acid and hindbrain patterning. J Neurobiol *66*, 705-725.

Gongal, P.A., and Waskiewicz, A.J. (2008). Zebrafish model of holoprosencephaly demonstrates a key role for TGIF in regulating retinoic acid metabolism. Hum Mol Genet *17*, 525-538.

Gongal, P.A., March, L.D., Holly, V.L., Pillay, L.M., Berry-Wynne, K.M., Kagechika, H., Waskiewicz, A.J. (2011). Hmx4 regulates Sonic Hedgehog signaling through control of retinoic acid synthesis during forebrain patterning. Dev Biol *335*, 55-64.

Hernandez, R.E., Rikhof, H.A., Bachmann, R., and Moens, C.B. (2004). vhnf1 integrates global RA patterning and local FGF signals to direct posterior hindbrain development in zebrafish. Development *131*, 4511-4520.

Higashijima, S., Hotta, Y., and Okamoto, H. (2000). Visualization of cranial motor neurons in live transgenic zebrafish expressing green fluorescent protein under the control of the islet-1 promoter/enhancer. J Neurosci *20*, 206-218.

Huang, D., Chen, S.W., and Gudas, L.J. (2002). Analysis of two distinct retinoic acid response elements in the homeobox gene Hoxb1 in transgenic mice. Dev Dyn *223*, 353-370.

Kudoh, T., Wilson, S.W., and Dawid, I.B. (2002). Distinct roles for Fgf, Wnt and retinoic acid in posteriorizing the neural ectoderm. Development *129*, 4335-4346.

Linville, A., Gumusaneli, E., Chandraratna, R.A., and Schilling, T.F. (2004). Independent roles for retinoic acid in segmentation and neuronal differentiation in the zebrafish hindbrain. Dev Biol *270*, 186-199.

Maden, M., Sonneveld, E., van der Saag, P.T., and Gale, E. (1998). The distribution of endogenous retinoic acid in the chick embryo: implications for developmental mechanisms. Development *125*, 4133-4144.

Maurus, D., and Harris, W.A. (2009). Zic-associated holoprosencephaly: zebrafish Zic1 controls midline formation and forebrain patterning by

regulating Nodal, Hedgehog, and retinoic acid signaling. Genes Dev *23*, 1461-1473.

Maves, L., and Kimmel, C.B. (2005). Dynamic and sequential patterning of the zebrafish posterior hindbrain by retinoic acid. Dev Biol *285*, 593-605.

Molotkova, N., Molotkov, A., Sirbu, I.O., and Duester, G. (2005). Requirement of mesodermal retinoic acid generated by Raldh2 for posterior neural transformation. Mech Dev *122*, 145-155.

Moroni, M.C., Vigano, M.A., and Mavilio, F. (1993). Regulation of the human HOXD4 gene by retinoids. Mech Dev *44*, 139-154.

Niederreither, K., Abu-Abed, S., Schuhbaur, B., Petkovich, M., Chambon, P., and Dolle, P. (2002). Genetic evidence that oxidative derivatives of retinoic acid are not involved in retinoid signaling during mouse development. Nat Genet *31*, 84-88.

Niederreither, K., and Dolle, P. (2008). Retinoic acid in development: towards an integrated view. Nat Rev Genet *9*, 541-553.

Niederreither, K., Subbarayan, V., Dolle, P., and Chambon, P. (1999). Embryonic retinoic acid synthesis is essential for early mouse post-implantation development. Nat Genet *21*, 444-448.

Niederreither, K., Vermot, J., Schuhbaur, B., Chambon, P., and Dolle, P. (2000). Retinoic acid synthesis and hindbrain patterning in the mouse embryo. Development *127*, 75-85.

Nyholm, M.K., Wu, S.F., Dorsky, R.I., and Grinblat, Y. (2007). The zebrafish zic2a-zic5 gene pair acts downstream of canonical Wnt signaling to control cell proliferation in the developing tectum. Development *134*, 735-746.

Ohishi, K., Nishikawa, S., Nagata, T., Yamauchi, N., Shinohara, H., Kido, J., and Ishida, H. (1995). Physiological concentrations of retinoic acid suppress the osteoblastic differentiation of fetal rat calvaria cells in vitro. Eur J Endocrinol *133*, 335-341.

Perz-Edwards, A., Hardison, N.L., and Linney, E. (2001). Retinoic acid-mediated gene expression in transgenic reporter zebrafish. Dev Biol *229*, 89-101.

Rossant, J., Zirngibl, R., Cado, D., Shago, M., and Giguere, V. (1991). Expression of a retinoic acid response element-hsplacZ transgene defines specific domains of transcriptional activity during mouse embryogenesis. Genes Dev *5*, 1333-1344.

Sakai, Y., Meno, C., Fujii, H., Nishino, J., Shiratori, H., Saijoh, Y., Rossant, J., and Hamada, H. (2001). The retinoic acid-inactivating enzyme CYP26 is essential for establishing an uneven distribution of retinoic acid along the anterio-posterior axis within the mouse embryo. Genes Dev *15*, 213-225.

Sanek, N.A., and Grinblat, Y. (2008). A novel role for zebrafish zic2a during forebrain development. Dev Biol *317*, 325-335.

Sanek, N.A., Taylor, A.A., Nyholm, M.K., and Grinblat, Y. (2009). Zebrafish zic2a patterns the forebrain through modulation of Hedgehog-activated gene expression. Development *136*, 3791-3800.

Simeone, A., Acampora, D., Nigro, V., Faiella, A., D'Esposito, M., Stornaiuolo, A., Mavilio, F., and Boncinelli, E. (1991). Differential regulation by retinoic acid of the homeobox genes of the four HOX loci in human embryonal carcinoma cells. Mech Dev *33*, 215-227.

Thisse, B., Heyer, V., Lux, A., Alunni, V., Degrave, A., Seiliez, I., Kirchner, J., Parkhill, J.P., and Thisse, C. (2004). Spatial and temporal expression of the zebrafish genome by large-scale in situ hybridization screening. Methods Cell Biol *77*, 505-519.

Vitobello, A., Ferretti, E., Lampe, X., Vilain, N., Ducret, S., Ori, M., Spetz, J.F., Selleri, L., Rijli, F.M. (2011). Hox and Pbx factors control retinoic acid synthesis during hindbrain segmentation. Dev Cell *20*, 469-482.

Waxman, J.S., and Yelon, D. (2011). Zebrafish retinoic acid receptors function as context-dependent transcriptional activators. Dev Biol *352*, 128-140.

Zhang, F., Nagy Kovacs, E., and Featherstone, M.S. (2000). Murine hoxd4 expression in the CNS requires multiple elements including a retinoic acid response element. Mech Dev *96*, 79-89.

Chapter 4: Results and Discussion

The role of Zic transcription factors in development of the vertebrate nervous system has been extensively studied, with functions in neural tube closure and forebrain development (Brown et al., 1998; Sanek and Grinblat, 2008), as repressors of neurogenesis (Brewster et al., 1998), and regulators of cell proliferation (Nyholm et al., 2007). We have identified an additional role for Zic2a and Zic2b in regulating embryonic RA synthesis, with depletion causing branchiomotor neuron defects – specifically in the posterior vagal motor neurons. Here we further investigate the role of Zic2a2b3 in neural differentiation and patterning. In addition, we examine potential transcriptional feedback mechanisms between Zic transcription factors themselves as well as RA.

4.1 Zic2a2b3 may have a role in hindbrain neurogenesis

To examine functions of Zic2a2b3 in neural development and differentiation, we carried out a series of experiments examining another class of hindbrain neurons and markers of hindbrain neurogenesis. The hindbrain commissural neurons, which extend axon projections across the hindbrain at segment boundaries, are labeled with the Zn-5 antibody (Higashijima et al., 2000). *Islet-1:gpf*–positive neurons were used to provide hindbrain positional information. The characteristic reduction in vagal domain in Zic2a2b3MO-injected embryos reported in previous chapter is visible (Figure 4.1 A, B, E, F). Within Zic2a2b3-depleted embryos, commissural neurons are mispatterned, with aberrant axon fasciculation at rhombomere boundaries (Figure 4.1 C, D, E, F). As Zn-5 also labels axon outgrowths in the cerebellum, we are also able to discern effects in this region. Of note, the neurons of the cerebellum are completely lost in Zic2a2b3 morphants (Figure 4.1 C, D). This is consistent with the role of Zics in regulating neural cell proliferation during murine cerebellar development (Aruga et al., 2002; Aruga et al., 1998) and is the first indication that Zics may

be necessary for proliferation or specification of Zn5-positive cerebellar neurons in zebrafish.

Zebrafish *her9* regulates neural progenitor populations by inhibiting neural differentiation within the inner ear and is postulated to have a similar, transient role in the hindbrain (Radosevic et al., 2011). In Zic2a2b3-depleted embryos, *her9* expression is unaffected within the tectum, cerebellum and lateral bands extending down the hindbrain (Figure 4.1 G, H). This suggests that the role of Zic2a2b3 in hindbrain neurogenesis is independent of *her9*. Notch signaling also maintains neural progenitor populations and acts by defining regions of progenitor versus differentiated cells (Louvi and Artavanis-Tsakonas, 2006). At 48 hpf, *notch1a* is expressed in stripes within the hindbrain, presumably with regions of differentiated neurons located between such *notch*-positive domains (Figure 4.1 I) (Nikolaou et al., 2009). *Notch1a* transcript levels are expanded to encompass entire rhombomeres in Zic2a2b3 morphants, suggesting an expansion of neural precursors within the hindbrain (Figure 4.1 I, J).

4.2 Zic2a2b3 morpholino injection does not result in non-specific neural apoptosis

Studies have identified potential non-specific effects of morpholino-medicated gene knockdown (Ekker and Larson, 2001; Robu et al., 2007). One side effect of particular importance for this work is upregulation of p53, which results in non-specific activation of the apoptotic pathway, predominantly within neural populations. To ensure that vagal neuron number in Zic2a2b3-depleted embryos is not affected by non-specific neural apoptosis, we used the anti-activated caspase-3 antibody to label cells actively undergoing apoptosis. For a complete analysis, we compared control uninjected embryos (AB; Figure 4.2 A, E, I), p53MO-injected embryos (Figure 4.2 B, F, J), Zic2a2b3MO-injected embryos (Figure 4.2 C, G, K), and Zic2a2b3p53MO-injected embryos (Figure 4.2 D, H, L). As expected, AB and p53MO-injected embryos have very few detectable apoptotic cells (Figure

4.2 E, F, I, J). While Zic2a2b3 morphants have a few apoptotic cells detectable within the anterior embryo – none of these co-localized with regions of branchiomotor neurons (Figure 4.2 C, K). With the addition of p53MO into the Zic2a2b3MO cocktail, apoptotic cells are reduced to levels similar to controls. Notably, the addition of p53MO partially rescues facial neuron mispatterning in Zic2a2b3 morphants (Figure 4.2 A-D). To this end, gene knockdown in experiments looking at differentiated hindbrain neurons were accomplished with the addition of p53MO.

4.3 Forebrain patterning is normal in Zic2a2b3-depleted embryos

Morphogenetic defects in mouse and human *Zic* mutants are predominantly within anterior neural tissue including defects in cerebellar development and neural tube formation and closure (Aruga, 2004; Nagai et al., 1997). Similarly, zebrafish *zic2a* is required for formation of the prethamalus region of the forebrain (Sanek and Grinblat, 2008).

We asked whether Zic2a2b3 morphants have forebrain defects similar to, or more severe than, those previously found. Markers of forebrain domains were used to analyze development and patterning of the telencephalon (*foxg1a*; Figure 4.3 A-D), the telencephalon, posterior diencephalon, and pretectum (*barhl2;* Figure 4.3 E-H), the diencephalon and prethalamus (*dlx2a*; Figure 4.3 I-L), and the ventral forebrain and midbrain (*nkx2.2a*; Figure 4.3 M, N). At 24 hpf there was no significant change to marker gene expression levels or domain within Zic2a2b3-depleted embryos as compared to controls, indicating that forebrain patterning is normal. A requirement for *zic2a* in formation of the prethalamus was not observed, based on the fact that *dlx2a* expression was unaffected. This is plausibly explained by differences in morpholino content. Sanek and Grinblat (2008) used three non-overlapping (two splice-blocking and one translation blocking) morpholinos to obtain Zic2a knockdown, while our cocktail contains a single splice-blocking Zic2a morpholino. Therefore, while defects in forebrain patterning resulting from Zic2a-depletion have been reported,

the dose of morpholino used in our experiments did not elicit anterior neural tube defects.

4.4 Zics compensate for depletion but are not sensitive to RA

Our studies have identified a reduction in RA signaling resulting from Zic2a2b-depletion, suggesting that Zic2a and Zic2b act upstream of RA by regulating RA synthesis. However, due to the propensity for feedback regulation within the RA signaling pathway we asked whether alterations in RA levels might affect *zic2a* or *zic2b* expression. *In situ* hybridization of tailbud stage embryos treated with 5 nM RA, 5 μM DEAB, or control DMSO was used to analyze *zic* transcription. Expression of both *zic2a* (Figure 4.4 A-C) and *zic2b* (Figure 4.4 D-F) was unaffected in response to RA increase or reduction, suggesting that there is no feedback regulation between RA and *zic2a/2b*.

There is evidence suggesting compensatory mechanisms between Zic transcription factors – including upregulation of paralogs in *Zic* mutants (Aruga et al., 2004). To determine if this is the case during zebrafish embryogenesis levels of *zic1*, *zic2a*, *zic2b*, and *zic3* transcripts were examined in Zic2a2b3-depleted embryos. We found evidence for transcriptional compensation, with upregulation of *zic2a*, *zic2b,* and *zic3* observed in morphants (Figure 4.5 B-D, F-G). The *zic2a* expression domain was expanded to include the entire dorsal embryo, while there was a strong and mild upregulation of *zic2b* and *zic3*, respectively. This upregulation of transcription is specific, as *zic1* was unaffected (Figure 4.5 A, E).

4.5 Conclusions

During development of the zebrafish nervous system Zic2a and Zic2b transcription factors act as important regulators of the RA synthesis gene, *aldh1a2*. In addition to their requirement for vagal neuron development, we have identified a possible role for Zic2a2b in other aspects of neurogenesis – formation of Zn-5-positive cerebellar neurons and defining regions of

hindbrain neurogenesis via *notch* regulation. While many aspects of RA signaling exhibit feedback activation or repression, Zic2a and Zic2b transcription is independent of RA levels.

4.6 Figures

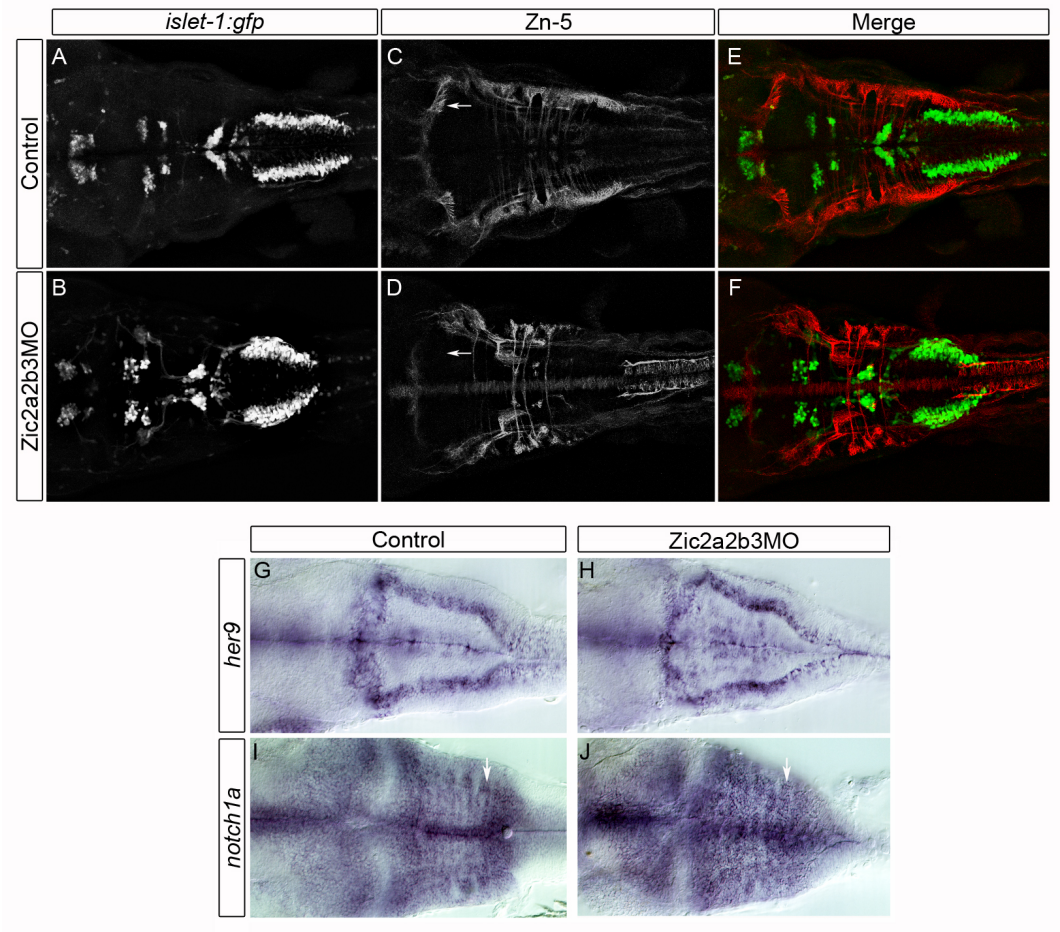

Figure 4.1: Zic2a2b3 depletion causes hindbrain neurogenesis defects.

Branchiomotor neurons (*islet-1:gfp*; A, B, E, F) and hindbrain commissural neurons (Zn-5 antibody; C, D, E, F) are visualized in un-injected (A, C, E) and Zic2a2b3MO-injected (2:2:3 ng; B, D, F) embryos. Markers used to assay hindbrain neurogenesis at 48 hpf include *her9* (cerebellum and lateral hindbrain; G, H) and *notch1a* (neurogenic-repressed bands in hindbrain; I, J; white arrowhead demarks central expression-lacking region of controls). Images are of 48 hpf embryos, dorsally mounted with anterior to left of *islet1:gfp* (A, B), Zn-5 (C, D), merge (E, F), or *in situ* hybridization (G-J).

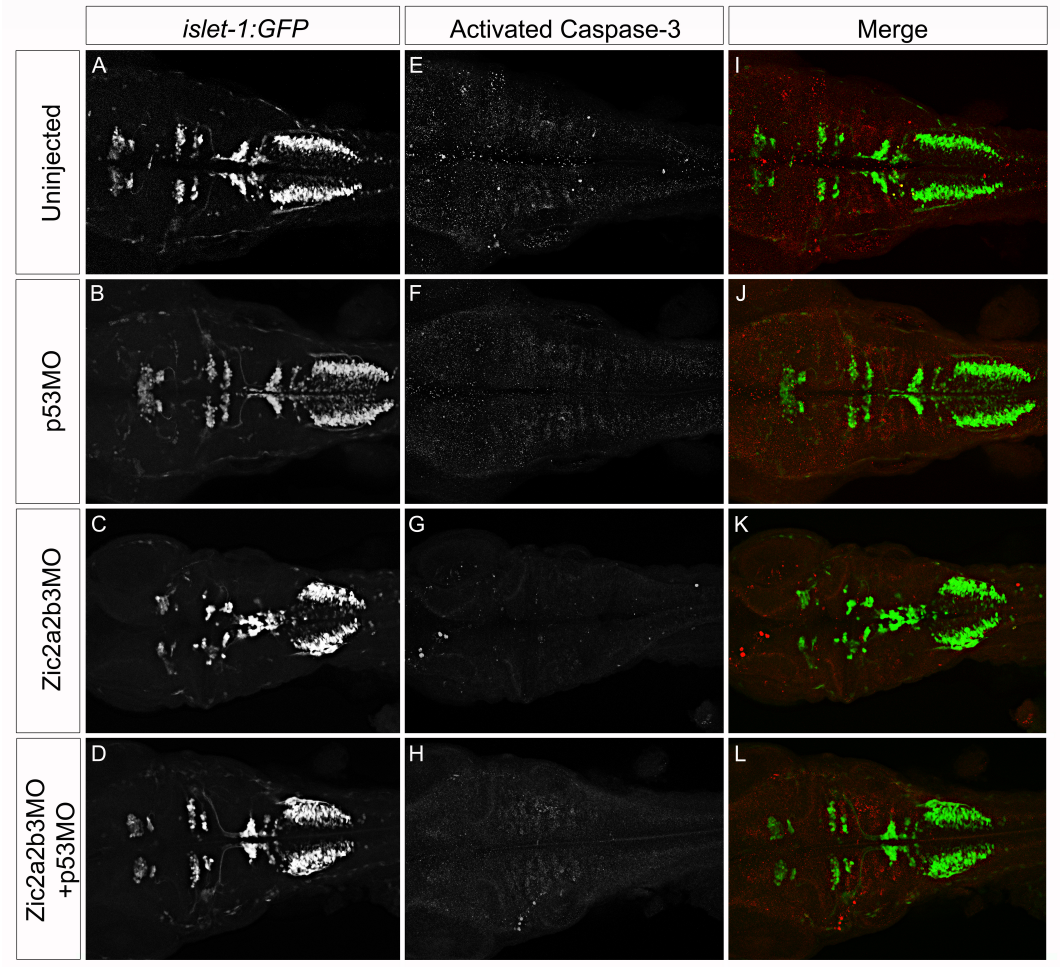

Figure 4.2: Combined injection of Zic2a2b3 morpholinos does not significantly increase non-specific cell death.

Visualization of branchiomotor neurons (*islet-1:gfp*; A-D, I-L) and anti-activated caspase-3 antibody (E-H, I-L) allows analysis of non-specific apoptosis within the motor neurons of un-injected (A, E, I), p53MO-injected (1 ng; B, F, J), Zic2a2b3MO-injected (2:2:3 ng; C, G, K), or Zic2a2b3p53MO-injected (2:2:3:1 ng; D, H, L). Images are of 48 hpf embryos dorsally mounted with anterior to left.

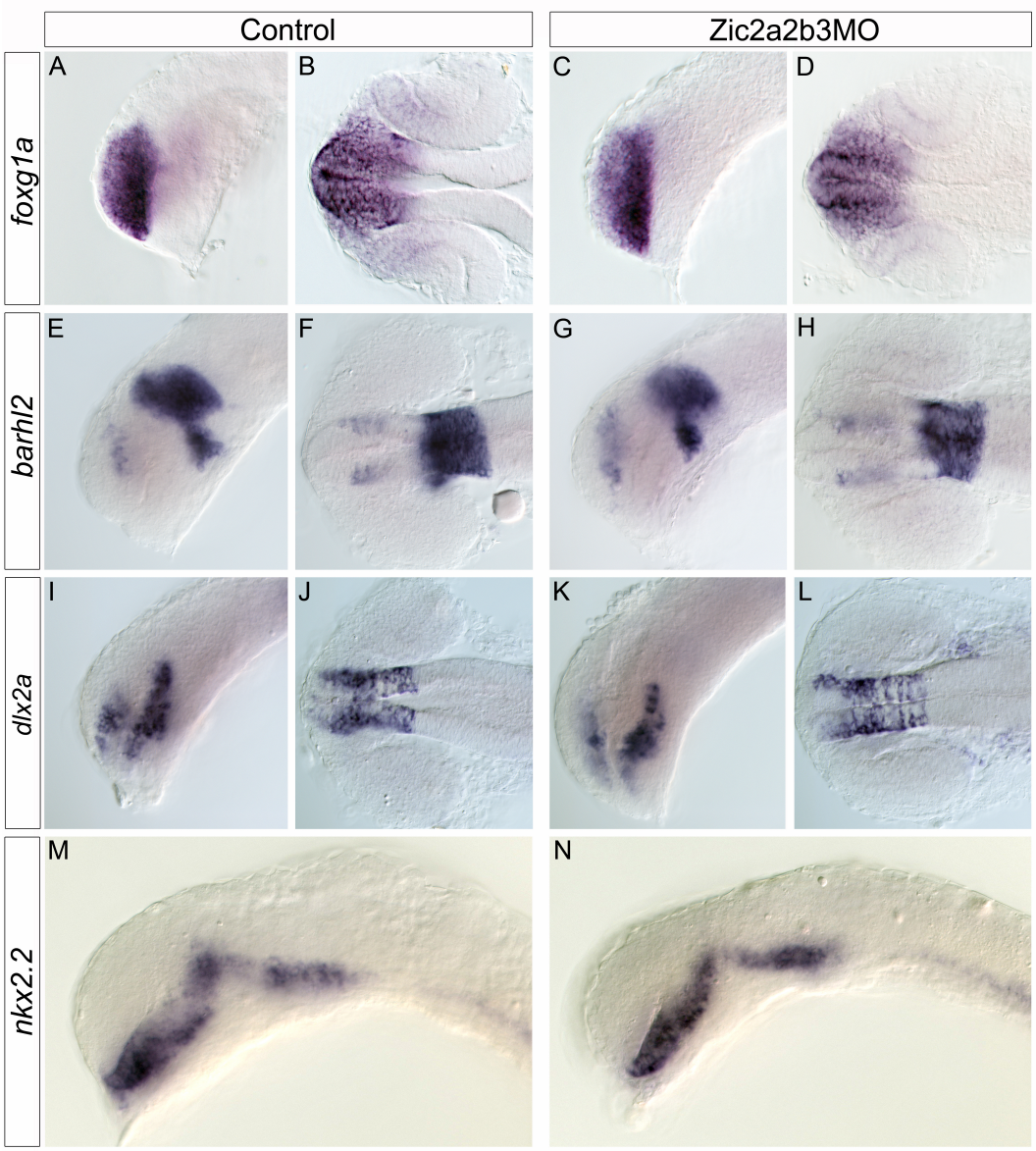

Figure 4.3: Anterior neural patterning is normal in Zic2a2b3 morphants.

Regions of the forebrain were examined using *in situ* hybridization for *foxg1a* (telencephalon; A-D), *barhl2* (telencephalon and thalamus; E-H), *dlx2a* (telencephalon, diencephalon, and prethalamus; I-L), *nkx2.2* (ventral forebrain and midbrain) in Zic2a2b3MO-injected embryos (C, D, G, H, K, L; 24 hpf) compared to un-injected controls (A, B, E, F, I, J; 24 hpf). Images are lateral (A, C, E, G, I, K, M, N) or dorsal (B, D, F, H, J, L, O-V) views with anterior to left.

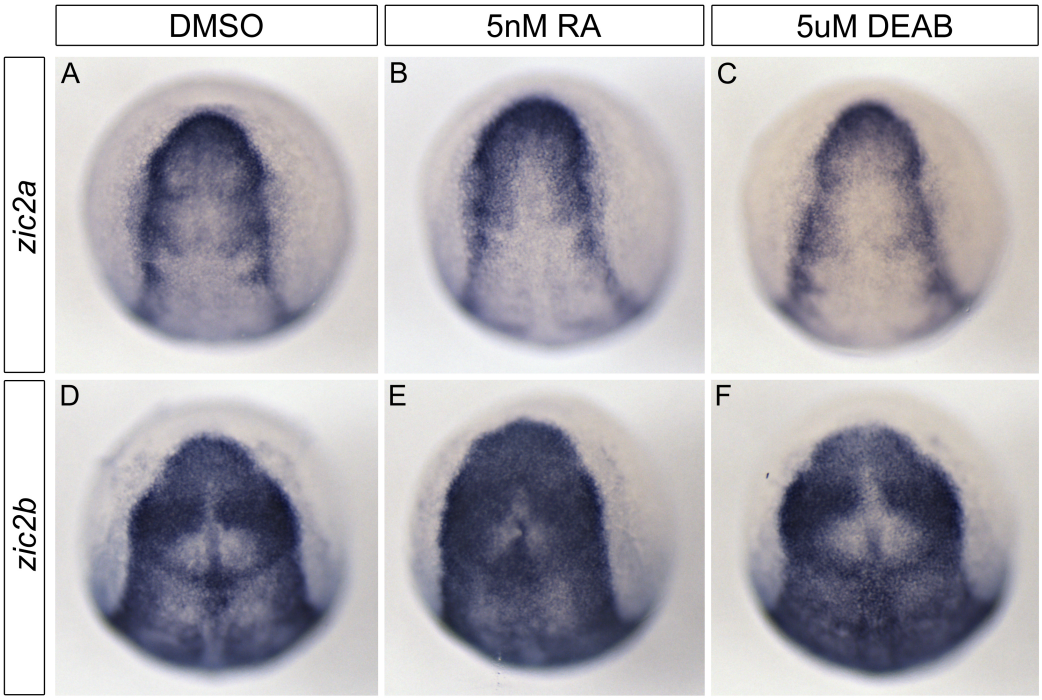

Figure 4.4: *zic2a* and *zic2b* transcription is not sensitive to RA levels.

Embryos were treated at ~50% epiboly with DMSO (A, D), 5 nM RA (B, E), or 5 μM DEAB (C, F). At tailbud stage, *zic2a* (A-C) and *zic2b* (D-F) transcripts were examined using *in situ* hybridization. All images are dorsal views with anterior to top.

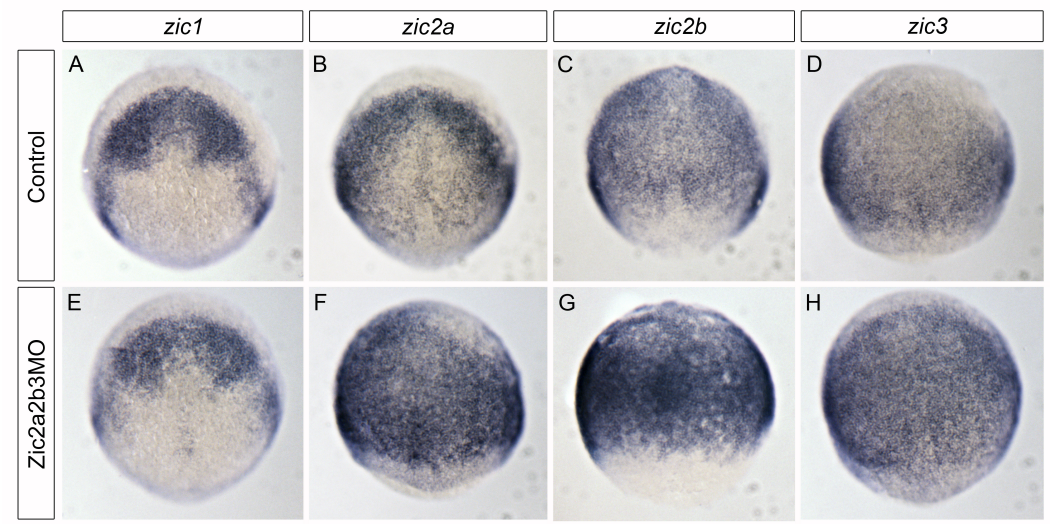

Figure 4.5: Zics can modulate each other's transcription.

Expression of *zic1* (A, E), *zic2a* (B, F), *zic2b* (C, G), and *zic3* (D, H) is analyzed in un-injected (A-D) or Zic2a2b3MO-injected (2:2:3 ng; E-H) embryos. Images are of 75% epiboly embryos, dorsal views with anterior to top.

4.7 Literature Cited

Aruga, J. (2004). The role of Zic genes in neural development. Mol Cell Neurosci *26*, 205-221.

Aruga, J., Inoue, T., Hoshino, J., and Mikoshiba, K. (2002). Zic2 controls cerebellar development in cooperation with Zic1. J Neurosci *22*, 218-225.

Aruga, J., Minowa, O., Yaginuma, H., Kuno, J., Nagai, T., Noda, T., and Mikoshiba, K. (1998). Mouse Zic1 is involved in cerebellar development. J Neurosci *18*, 284-293.

Brewster, R., Lee, J., and Ruiz i Altaba, A. (1998). Gli/Zic factors pattern the neural plate by defining domains of cell differentiation. Nature *393*, 579-583.

Brown, S.A., Warburton, D., Brown, L.Y., Yu, C.Y., Roeder, E.R., Stengel-Rutkowski, S., Hennekam, R.C., and Muenke, M. (1998). Holoprosencephaly due to mutations in ZIC2, a homologue of Drosophila odd-paired. Nat Genet *20*, 180-183.

Ekker, S.C., and Larson, J.D. (2001). Morphant technology in model developmental systems. Genesis *30*, 89-93.

Higashijima, S., Hotta, Y., and Okamoto, H. (2000). Visualization of cranial motor neurons in live transgenic zebrafish expressing green fluorescent protein under the control of the islet-1 promoter/enhancer. J Neurosci *20*, 206-218.

Louvi, A., and Artavanis-Tsakonas, S. (2006). Notch signalling in vertebrate neural development. Nat Rev Neurosci *7*, 93-102.

Nagai, T., Aruga, J., Takada, S., Gunther, T., Sporle, R., Schughart, K., and Mikoshiba, K. (1997). The expression of the mouse Zic1, Zic2, and Zic3 gene suggests an essential role for Zic genes in body pattern formation. Dev Biol *182*, 299-313.

Nikolaou, N., Watanabe-Asaka, T., Gerety, S., Distel, M., Koster, R.W., and Wilkinson, D.G. (2009). Lunatic fringe promotes the lateral inhibition of neurogenesis. Development *136*, 2523-2533.

Nyholm, M.K., Wu, S.F., Dorsky, R.I., and Grinblat, Y. (2007). The zebrafish zic2a-zic5 gene pair acts downstream of canonical Wnt signaling to control cell proliferation in the developing tectum. Development *134*, 735-746.

Radosevic, M., Robert-Moreno, A., Coolen, M., Bally-Cuif, L., Alsina, B. (2011). Her9 represses neurogenic fate downstream of Tbx1 and retinoic acid signaling in the inner ear. Development *138*, 397-408.

Robu, M.E., Larson, J.D., Nasevicius, A., Beiraghi, S., Brenner, C., Farber, S.A., and Ekker, S.C. (2007). p53 activation by knockdown technologies. PLoS Genet *3*, e78.

Sanek, N.A., and Grinblat, Y. (2008). A novel role for zebrafish zic2a during forebrain development. Dev Biol *317*, 325-335.

Chapter 5. Future Directions

Retinoic acid (RA) acts as a morphogen during embryonic development and is necessary for induction of posterior neural tissue, patterning of the neural tube, and regulating proliferation and differentiation of neural populations (Dupe and Lumsden, 2001; Glover et al., 2006; Moens and Selleri, 2006; Papalopulu et al., 1991). The factors that regulate RA signaling have been the topic of study for decades. We have identified a novel regulatory mechanism whereby Zic2a and Zic2b transcription factors regulate retinoic acid synthesis through *aldh1a2*. Zic2a2b depletion causes reduced RA signaling levels and a concomitant reduction in posterior neural domains, both phenotypes nearly identical to Aldh1a2-depletion. This chapter outlines areas of future study, focusing on methodology and tools that will both clarify and deepen our understanding of Zic function.

5.1 Zic mRNA over-expression and rescue experiments

In zebrafish, over-expression analysis using microinjection of pre-synthesized mRNA has yielded great experimental insight. However, this method of over-expression is not without disadvantages, including the fact that ubiquitous over-expression itself can cause developmental defects. Furthermore, mRNAs are degraded over time such that alterations at later stages are difficult to obtain (Malicki et al., 2002). Experiments from our group and others (Maurus and Harris, 2009; Sanek and Grinblat, 2008) found that *zic2a* over-expression results in embryonic lethality, with failure to complete gastrulation. This defect may result from a requirement for regional *zic2a* expression during gastrulation or may be a broad over-expression defect. To complement our experiments, a method of temporal or regional over-expression would allow the embryo to develop through gastrulation stages. This would allow Zic mRNA overexpression to examine whether RA –metabolism gene expression is concurrently upregulated, as we would expect based on the knockdown phenotypes described in Chapter 3.

Additionally, experiments that examine rescue of morpholino knockdown phenotypes with mRNA overexpression and analysis of Zic function at different time-points of neural development will be informative.

The most common method of temporal regulation is using the *hsp70* heat-shock inducible promoter driving expression of the gene of interest (Halloran et al., 2000). This method involves creation of a transgenic zebrafish strain and inducing expression by incubation at 38^{o}C for one hour. Alterations in gene expression are visible between two and four hours later. While this method still results in ubiquitous over-expression, it likely can overcome the early developmental lethality and would allow functional studies within narrow developmental windows.

An alternative approach for spatially controlled gene expression is the GAL4/UAS system. In an activator strain, zebrafish express GAL4 under a tissue specific promoter. Several enhancer trap screens have now generated transgenic zebrafish lines expressing GAL4 within a variety of tissues (Asakawa and Kawakami, 2008; Distel et al., 2009; Scott et al., 2007). A second effector strain carries the gene of interest under control of GAL4-responsive promoter. By crossing these strains you achieve tissue- and temporal-specific over-expression of the gene. While this approach allows tissue-specific alterations to gene expression, there is a temporal limitation as to when GAL4 is expressed within the activator strain. The production of stable GAL4 and UAS strains, followed by a stable GAL4/UAS is also time consuming as at least three months are required for fish to reach maturity.

Regarding *zic2a2b*, the GAL4/UAS method of gene regulation would be useful in producing *zic2a2b* expression within *islet-1*-positive cells to ascertain cell-autonomous versus cell-non-autonomous requirements for these transcription factors. Additionally, the temporal requirement for *zic2a2b* could be analyzed by *zic2a2b* expression within the developing dorsal neural tube. The effects of neural tube specific upregulation on resulting neural populations could be determined, as well as the ability of neural tube–derived Zic2a2b to rescue vagal neuron defects in Zic2a2b-

depleted embryos. However, if the requirement for these genes is significantly earlier in development (e.g. in establishing RA signaling levels), no rescue would be visible. Interestingly, expression of *zic2a2b* within the posterior hindbrain and spinal cord, for example within the *hoxb4* expression domain, could potentially rescue the posterior truncation of Zic2a2b-depleted embryos.

We postulate that the posterior truncation in Zic2a2b-depleted embryos results from an early reduction in *aldh1a2*. We have shown that supplying RA, the product of the Aldh1a2-catalyzed reaction, rescues the vagal neuron defect within morphants. To support the key role of Aldh1a2, treatment of embryos with exogenous retinol (Vitamin A), the RA precursor, would be interesting as it would allow the study of potential retinol-independent mechanisms of RA metabolism. If Zic2a2b morphants are deficient in *aldh1a2*, and Aldh1a2 is the crucial metabolite for RA synthesis during embryogenesis, we would expect the vagal neuron defect to persist with retinol treatment.

To differentiate between the requirements for RA during early neural patterning and later regulation of neural proliferation and differentiation, varying the embryonic stage of exogenous RA treatment would be informative. In our experiments, RA was added at mid-gastrulation stages with concentrations remaining constant until the time of embryo fixation (48 hpf). However, birth of the branchiomotor neurons begins at approximately 26 hpf. Therefore, to address RA requirements during these later neurogenesis events, RA treatment between 15-22 somite stage would be necessary. If the vagal neuron defect observed in Zic2a2b-depleted embryos was rescued with this treatment, we would conclude that RA is acting independently of neural patterning.

5.2 Zic2a2b gene knockdown and mutants

The use of morpholinos to achieve gene knockdown, while a useful and common tool in zebrafish, can result in experimental obstacles.

Morpholinos can cause non-specific defects including activation of the p53-apoptotic pathway, most commonly resulting in neuronal cell death, as well as necrosis, somatic defects, and heart adema (Robu et al., 2007). Often, the use of multiple morpholinos (or a high dose) is required to appropriately reduce expression levels. In our experiments single Zic2a and Zic2b splice-blocking morpholinos were used. To ascertain morpholino specificity, essential experiments should be completed with control morpholinos examining for production of similar phenotypes. A control splice –blocking morpholino targeting a different intron -exon boundary (for example, the first exon and second intron) would theoretically produce a non-functional protein. However, if cryptic splice sites are present, the use of splice –blocking morpholinos could produce a differentially spliced, functional protein product. Alternatively, translation blocking morpholinos could effectively reduce protein translation. As neither Zic2a nor Zic2b are maternally expressed, a slice -blocking and translation blocking morpholino should produce similar phenotypes as both act on zygotically expressed Zic2a and Zic2b mRNA.

To clarify the role(s) of Zics, while reducing non-specific side-effects, dominant negative protein constructs or the production of mutant zebrafish would be informative. Drosophila and Xenopus dominant negative Gli2/3 transcription factors were produced using C-terminal truncations. These truncations eliminate the regions of Gli2/3 that are not involved in DNA binding, therefore removing regulatory regions and leaving the zinc-finger DNA binding domains (Brewster et al., 1998) (Ruiz i Altaba et al., 2003). The predicted ZOC (Zic-Opa related) regulator domain is located within the N-terminus of Zic2a and Zic2b, opposite the zinc-finger domains (Figure 1.4) (Aruga, 2004). Creating a N-terminal Zic2a/2b truncation, lacking the ZOC-domain, may produce a "dominant negative" protein. As Zics can interact with Glis and potentially other Zics via their DNA binding domain, a dominant negative transcription factor could produce a strong phenotype correlating with knockdown/loss of multiple Zics (Koyabu et al., 2001). Of

note, although there is significant protein similarity and expression domain overlap, Zic family members are regulated differently and could have varying roles within target cells. Additionally, due to their single-amino acid stretches, Zics were initially thought to act as repressors, however activator functions have also been identified (Houston and Wylie, 2005). Therefore, care must be taken in analyzing effects of "dominant repressor" assays to correctly ascertain whether potentiation of Zic function or loss of Zic function results.

While large-scale TILLING projects are ongoing, zebrafish *zic* mutants have yet to be identified (Sood et al., 2006). There are several mechanisms with which zebrafish mutants can be created, such as zinc finger nucleases and TALENs. Zinc-finger nucleases act to target specific DNA sequences and introduce double stranded breaks (Meng et al., 2008). Within these cells, error-prone non-homologous end joining repairs DNA breaks, often resulting in insertions and deletions. There are reported success using zinc finger nucleases to create zebrafish mutants – however, this success requires a specific recognition site: two 9 base-pair zinc finger recognition sites, flanking a 6 base-pair spacer (Meng et al., 2008). Unfortunately, Zic2a has only moderately acceptable zinc finger recognition sites suggesting that creation of a mutant using this method would be challenging.

Recently, the use of TALENs to induce mutations has received significant attention after successful use in human cell culture (Hockemeyer et al., 2011). Fusion of plant-derived transcription-like activators (TAL) to the FokI nuclease creates an efficient protein that targets and creates double-stranded DNA breaks. This method has been successful in generating heritable mutations within zebrafish (Huang et al., 2011; Sander et al., 2011).

With the formation of Zic2a/2b single mutants, analysis of individual gene function will be more clear, as off-target morpholino effects are avoided. In addition, analyzing redundant functions of Zics will be significantly easier via creation of doubly mutant fish as well as morpholino-mediated knockdown in conjunction with mutants.

5.3 Regulatory interactions of Zic2a2b

In addition to Zic2a2b, transcription factors that act upstream of *aldh1a2* include Tgif, Hmx4, and Hox-Pbx complexes (Gongal et al., 2008; Gongal et al., 2011; Vitobello et al., 2011). Similar to the known role of Tgif, we have identified a regulatory mechanism between Zic2a2b and RA metabolism genes, regulating transcription of both *aldh1a2* and *cyp26a1*. Very few transcription factors identified to date act upstream of both potentiation and inhibition of a signaling pathway. Therefore, further examining the mechanisms by which these transcription factors act would be informative. For example, morpholino-mediated knockdown of Tgif, Hmx4, Zic2a2b, and Pbx-depletion in paired combinations or rescue of Zic -depletion phenotypes with mRNA overexpression (using Tgif, Hmx4, or Pbx mRNA) would provide useful information. These experiments would examine whether Zic2a2b, Tgif, Hmx4, and Hox-Pbx act within the same pathway to modulate RA levels.

Finally, Zic transcription factors are capable of binding Gli regulatory sequences *in vitro*, implicating a putative role for Zic in mediating Shh signaling (Koyabu et al., 2001). Additionally, yeast one-hybrid has identified interaction between Zics and cis-regulatory regions of ApolipoproteinE, Dopamine receptor1a, and Math1 (Aruga, 2004). However no large-scale method has been used to identify genes directly regulated by Zics. Chromatin immunoprecipitation (ChIP) and sequencing is a common technology used to assay high-throughput protein-DNA interactions and would be essential to further clarify the transcriptional role of Zics. This would allow identification of Zic2a/2b binding sites within *cyp26a1* and *aldh1a2* enhancer regions. While there is a putative Gli binding site within the zebrafish *cyp26a1* promoter, a direct regulatory relationship has not been shown (Hu et al., 2008). In addition, regulatory relationships between Zics themselves, Zics and Shh signaling, and Zics and neurogenic factors, could be investigated at one or many stages of zebrafish embryonic development.

5.4 Literature Cited

Aruga, J. (2004). The role of Zic genes in neural development. Mol Cell Neurosci *26*, 205-221.

Asakawa, K., and Kawakami, K. (2008). Targeted gene expression by the Gal4-UAS system in zebrafish. Dev Growth Differ *50*, 391-399.

Brewster, R., Lee, J., and Ruiz i Altaba, A. (1998). Gli/Zic factors pattern the neural plate by defining domains of cell differentiation. Nature *393*, 579-583.

Distel, M., Wullimann, M.F., and Koster, R.W. (2009). Optimized Gal4 genetics for permanent gene expression mapping in zebrafish. Proc Natl Acad Sci U S A *106*, 13365-13370.

Dupe, V., and Lumsden, A. (2001). Hindbrain patterning involves graded responses to retinoic acid signalling. Development *128*, 2199-2208.

Glover, J.C., Renaud, J.S., and Rijli, F.M. (2006). Retinoic acid and hindbrain patterning. J Neurobiol *66*, 705-725.

Gongal, P.A., and Waskiewicz, A.J. (2008). Zebrafish model of holoprosencephaly demonstrates a key role for TGIF in regulating retinoic acid metabolism. Hum Mol Genet *17*, 525-538.

Gongal, P.A., March, L.D., Holly, V.L., Pillay, L.M., Berry-Wynne, K.M., Kagechika, H., Waskiewicz, A.J. (2011). Hmx4 regulates Sonic Hedgehog signaling through control of retinoic acid synthesis during forebrain patterning. Dev Biol *335*, 55-64.

Halloran, M.C., Sato-Maeda, M., Warren, J.T., Su, F., Lele, Z., Krone, P.H., Kuwada, J.Y., and Shoji, W. (2000). Laser-induced gene expression in specific cells of transgenic zebrafish. Development *127*, 1953-1960.

Hockemeyer, D., Wang, H., Kiani, S., Lai, C.S., Gao, Q., Cassady, J.P., Cost, G.J., Zhang, L., Santiago, Y., Miller, J.C., *et al.* (2011). Genetic engineering of human pluripotent cells using TALE nucleases. Nat Biotechnol *29*, 731-734.

Houston, D.W., and Wylie, C. (2005). Maternal Xenopus Zic2 negatively regulates Nodal-related gene expression during anteroposterior patterning. Development *132*, 4845-4855.

Hu, P., Tian, M., Bao, J., Xing, G., Gu, X., Gao, X., Linney, E., and Zhao, Q. (2008). Retinoid regulation of the zebrafish cyp26a1 promoter. Dev Dyn *237*, 3798-3808.

Huang, P., Xiao, A., Zhou, M., Zhu, Z., Lin, S., and Zhang, B. (2011). Heritable gene targeting in zebrafish using customized TALENs. Nat Biotechnol *29*, 699-700.

Koyabu, Y., Nakata, K., Mizugishi, K., Aruga, J., and Mikoshiba, K. (2001). Physical and functional interactions between Zic and Gli proteins. J Biol Chem *276*, 6889-6892.

Malicki, J., Jo, H., Wei, X., Hsiung, M., and Pujic, Z. (2002). Analysis of gene function in the zebrafish retina. Methods *28*, 427-438.

Maurus, D., and Harris, W.A. (2009). Zic-associated holoprosencephaly: zebrafish Zic1 controls midline formation and forebrain patterning by regulating Nodal, Hedgehog, and retinoic acid signaling. Genes Dev *23*, 1461-1473.

Meng, X., Noyes, M.B., Zhu, L.J., Lawson, N.D., and Wolfe, S.A. (2008). Targeted gene inactivation in zebrafish using engineered zinc-finger nucleases. Nat Biotechnol *26*, 695-701.

Moens, C.B., and Selleri, L. (2006). Hox cofactors in vertebrate development. Dev Biol *291*, 193-206.

Papalopulu, N., Clarke, J.D., Bradley, L., Wilkinson, D., Krumlauf, R., and Holder, N. (1991). Retinoic acid causes abnormal development and segmental patterning of the anterior hindbrain in Xenopus embryos. Development *113*, 1145-1158.

Robu, M.E., Larson, J.D., Nasevicius, A., Beiraghi, S., Brenner, C., Farber, S.A., and Ekker, S.C. (2007). p53 activation by knockdown technologies. PLoS Genet *3*, e78.

Ruiz i Altaba, A., Nguyen, V., and Palma, V. (2003). The emergent design of the neural tube: prepattern, SHH morphogen and GLI code. Curr Opin Genet Dev *13*, 513-521.

Sander, J.D., Cade, L., Khayter, C., Reyon, D., Peterson, R.T., Joung, J.K., and Yeh, J.R. (2011). Targeted gene disruption in somatic zebrafish cells using engineered TALENs. Nat Biotechnol *29*, 697-698.

Sanek, N.A., and Grinblat, Y. (2008). A novel role for zebrafish zic2a during forebrain development. Dev Biol *317*, 325-335.

Scott, E.K., Mason, L., Arrenberg, A.B., Ziv, L., Gosse, N.J., Xiao, T., Chi, N.C., Asakawa, K., Kawakami, K., and Baier, H. (2007). Targeting neural circuitry in zebrafish using GAL4 enhancer trapping. Nat Methods *4*, 323-326.

Sood, R., English, M.A., Jones, M., Mullikin, J., Wang, D.M., Anderson, M., Wu, D., Chandrasekharappa, S.C., Yu, J., Zhang, J.*, et al.* (2006). Methods for reverse genetic screening in zebrafish by resequencing and TILLING. Methods *39*, 220-227.

Vitobello, A., Ferretti, E., Lampe, X., Vilain, N., Ducret, S., Ori, M., Spetz, J.F., Selleri, L., Rijli, F.M. (2011). Hox and Pbx factors control retinoic acid synthesis during hindbrain segmentation. Dev Cell *20*, 469-482.